Model biological membranes, studied by AFM imaging and force manipulation

Bestudering van model biologische membranen met behulp van AFM afbeeldingen en krachtmetingen

(met een samenvatting in het Nederlands)

Proefschrift

ter verkrijging van de graad van doctor aan de Universiteit Utrecht op gezag van de rector magnificus, prof. dr. W.H. Gispen, ingevolge het besluit van het college voor promoties in het openbaar te verdedigen op maandag 15 januari 2007 des middags te 4.15 uur

door

Dragomir Nikolov Ganchev
geboren op 2 mei 1970 te Veliko Tarnovo, Bulgarije

Promotoren	Prof. dr. B. de Kruijff
	Prof. dr. A. J. Killian

This work was financed by the Division of Chemical Sciences
of The Netherlands Organization for Scientific research (NWO)

Ganchev, Dragomir Nikolov
Model biological membranes, studied by AFM imaging and force manipulation
Bestudering van model biologische membranen met behulp van AFM afbeeldingen en krachtmetingen
Proefschrift, Utrecht University

CONTENTS

Chapter 1. General introduction

1.1 The membrane is an omnipresent, important and highly complex biological structure

All living cells, from the unicellular organisms to the cells in our own body, are surrounded by membranes. The cytoplasmic membrane determines the boundaries of the cell, defining in and out and preventing the vital cell ingredients to dissipate in the surrounding. In addition to this membrane, a number of membranes are present within the eukaryotic cells, determining the boundaries of cell organelles [1].

The established model for the structure of the biological membrane describes it as a lipid bilayer with which proteins are associated in a number of different ways. Proteins can be either adsorbed on the surface of the membrane (peripheral proteins), or could traverse the lipid bilayer (integral proteins). Some of the membrane proteins could be modified with acyl chain, which anchors the protein to the membrane (for representation of some of the types of membrane proteins see figure 1.) The lipid bilayer hypothesis was proposed in 1925, when Gorter and Grendel performed their fundamental experiment, in which they determined the limiting area per molecule for lipid molecules, extracted from red blood cells [2]. Comparing the obtained limiting area, multiplied with the number of lipid molecules per cell, with the available surface area of the erythrocyte, they found a 2:1 ratio and therefore postulated that the membrane consist of two layers of lipid molecules. Later on it was argued that this result is achieved through a fortunate compensation of two errors, acting in opposite directions, but nevertheless, the correct concept of the biological membrane as a lipid bilayer was born.

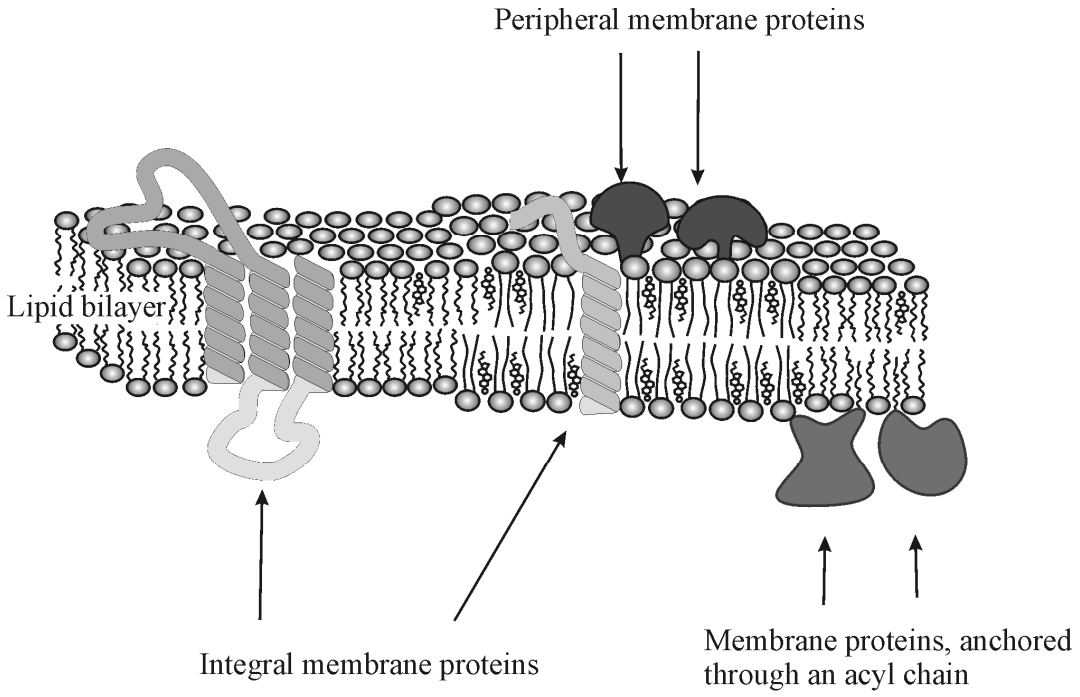

Figure 1. Schematic representation of the organization of the biological membrane. For simplicity, some classes of lipids (glycomodified lipids) and proteins are not presented.

However, the membrane is much more than a lipid bilayer which defines the cell boundaries and provides compartmentization within the cell. A number of vital cell processes are performed by the membrane proteins. They are encoded by ~ ¼ of the open reading frames and are complex molecules, sometimes assembling in multimolecular protein complexes. Membrane proteins serve as an active interface between the cell and the environment, providing mass transport between the cell and surrounding, signal transduction and specific recognition. Since these functions are crucial for the cell survival, the life of the cell depends on the proper functioning of the membrane proteins.

The importance of the membrane as a vital part of the cell attracted the attention of researchers and the biological membrane became a subject of rather extensive scientific investigations. As a result of this, nowadays it is established that the membrane is a highly complex and sophisticated structure. The lipid bilayer comprises a multitude of lipid species and serves as a matrix, providing an appropriate environment for the wide variety of membrane proteins (Figure 1). Moreover, lipids and proteins are not homogeneously distributed throughout the membrane and could form assemblies with a specific composition, such as lipid domains, and this further increases the level of complexity of the membrane. In the next sections we will provide a brief description of the lipids and proteins, their functions and the structures they form within the membrane.

1.2 Lipids. More than 500 lipid species are identified in biological membranes in different cells and organisms, and the composition of specialized membranes within the cells varies significantly [3]. Each lipid species possesses certain physical and chemical properties, and consequently, its presence in the membrane regulates in a certain manner the properties of the membrane. Some of the common membrane lipids in eukaryotic organisms, such as phosphatidylcholine, sphingomyelin and cholesterol, are presented in figure 2.

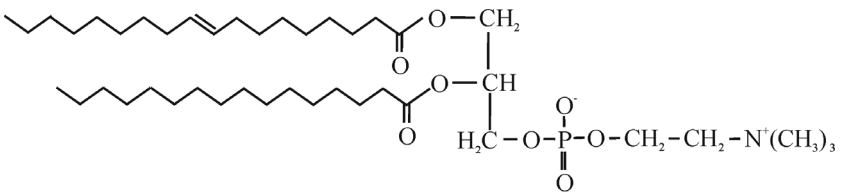

Glycerophospholipids (phosphatidylcholine)

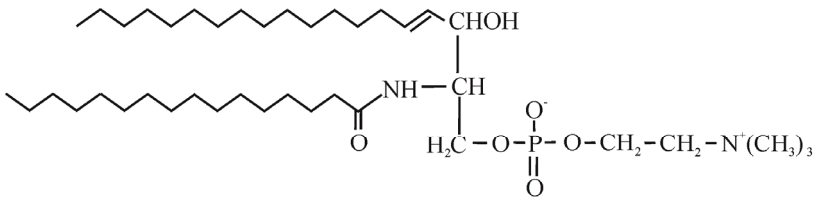

Phosphosphingolipids (sphingomyelin)

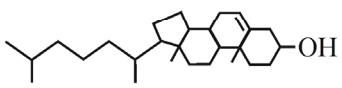

Cholesterol

Figure 2. Structure of some of the membrane lipids.

One important feature of a lipid molecule is its amphipatic character, meaning that it has both a hydrophobic part, containing one or more acyl chains, and a hydrophilic part - a polar head group. This dual character is crucial for the behaviour of the lipid molecules in an aqueous environment and determines their self-assembly in different structures, including a lipid bilayer. Importantly, the ratio between the sizes of the hydrophobic and hydrophilic parts is crucial in determining whether a certain lipid forms a bilayer, when dispersed in an aqueous environment (Figure 3) [1]**.** If this ratio is close to 1, a stable bilayer is formed.

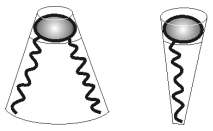

Lipids, forming non-bilayer structures

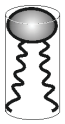

Bilayer forming lipid - the ratio between areas of the head group and the hydrophobic part is ~ 0.5 - 1

Figure 3. The sizes of the hydrophobic and hydrophilic parts of the lipid molecule are important in determining the structures, which they form in aqueous environment.

The predominant state in biological membranes is the so-called liquid crystalline state (L_α) (figure 4). In this state the acyl chains of the lipid molecules are disordered, the bilayer has fluid-like behaviour and molecules within the bilayer are highly mobile (thus the other term for this phase – "liquid disordered, l_d"). When the temperature is below a certain value, the lipid bilayer is in a gel state - L_β. In this state the acyl chains in the lipid molecules are straightened and the molecule occupies a minimal area. The lateral mobility of the molecules within this highly ordered state is strongly suppressed. The state of the bilayer depends on the length and degree of unsaturation of the acyl chains of the lipid molecules. Generally, the longer or the more saturated the acyl chains are, the higher is the respective transition temperature (the temperature, at which the bilayer changes its state from gel to liquid-crystalline). The state of the bilayer is crucially important for the overall physical properties of the bilayer – fluidity and elasticity of the bilayer itself, as well as for the mobility and functionality of the membrane incorporated molecules.

The acyl chains – the hydrophobic part of the lipid molecule - can be connected through a glycerol (glycerolipids) or sphingosine (sphingolipids) backbone to a hydrophilic head group, which also varies in its chemical composition. The polar head group of the lipid molecule varies in charge and size and these characteristic features of the lipid head group are important in certain membrane processes. One abundant class of glycerolipids in animal cell membranes is phosphatidylcholine (PC). PC lipids have two acyl chains and are so-called bilayer-forming lipids, because they spontaneously self-assemble in an aqueous environment into bilayers. Another important feature of the PC lipids is their zwitterionic character. The choline group is positively charged, which compensates the negative charge of the phosphate. As a result the PC molecule bears zero net charge.

Another important group of lipids, encountered in the plasma membrane of many mammalian cells, are sphingolipids. A typical representative of sphingolipids is sphingomyelin (SM) which has a same polar head group as PC glycerolipids (figure 2). Despite having the same head group, these two groups of lipid species differ significantly

in their properties [4]. Sphingolipids are characterized by long and largely saturated acyl chains. Due to this acyl chain composition they have a relatively high transition temperature. Perhaps even more important from a biological point of view is the higher affinity of sphingomyelin for sterols - another major class of membrane lipids.

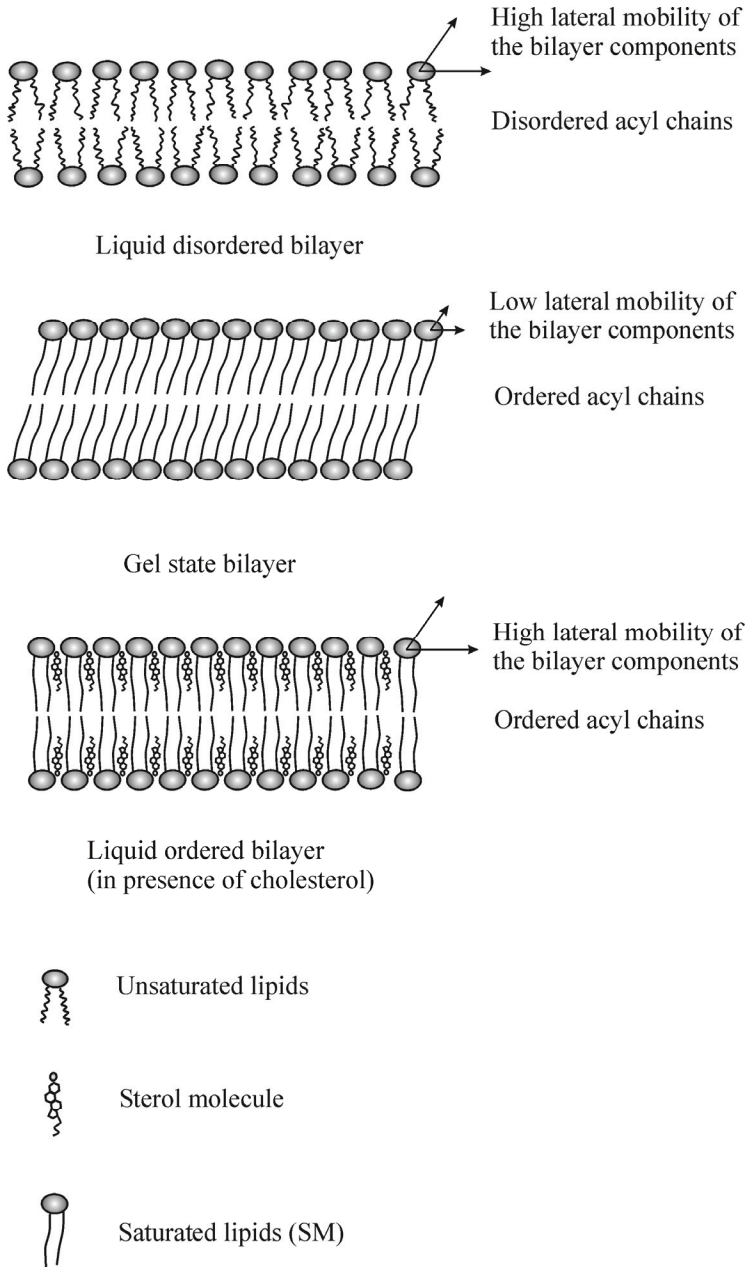

Figure 4. Some of the states of the lipid bilayer, encountered in biological membranes.

A representative of the sterols is cholesterol, which is a non-charged lipid molecule of crucial importance in eukaryotes and which in some animal cells accounts for up to 50 % of the lipid content of the plasma membrane. Cholesterol has a small hydrophilic head group, consisting of a hydroxyl group, and a hydrophobic part, which contains a rather rigid structure of four fused rings. The precise mechanisms of the interaction between cholesterol and phospholipids are still under intensive investigations and a point of debates. However, it is generally accepted that the

ring structure of cholesterol interacts with the acyl chains of surrounding phospholipids, optimizing the hydrophobic interactions. A strong interaction between the hydroxyl group of cholesterol and the PC polar head group was also proposed. Cholesterol also interacts strongly with glycolipids. The demonstrated strong affinity between cholesterol and sphingolipids was explained by a proposed formation of a hydrogen bond between the hydroxyl group of the cholesterol and the sphingosine backbone of sphingomyelin.

Due to these specific interactions, cholesterol significantly modifies the physical properties of the lipid bilayer. When present in a membrane above a certain threshold level, and when saturated lipids are present, cholesterol can induce the formation of a lipid bilayer in a specific state, called the liquid ordered (l_o) state. In this state the bilayer is characterized by a high lateral mobility of its components, as in the case of the liquid disordered state, but the ordering of the acyl chains is as in the gel phase bilayers. In the l_o phase the physical properties of the bilayer are significantly different from the properties of both L_α and L_β phases. For instance, the thickness of the bilayer is modified in the presence of cholesterol, and quite significantly from a biological point of view, the bending and compression moduli of the bilayer are substantially increased [5].

1.3 Phase separation in membranes and lipid bilayers

The complexity of the membrane is determined not only by the huge diversity and complexity of its components, but also by the fact that they are not uniformly distributed. This asymmetry is both between leaflets, causing enrichment of each leaflet in certain lipid species, and lateral, leading to formation of domains with defined lipid composition within the membrane. The existence of such domains was postulated after the discovery that lipid fractions, enriched in SM and cholesterol, can be extracted from biological membranes upon treatment with the surfactant Triton X-100 at low temperatures (~5^o C). Supposedly these domains are involved in important cell processes, such as signaling and protein sorting [6]. The isolated membrane fractions are enriched in certain proteins, while depleted in others. A necessity of certain proteins to be present in such domains (also known as rafts) in order to function properly was also proposed [7]. The phase separation, leading to domain formation, is a complex process, influenced both by the head group and the order of the acyl chains of the lipid. A crucial role plays the already described effect of cholesterol on properties of saturated lipids, leading to the formation of a liquid ordered phase (figure 5).

The proposed important role of the lipid rafts generated a great interest, and many studies were concentrated on characterizing their composition, sizes and physical properties [8]. Since the possibilities for studying the processes of domain formation and the properties of the formed domains in real membranes are rather limited, model systems were predominantly studied. Monolayers and bilayers with a lipid composition, resembling the lipid composition of biological membranes, were extensively investigated. In these systems a process of spontaneous domain formation is visualized. Using different techniques, such as fluorescence microscopy and Atomic Force Microscopy, insight in the organization and sizes of lipid domains within model membranes was obtained. Numerous studies demonstrated the subtle manner in which the precise chemistry of lipids influences the process of phase separation within the bilayers [9]. Quite significant is the observation of detergent resistant domains in model bilayers [10]. Protein/lipid interactions also can be studied and ordering of model transmembrane peptides within lipid bilayers was demonstrated [11]. This suggests that investigating the behaviour of lipid bilayers with different composition and the effect of incorporated model peptides on the bilayer will give us insight in the organization of a biological membrane.

The enormous diversity of membrane lipids and the subtle way, in which properties of the membrane depend on the lipid composition, provide an ingenious way for regulation of membrane properties. By adjustments of a length and saturation of acyl chains of the lipids and by preferential location of certain lipids on a specific place the local properties of the membrane can be controlled through the formation of lipid domains. This could provide a proper lipid environment for proteins - the active components, associated with the membrane.

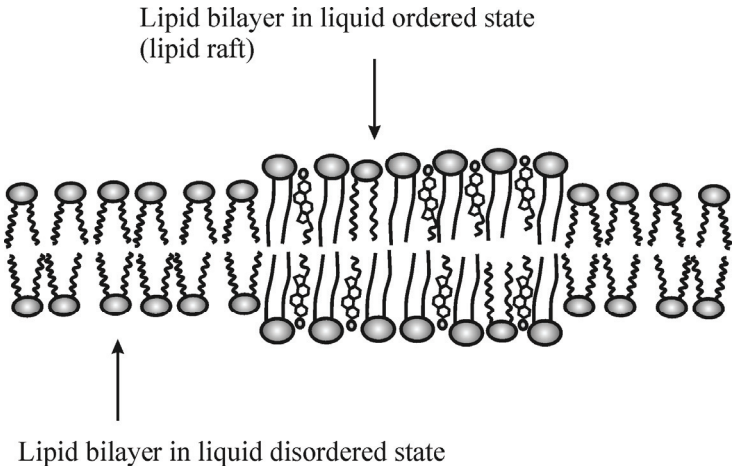

Figure 5. Schematic representation of raft organization in membranes.

1.4 Proteins.

The lipid matrix of the membrane provides an appropriate environment for the membrane proteins. In different types of membranes the content of these proteins, incorporated in or associated with the membrane, is between 20 and 80 mass %.

A common motif in the sequence of the integral membrane proteins is a span of ~ 20 consecutive hydrophobic amino acids residues. They form a hydrophobic α-helix, which traverses the hydrocarbon region of the membrane. Quite often specific amino acid residues, such as tryptophans, are found to flank α-helices of the membrane proteins [12]. Tryptophans were shown to have an affinity for the interfacial region of the bilayer and they anchor the α-helix of the protein in a certain position in the membrane. Some of the membrane proteins are rather complex molecules, having 10 and even more α-helices, spanning the membrane. Due to this complexity often model peptides, featuring a hydrophobic α-helix are used as a model system to get insight in membrane proteins [13].

One group of such model peptides are the so-called WALP peptides, which have been extensively studied as a suitable model for the transmembrane part of the membrane proteins [14]. These synthetic peptides combine two characteristic features of membrane proteins. The first feature is a stretch of a desired number of hydrophobic residues, in this case a series of alternating leucine and alanine residues. The length of the stretch can be designed to match (or mismatch) a desired bilayer thickness. The second feature is the presence of tryptophans on both sides of the A/L repeat. Extensive studies of these peptides provided valuable insight in the behaviour and properties of a transmembrane α-helix, incorporated in lipid bilayers with a different composition [15]. Since the composition of these peptides closely resembles the membrane spanning part of proteins, the obtained knowledge provided us with better understanding of behaviour of membrane proteins.

1.5 Lipid – Protein interactions

Membrane proteins are amazing molecular machines. Under normal circumstances they perform their functions with high efficiency. The complex architecture of these proteins determines their functionality. However, the membrane lipids are not only the passive matrix, which surrounds the proteins. The process of protein insertion and assembly within the membrane, as well as proper functioning of the proteins is modulated by the membrane lipids. In these processes both protein-protein (P/P) and lipid-protein (L/P) interactions are operative. The dependence of protein targeting and sorting on P/P and P/L interactions was also recognized [16]. The membrane/peptide interactions of some extracellular peptides, such as prion proteins and antimicrobial peptides are also dependent on P/L interactions between these molecules and the target membrane. In each of these processes a number of interactions are operative which differ in nature. For instance, hydrophobic interactions are dominant in the process of insertion of transmembrane proteins [17] and electrostatic interactions mediate the recognition process of antimicrobial peptides with the target membranes [18].

This dependence of the protein localization, conformation and functionality on the L/P and P/P interactions is quite significant and knowledge in this area will substantially increase our understanding on the behaviour of membrane proteins and of the processes, performed by them. Some progress has been made in characterizing these interactions. The preferential location of each amino acid in a certain position with respect to the bilayer has been described. For instance, hydrophobic residues with a typical representative leucine prefer the hydrophobic core of the bilayer, while tryptophans prefer the interfacial region of the bilayer and charged residues such as lysine are more likely to be found in the parts of the protein, residing in the aqueous environment [19].

However, still many obscure points remain and on a molecular level our understanding is still limited. Nonetheless, information for the interaction between single protein and lipid molecules within a bilayer will be needed in order to understand in detail the way in which membrane proteins insert, assemble and perform their functions. The problem with the complexity of the proteins is also encountered here and this suggests that model peptides, such as the already described WALP peptides would be a convenient system to study P/L interactions in more detail.

1.6 Membrane as a target for antimicrobial peptides.

The cell membrane is important not only as a structure, defining the boundary of the cell and performing vital cell functions through the incorporated proteins. It is well established that the membrane also is a target for certain molecules, which attack the cell. From a practical point of view rather important is the group of substances, which selectively attack the bacterial membrane and provide us with weapons in the war against bacteria. This group of bactericides consists of small proteinaceous molecules, commonly referred to as antimicrobial peptides, which are synthesized by different organisms as a weapon against target cells. These molecules target the bacterial membrane and through different mechanisms kill the bacteria. They vary in their precise chemical structure, but the large part of them are ~ 15 - 45 amino acid residues long peptides [20]. They are amphipatic molecules, quite often they have a non-defined secondary structure in an aqueous environment and adopt an α-helical conformation upon binding to the membrane surface. Their predominantly cationic character suggests that the anionic lipids, commonly located in the outer leaflet of the bacterial membranes are important in the membrane recognition and penetration of these peptides.

The action of the antimicrobial peptides can be non-specific, when the binding to the membrane does not require a specific target molecule (see figure 6). Typical examples of such peptides are the antimicrobial peptides from the families of the magainins and clavanins. Through binding to the membrane this type of antimicrobial peptides

accumulate on its surface and upon reaching a certain threshold level they disrupt the barrier properties of the membrane. Various models for the process of membrane disruption are proposed. One of the discussed mechanisms is pore formation, where the antimicrobial peptide forms defined pores within the membrane, and pores of different topologies were proposed [21]. Another mechanism is carpet-like membrane destabilization [22]. In both proposed mechanisms the barrier properties of the membrane are lost and this causes cell ingredients to flow out in the environment. This eventually kills the targeted microbial cell.

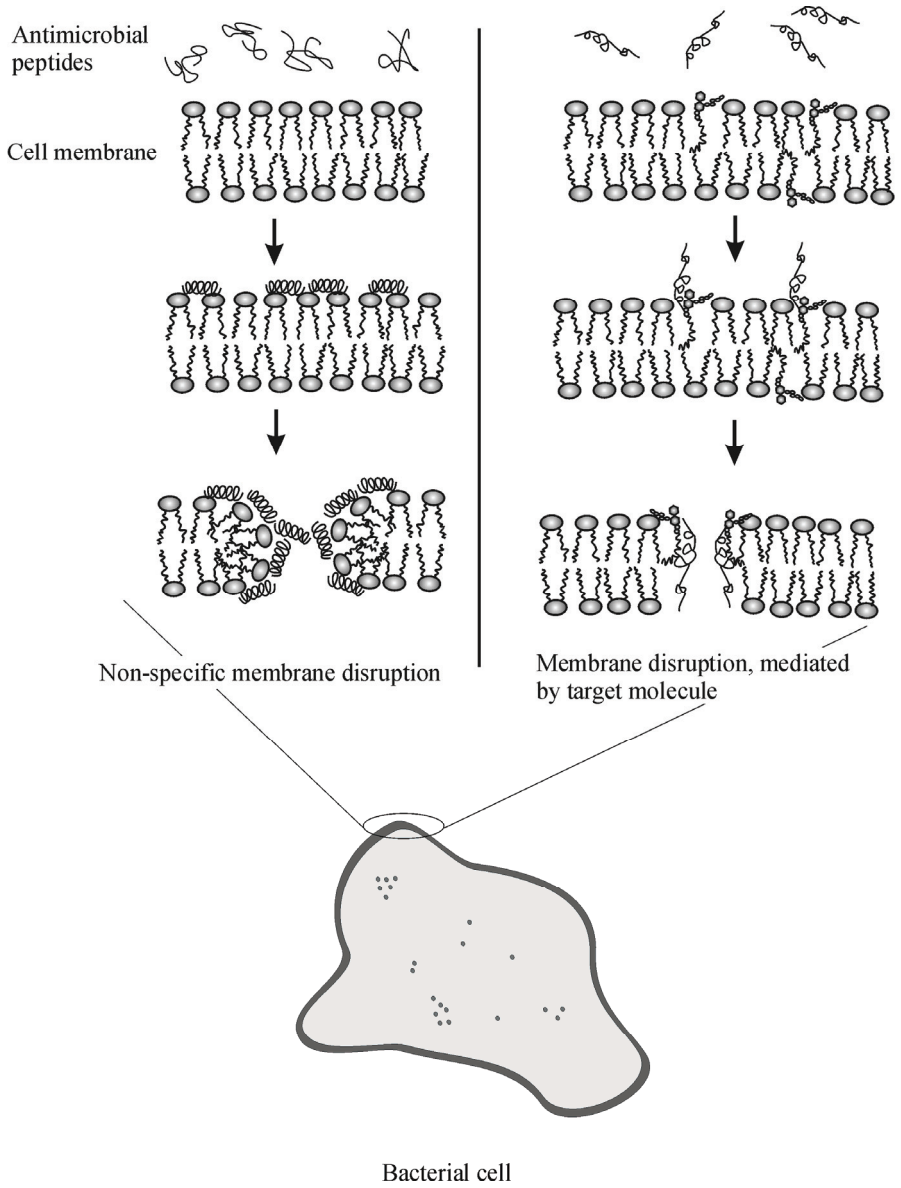

Figure 6. Two different mechanisms are operative in the action of membrane-interacting antimicrobial antibiotics. The targeting of the cell membrane by antibacterial peptides can be non-specific, as in the case of clavanins, when no presence of a specific molecule is required for the antimicrobial action (A), or mediated by a specific target molecule, as in the case of nisin, which forms pore complexes with lipid II (B).

Another group of antimicrobial peptides interacts specifically with target molecules within the membrane in the process of their antimicrobial action. Such a target molecule is Lipid II (L II), (Figure 7), a complex lipid molecule,

containing a long bactoprenyl chain connected via a pyrophosphate to a large hydrophilic group, consisting of a disaccharide-pentapeptide unit. L II plays a key role in the synthesis of the bacterial cell wall. The bacterial cell wall is a specific structure, encountered in bacteria and is vital for the bacterial survival. This makes the cell wall and molecules, taking part in its synthesis, an ideal target for selective antimicrobial action. Some of the antimicrobial peptides, specifically targeting Lipid II, are vancomycin and mersacidine. For instance, vancomycin specifically binds to the last two alanines in the pentapeptide of the L II head group and prevents cell wall synthesis. Another antibiotic with practical implementation, and with L II as target, is nisin. Nisin is a pore-forming peptide and forms together with L II a pore in the bacterial membrane with a defined 2:1 nisin:L II ratio [23]. The pore formation leads to dissipation of the membrane potential and this eventually kills the bacteria. Nisin is produced by the gram-positive bacteria *Lactococcus lactis* and belongs to the group of lantibiotics. Lantibiotics form a specific class of antimicrobial peptides, containing uniquely modified amino acids [24]. These amino acids form lanthionine rings, which have been demonstrated to be important in their antimicrobial action [25]. Nisin contains 34 amino acids, has 5 lanthionine rings and is positively charged. It is highly effective against a broad range of Gram-positive bacteria. Due to their high selectivity towards bacteria (a result of targeting of the Lipid II molecule), lantibiotics are promising antibiotics.

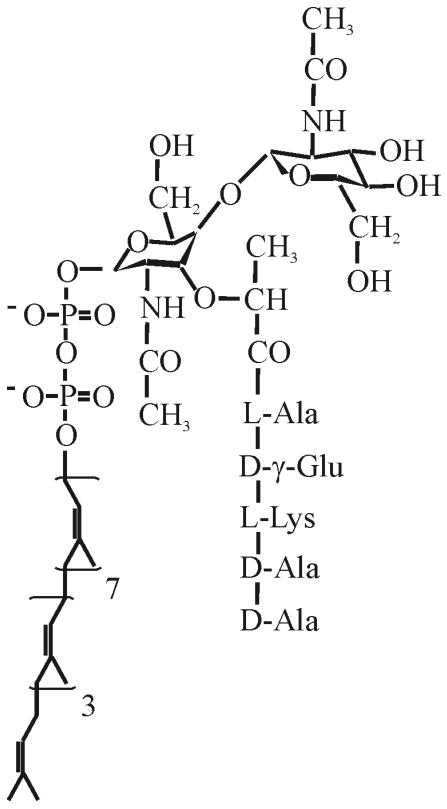

Figure 7. Lipid II structure.

1.7 Supported lipid bilayers as a model system for a biomembrane and techniques, used for their characterization. The membrane can be considered as a two-dimensional structure with a surface organization which can reveal many of its structural features, such as domain formation and the location and conformation of membrane proteins. Therefore it is of prime interest to obtain reliable information on the surface organization of biological membranes. Unfortunately, due to the complexity of the membrane, it is difficult to study its surface in an intact cell.

Therefore, an appropriate model system which is suitable for investigations of its surface organization and properties is needed. We should be able to control the composition of the studied model system, in order to closely reproduce the composition of a biological membrane of interest. Acquired results for a chosen model system, if obtained at physiological conditions, will give us insight into the organization and properties of biological membranes.

One model system, which fulfills these requirements, is a supported lipid bilayer, formed on an (atomically) flat support (mica, silica or other hydrophilic surface). The supported lipid bilayer closely resembles the biological membrane. A water layer, app. 1 nm thick [26] is situated between the bilayer and the supporting surface and isolates the bilayer from the support, ensuring mobility of the bilayer species similar to the mobility of the components in a membrane [27]. Using established protocols, we have the possibility to prepare supported bilayers with desired composition and to investigate them at controlled conditions. Moreover, with supported bilayers one can follow adsorption processes of different membrane-interacting molecules, such as antimicrobial peptides, which gives the possibility to study membrane/drug interactions [28]. The possibility to follow in-time interactions of supported bilayers with molecules of interests also suggest that supported lipid bilayer can be used as biosensors.

Supported bilayers can be formed by the Langmuir-Blodgett technique [29], by the vesicle fusion method [30] or by spin-coating [31]. The first technique allows to deposit and study bilayers at predetermined surface pressures and with different compositions of each monolayer, while vesicle fusion allows formation of a bilayer at surface pressures, presumably resembling surface pressure in a cell membrane. Moreover, with the vesicle fusion method one could incorporate a (part of) a protein in the bilayer. Unfortunately, the process of formation of the bilayer from vesicle suspensions is not yet completely understood. However, some insight in this area has been gained, following the early stages of adsorption of single vesicles, their interaction and spreading over the substrate [32]. The latter technique, spin coating was recently developed and allows formation of multilamellar bilayer stacks. Controlling the deposition parameters, it is possible to deposit large-scale ordered samples, containing from 2 up to 30 bilayers. Supported bilayers are also a convenient system to study lipid phase separation and peptide aggregation within lipid bilayers. Lipid and lipid/peptide domains with a specific composition were observed and the dependence of their morphology on the exact chemistry of lipids and peptides was described [33].

The diversity of processes that can be studied using supported bilayers and the fact that they closely resemble biological membranes makes them a suitable model system to study properties of membranes. Therefore, currently they are receiving increasing attention. A number of techniques can be used to get insight in the structure and properties of supported bilayers. Here we will mention only a few techniques as an example for the possibilities to investigate and characterize supported lipid bilayers. The NMR technique is used to probe the ordering of the acyl chains in multilamellar bilayer stacks [34]. Fourier Transformed InfraRed (FTIR) spectroscopy provides information on the chemical structure of the supported bilayers, conformation of incorporated proteins [35] and lipid/protein interactions [36]. Adsorption and desorption processes on lipid bilayers can be followed by Surface Plasmon Resonance (SPR) technique [37] or quartz crystal microbalance [38].

Surface imaging techniques can further provide information on specific features on the surface of the investigated samples, and they are extensively used on supported bilayers. One of these techniques is fluorescence microscopy. It allows visualization of formed lipid domains and localization of protein molecules in supported bilayers. However, its resolution is limited to several hundred nanometers, and since many features in membranes and membrane-mimicking systems are smaller than this limit, a more powerful surface imaging technique is needed. Such technique, proved to be rather fruitful for characterization of supported bilayers is Atomic Force Microscopy (AFM).

The first article, in which the AFM technique was described, was published in 1986 [39]. Since than this technique provided a wealth of data, concerning biological systems, such as bilayers [40], proteins [41], DNA molecules [42] and cells [43]. These studies demonstrated the possibility of the AFM method to visualize with nanometer resolution the topography of the investigated supported sample. Imaging can be performed at physiological conditions - in an aqueous environment and at room temperature, and without the necessity chemically to modify the investigated molecules. Moreover, we could mechanically manipulate molecules of interest, which makes AFM rather unique amongst the other biophysical techniques. In the following part we will discuss the principle of operation of AFM, its capabilities and limitations, and we will give some of the more significant achievements, obtained by the AFM technique.

1.8 AFM – principle of operation, possibilities and limitations.

AFM "sees" the investigated sample via interaction of a sharp tip with the underlying sample. This technique allows visualization of the sample with nanometer (and in some cases, with sub-nanometer [44]) resolution, in contrast with optical microscopy, where light is used to create an optical image of the investigated specimen and the resolution is limited by the diffraction limit of the used light (~ 500-600 nm). A sharp, nanometer sized AFM tip is mounted on the end of a long flexible cantilever, connected to a holder (Figure 8).

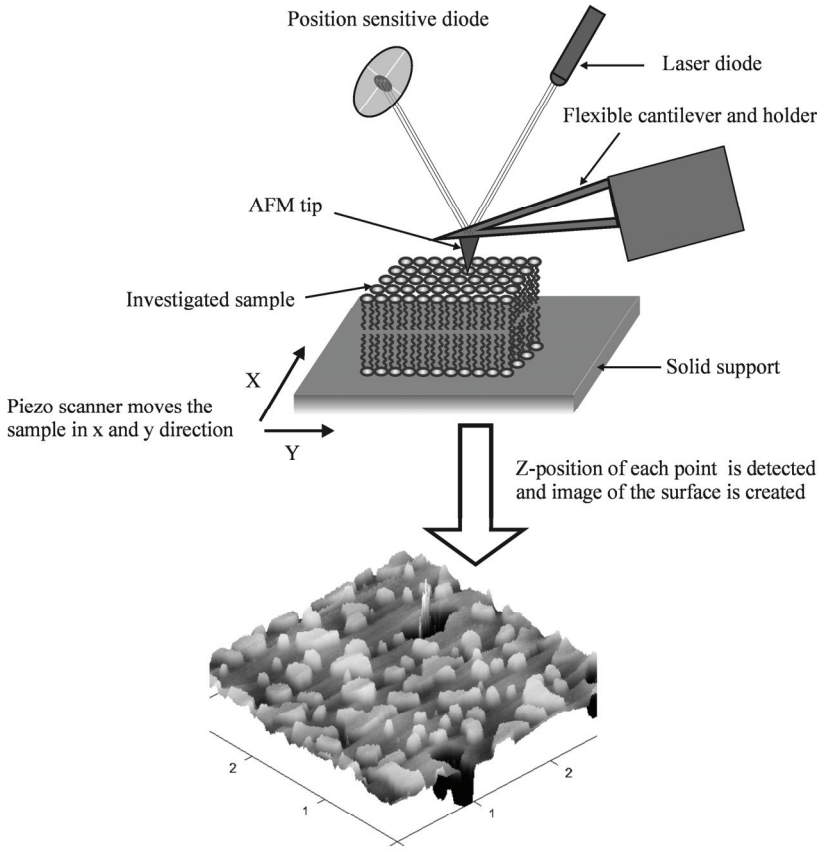

Figure 8. AFM technique – principle of operation

The backside of the cantilever is highly reflective and a beam from a laser diode is projected onto the end of the cantilever and reflected on the position sensitive diode. The slightest movement of the tip in the z direction will reflect the laser beam on a different spot on the position sensitive diode, which creates a signal, used by the AFM to maintain the z-position of the tip. The studied sample is adsorbed on an atomically flat support (mica for instance) and the tip is brought in contact with the sample, until some preset value of the force between tip and the sample is reached. Either the tip assembly, or the support with the sample, is mounted on a three-dimensional piezoscanner, which can move the tip (or alternatively, the sample) in the x, y and z directions. For clarity, further we will assume that the tip is fixed and the sample is moved by the piezoscanner. The sample is moved by the piezoscanner in the x and y directions, thus being raster-scanned by the tip. The electronics of the AFM keeps, by moving the piezoscanner in z direction, the force between the tip and the sample constant at each point, scanned in the x and y directions, which allows simultaneous information on the height of the sample at the respective x-y coordinate to be registered. In this way we collect the data for the location of each point on the surface of the sample in three-dimensional space, which allows a 3D image of the surface of the sample to be reconstructed. In the created image the lower areas in the sample are presented as darker, and the higher areas as lighter.

The use of the laser diode and position sensitive diode create a so-called optical lever with a light-path of a few centimeters, which allows detection of the z-position of the tip with a precision of 0.1 nm. This determines the vertical resolution of the AFM and this high sensitivity allows discrimination between areas with very small height differences, such as phase-separated lipid bilayers [45]. The resolution in the x and y direction is directly determined by the radius of the tip, which can be as low as several nanometers. This allows nanometer and sub-nanometer resolution to be achieved, but in the same time could be one of the drawbacks of this technique. Even if we use a sharp tip, it could be polluted with material from the sample during scanning, thus deteriorating the resolution [46]. This is especially a potential threat in imaging of soft biological samples. With such samples another problem could arise due to their softness. Since a certain force, exerted on the tip is needed for visualization, the tip could deform the sample and even penetrate through it, which results in images, which do not represent correctly the surface of the sample. The basic principle of operation of the AFM - imaging the sample through surface forces, could cause still another problem. If the surface properties of the sample, and as a consequence – tip/sample interaction – are substantially different in different sample points, than the obtained image would not represent correctly the true surface profile of the sample, and the image would be influenced by the surface inhomogenities [47]. These considerations come to show that, as every other technique, the AFM is not a perfect tool. However, being aware of the potential pitfalls, one can (almost) always construct an experiment and interpret the data in such a way that reliable information for the sample can be achieved.

1.8.1 AFM is a technique, allowing imaging of biological samples at physiological conditions.

Since no vacuum or low temperatures are required for the AFM to operate, this technique is ideally suited to investigate biological samples at physiological conditions – in aqueous environment and at room temperature. This feature places it in a rather unique position amongst other microscopic techniques, being the only one which allows visualization at such conditions with a nanometer and sub-nanometer resolution. Moreover, the composition of the aqueous media can be exchanged during the experiment, which allows additional flexibility. In this way in-time adsorption of different molecules of interest can be investigated [48], as well as the reaction of the sample to the change in the experimental conditions. This suitability of the technique to image biological samples at relevant

conditions quickly established AFM as a valuable tool in biophysical laboratories. A constantly growing number of AFM studies revealed a wealth of data on a wide variety of biological systems (for a recent review, see [49]). Next we will discuss some of the more significant achievements in this field.

One of the systems, most intensively studied by AFM, are supported lipid bilayers of different composition [50]. The thickness of bilayers is the most direct parameter, which can be derived [51]. It was shown that depending on the state and composition of the bilayer, the thickness of the supported bilayer is between 4 and 6 nm. This value includes a water layer, approximately one nanometer thick, lying between the support and the bilayer and is in good agreement with the data from other techniques. The water layer isolates the bilayer from the support and provides a mobility of the bilayer components, comparable to the mobility in non-supported bilayers [52]. When more than one lipid species is present in the bilayer, a phase separation may be observed [53], clearly demonstrating the possibility of the AFM to resolve gel and liquid crystalline domains within the bilayer. Further elaborations of the system are also possible, allowing observation of ternary lipid mixtures. Quite significant is the observation of detergent resistant domains in cholesterol-containing ternary mixtures, which system is a direct model for lipid rafts in biomembranes [54].

Other highly informative experiments are the observations of ordered arrays of membrane proteins. Classical examples are the imaging of the purple membrane in *Halobacterium Salinarium* [55], and the Hexagonally Packed Intermediate layer in *Deinococcus radiodurans* [56]. On these samples, as well as on the number of other membrane proteins [57], a sub-nanometer resolution was achieved, allowing identification of individual α-helices of these membrane proteins. Since the α-helix is a predominant motif of membrane proteins, some studies concentrated on the behaviour of model peptides with a single α-helix, incorporated within a lipid bilayer. Intriguing self-assembling ordered domains were observed in such systems, using so-called WALP peptides [58]. Observed domains consist of regularly spaced dark (lower) lines with defined repeat distance, separated by lighter (higher) areas. The domains are typically connected by cracks in the bilayer. The observed ordering phenomenon is similar to the already observed ordering of gramicidin A in a lipid bilayer [59], which suggest that the ordering within a bilayer could be a more general property of transmembrane peptides.

Another intensively studied area in membrane research is the interaction between membrane interacting antimicrobial peptides and lipid bilayers of different composition. Understanding the process of action of these peptides is an important step in developing new weapons in the war against bacteria. The process of interaction between membrane interacting substances and lipid bilayers could be conveniently followed in time, using the imaging capabilities of the AFM [60]. The damage, caused by antimicrobial peptides to the membrane, also can be visualized [61].

AFM can visualize not only membrane mimicking systems and their interactions with biologically relevant molecules, but also individual biological molecules, such as DNA [62] and single protein molecules [63]. In these experiment the characteristic helical pattern of the DNA molecule was resolved, as well as the specific shape of investigated proteins. Problems in such systems could arise from the requirements for proper adsorption of the investigated molecule to the solid support. The protein or DNA should be attached strongly enough to allow a stable scanning and in the same time not to be deformed by exceedingly strong interaction forces with the substrate. This requires from the researcher to fine-tune the chemical composition of the imaging buffer and/or the substrate [64].

The possibility of the AFM method to follow in-time processes on a single molecular level recently was employed to study the aggregation and fibrilization of amyloid-forming peptides. These peptides are present in the human body usually as monomers, but under some circumstances they start to aggregate, forming fibrils, which could damage the cell. Since this process leads to some life threatening diseases, a profound understanding of the process of fibrilization is of vital importance. A number of emerging AFM studies, providing information on processes of fibrilization [65] and the fibril/membrane interactions [66] demonstrated the possibility of the AFM to be implemented in this field. The possibility to change the environment during an experiment will allow the researcher to study the fibrilization process at different conditions.

1.8.2 AFM can mechanically manipulate the investigated samples, increasing the possibilities for characterization.

Soon after the development of AFM, its potential not only to image, but also to manipulate mechanically the sample on a single molecular level and to measure inter- and intra-molecular forces was realized. The first description of the force measurement approach was published in 1992 [67] and since then the area of force measurements became an extensively studied research field (for recent review, see [68]). The main idea behind force manipulation is that the AFM tip can in a controlled way either push or pull the target molecules within the investigated sample. Since in each moment the z-position of the tip is known, and the spring constant of the cantilever can be determined, the force, which the tip exerts on the sample, is known with a good precision.

When AFM is used as a force measuring device, the tip is positioned over a point of interest on the surface of the sample and the movement of the sample is restricted in the x and y directions. Then the sample performs a cycle, approaching the tip, making a contact with it, and after reaching the predetermined position the sample is retracted to its initial position. At each moment the position of the tip and the cantilever is known and from this information the so-called force-distance curve is created. According to Hook's law the force, exerted by the tip on the sample (in the case we want to push the sample) or by which the tip is held in contact with the sample (in case of measurement of the inter- and intra-molecular forces) is:

$$F=d.k,$$

where d is the displacement of the tip and k is the spring constant of the cantilever (Figure 9).

When we exert the force on the sample, we can use the tip as a tool to probe local mechanical properties of the sample, such as elasticity, or the force, needed to penetrate through the investigated specimen. In this way the force, needed to penetrate through a lipid bilayer can be measured. The dependence of this penetration force on the lipid composition was investigated [69]. This possibility renders AFM as an alternative, or complementary technique, to the surface force apparatus (SFA). While AFM offers the possibility to image the sample, SFA provides much better characterization of the shape and size of the surfaces with a possibility for following a more rigorous theoretical interpretation.

Another fruitful application of AFM as a force sensor is to determine inter- and intra-molecular forces with a picoNewton precision. This possibility, combined with the imaging capability of AFM, lacking in any other force measuring technique (such as laser tweezers [70] or biomembrane force probe [71]) makes a unique combination, which provided some amazing results during the last few years. A more detailed description of the force measurement procedure and some of the most prominent examples will be discussed further.

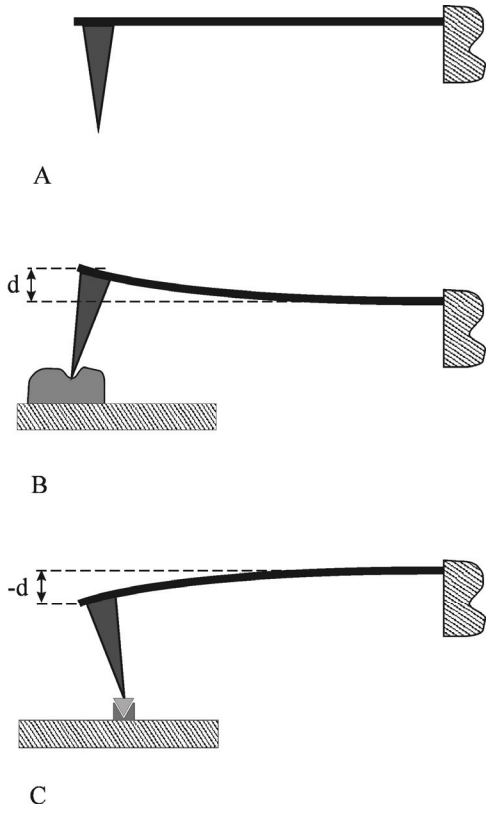

Figure 9. AFM tip can be implemented as a tool to mechanically manipulate the sample. In (A) the cantilever is in equilibrium and no mechanical force is applied on the tip. In (B) the positive displacement of the tip from its equilibrium position causes the underlying sample to be mechanically pressed and possibly deformed with a defined force. In (C) the negative displacement of the tip applies a pulling force on the formed molecular complex, thus probing the strength of the assembly.

1.9 AFM as a tool to measure forces of interaction between biomolecular complexes and mechanical properties of single molecules.

The AFM technique allows detection of the smallest deflections in the position of the cantilever. Transformed in forces, according to the Hook's law, the resolution limit of one Ångstrom in the z-direction theoretically gives a force sensitivity of ~ 1-2 pN for the softest cantilevers! However, due to thermal motions of the cantilever, caused by the Brownian motion of the molecules in the aqueous medium, the sensitivity is limited to app. 10-20 pN.

First we will discuss measurements of the internal mechanical properties of molecules. The basic idea is rather straightforward. The molecules of interests are immobilized on the support, possibly visualized, and afterwards the tip is positioned on a point of interest on the sample. Then a force-distance curve is recorded and as the tip is brought in contact with the sample, a part of the investigated molecule is attached to the tip, either by the applied force (physisorption), or by chemical interaction between the modified tip and the investigated molecule (chemisorption). In this way a molecular bridge between the tip and sample is created. Only one molecule should be captured between the tip and the sample in order for a reliable data interpretation to be possible. This can be achieved by varying the concentration of the molecules under investigation.

When a stable attachment of the molecule to both the substrate and the tip is achieved, upon retraction of the sample the molecule will be stretched. As a result of this the cantilever will bend and will start to apply gradually increasing force to the bridging molecule. As an example let us consider a modular protein molecule, such as a muscle protein titin, having a number of folded domains (Figure 10). This molecule is fixed on one end to the substrate and on its other end to the tip. Upon separation, at a certain moment the elastic force of the cantilever, exerted on the molecule becomes larger than the unfolding strength of its weakest domain and this domain unfolds, adding its unfolded length to the bridge between the tip and sample, thus releasing (part of) the elastic force. The continuing separation between the tip and the sample loads again the remaining folded domains of the molecule, until a critical unfolding force for the next domain is reached and this domain yields and unfolds. This sequence continues until all domains in the protein are unfolded, and/or the attachment to the tip or substrate is broken.

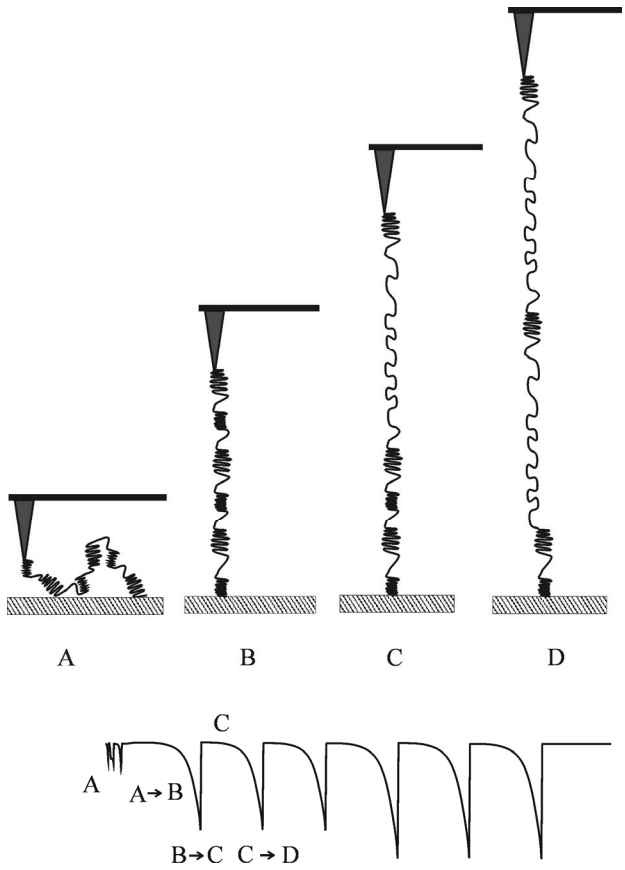

Figure 10. AFM force apparatus, used as a set-up to measure intramolecular forces, such as unfolding strength of a modular protein. The recorded force-distance curves demonstrate the unfolding of each individual protein domain. The peaks in the curve (B-C, C-D, etc.) indicate for the strength of the unfolded domain.

During the process of the molecule pulling, the position of the tip is registered at each moment. From the recorded force-distance curve we can directly determine the force, applied by the cantilever through the tip on the sample. In

this way the value of the force, at which a certain domain within the studied molecule unfolds, can be precisely determined from the height of the respective peaks. In order to have a reliable statistics, many force curves should be recorded and analyzed (usually > 100, depending on the system). Differences in the mechanical strength of different domains in the studied molecule can be reliably detected, as demonstrated in [72]. The shape of the curves, preceding each peak in the force curve usually is fitted with a theoretical curve according to two proposed models, Worm-Like Chain (WLC) and Freely Jointed Chain (FJC). The parameters, obtained from both models are the persistence length (usually interpreted as the smallest non-deformable part in the studied molecule) and the contour length of the molecule (its fully extended length). Moreover, using an appropriate theory (described in part 1.10 of the present thesis) other parameters of the molecule, such as the natural rate of unfolding of domains can be estimated. In a study on polysaccharides it was demonstrated that even the chair-boat transition in the sugar monomer could be detected by AFM [73]. In all these and many other studies it was demonstrated that by mechanical manipulation of a target molecule, one can get information about some of its fundamental properties.

The AFM as a force-measuring device is used not only to determine the properties of single molecules. A rather fruitful field during the last years was the determination of the strength of binding of different biomolecular complexes [74]. In this way the interaction strength of many ligand/receptor and antibody/antigen couples were determined and interpreted [75]. The procedure in this case is as follows (Figure 11). One of the molecules in the couple is immobilized on the solid support, and the tip is incubated with the other molecule. Sometimes a special chemical treatment of the tip and/or the support is needed in order to have the molecules properly attached. Often this treatment includes introduction of a so-called spacer, a long polymer molecule between the immobilized molecule and the support or the tip, which allows conformational freedom of the attached molecule. Since the precise geometry of contact in the antigen/antibody complex is crucial for a proper recognition, sometimes this spacer molecule is essential for successful experiments in these systems. The preferential experimental condition is when only a single complex is formed between the tip and the sample. This is achieved by controlling the density of the coverage of the tip and the substrate with the investigated molecules [76]. The length of the spacer molecule also can be varied, changing the effective radius, in which the molecule, connected to the spacer could probe for the other molecule in the complex. However, controlling these factors is not always possible and sometimes more than one couple is formed and at the retract cycle of the tip more than one bond is broken in succession or even almost simultaneously. If multiple rupture events occur, the obtained force distribution should be scrutinized and correlation analysis to be preformed in order strength of the single complex to be determined. As in the case of force measurements within a single molecule, in the case of intermolecular force determination, hundred and sometimes even thousands of force events are collected and analyzed.

As a classical example for force measurements we could mention the determination of strength of integration of a bacteriorhodopsin (BR) molecule in a purple membrane [77]. This protein has seven transmembrane α–helices and assembles as a trimer in a so-called purple membrane. After visualization of the sample, the tip was brought in contact with the protein molecule and a part of the protein was attached to the tip. Upon withdrawal of the tip a characteristic saw-tooth pattern was observed with up to four separate peaks. The intricate pattern of observed force peaks were analyzed in detail and to each peak withdrawal and unfolding of a specific helix/helices was ascribed [78]. Remarkably, after each recorded force curve, a vacancy in the 2D ordered protein assembly of the purple membrane was observed, which is an indication for the absence of a BR molecule, removed during the force manipulation. Another interesting example of intermolecular force measurements is the determination of force between

complementary strands of DNA molecules. In these experiments a value for the strength of the bond between the complementary DNA bases were determined [79]. In another AFM study [80] on complementary DNA strands some thermodynamic properties and the range of the interaction between DNA strands were determined, using an earlier developed theory [81], which describes the dissociation of the biological bonds as a thermally activated process. The next part presents the key points in this theory.

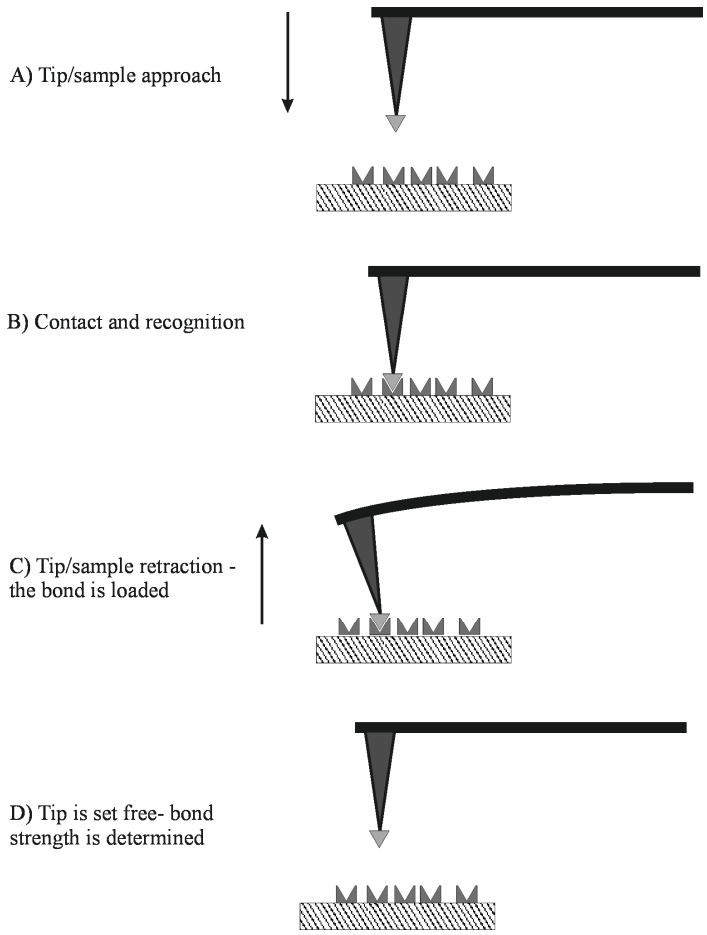

Figure 11. AFM as a tool to measure intermolecular forces between molecular complexes, such as complementary DNA strands, ligand/receptor couples, etc.

1.10 The strength of a biomolecular bond depends on the way we load it upon probing its strength.

So far we discussed the force measurements in biological systems as if each biological bond has a defined value, independent of the experimental conditions. In fact, the first studies (up to 1997) treated the subject in this way. Then in 1997 a theory was proposed by Evans [82], based on the previous work of Bell [83]. This theory placed the force measurements on a completely new, quantitative basis.

1.10.1 The natural lifetime of each bond is the fundamental property, which determines the behaviour of the bond upon loading.

The key idea in the proposed theory, which already is established as an indispensable tool in the interpretation of force measurements, is that each bond is characterized not by some inherent strength, but rather by a defined lifetime. This lifetime in the case of biological non-covalent bonds could be from a few milliseconds up to days or even longer. In a period longer than the lifetime of the bond, it has zero strength due to spontaneous dissociation of the complex. The natural lifetime of the bond is determined by the height and position of the energy barrier preventing the thermal dissociation of this bond. The applied force deforms the energy landscape of the interaction and lowers the energy barrier which prevents the spontaneous dissociation, thus decreasing the lifetime of the bond (Figure 12).

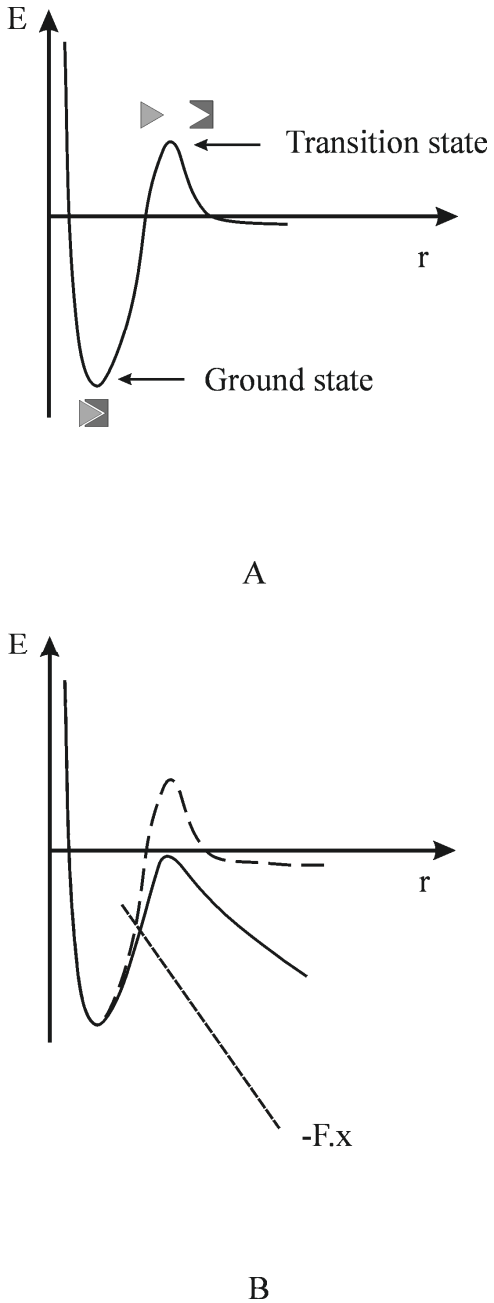

Figure 12. Energy landscape of a bond between biomolecules in the absence of an applied external force (A) and in the presence of external force, which deforms the landscape and lowers the energy barrier (B).

In the AFM force measurement we do not load the bond instantaneously, but the force increases gradually with time, as the tip retracts from the support. From the experimental point of view this means that if we load the investigated bond slowly enough, we will not detect any bond rupture due to the spontaneous dissociation of the bond during the experiment! However, at a certain loading rate the accumulated force within the lifetime of the bond will lower sufficiently the energy barrier and dissociation will be registered at a certain applied force. In this way a defined rupture strength, different from zero is registered. These considerations show that the measured strength of the bond depends on the rate, at which we load it.

Once realizing that no definitive value could be ascribed to the studied bond, but that its behaviour depends on its natural lifetime, determined by the energy barriers involved, it is easy to follow the theory in more detail. After the decrease in the energy for dissociation ΔE_0 by an applied external force F, postulated by Bell, the theory was further developed for the case of gradual loading, as in AFM experiments. Evans [84] derived a simple relation of the registered bond strength as a function of loading rate, predicting the dependency of the registered most probable force F* on the loading rate:

$F^* = (k_bT/ X_b)\ln (r/((k_bT/X_b).K_{off}))$

Here X_b is the distance between the ground state (the potential well, where the molecular complex resides) and the transition state (the position of the energy barrier), r is the loading rate, k_bT is the thermal energy and K_{off} is the natural off-rate of the complex (1/lifetime). An important assumption in this equation is that the energy barrier is sharp, which means that it does not change its position under influence of the applied external force. From this equation one sees that the registered force will increase linearly with the natural logarithm of the loading rate. Moreover, probing the strength of a biological complex over several orders of magnitude of loading rates will give us information about the energy landscape of the interaction. From the slope (k_bT/ X_b) and the x-intercept of each linear regime we can get information on the position X_b of each energy barrier along the dissociation pathway. The intercept with the x - axis gives the off - rate at zero applied force K_{off} through the dependency $r(F=0) = (k_bT/ X_b).K_{off}$.

The potential of the proposed theory was quickly appreciated and in almost all recent force measurement studies a force/loading rate dependency was investigated and the data were interpreted according to this theory. Some ligand/receptor and antigen/antibody couples were characterized and details in their energetic landscapes were described [85, 86]. Moreover, in some cases the natural off-rate, determined by the AFM force measurement is compared with the data, obtained by bulk techniques, giving additional information for the energy landscape of the studied couple [87]. The interpretation of the obtained parameters – distances bound/transition state and natural off-rates - in terms of the macroscopic functions, performed by the studied molecular complexes, is also attempted [88]. A number of important biomolecular couples (or molecular assemblies), which interactions are not characterized yet, promise the appearance of new interesting studies.

Scope of the thesis

In the present thesis AFM was used as an image and force measuring device on a variety of membrane mimicking systems. In **Chapter 2** the behaviour of the model WALP peptide, which resembles the transmembrane part of integral membrane proteins, and its ability to form a specific ordered domains in lipid bilayers of different compositions is studied. In **Chapter 3** we studied further the behaviour of WALP in lipid bilayers and investigated the

strength of integration of this transmembrane peptide, using the force measuring possibilities of the AFM. Data analysis according to the described theory gives insight in the factors, governing the stability of integration of transmembrane proteins. Another example for possibilities of the AFM as a manipulating tool is presented in **Chapter 4**, where Lipid II - an important biological molecule, is studied and size and orientation of its head group, when the molecule is incorporated in a bilayer, was obtained. The thesis finishes with a summary and perspectives in **Chapter 5**.

[1] Gennis, R.B., Biomembranes: Molecular structure and function Springer-Verlag, London, 1989

[2] Gorter, E. and Grendel, F. 1925. On bimolecular layers of lipoids on the chromocytes of the blood. J. Exp. Med. 41:439-443.

[3] Veerkamp JH. Lipids of the cell plasma membrane. Biomembranes. 1972; 3:159-79

[4] Niemela P, Hyvonen MT, Vattulainen I.Structure and dynamics of sphingomyelin bilayer: insight gained through systematic comparison to phosphatidylcholine. Biophys J. 2004; 87(5):2976-89.

[5] Tierney KJ, Block DE, Longo ML.Elasticity and phase behavior of DPPC membrane modulated by cholesterol, ergosterol, and ethanol. Biophys J. 2005; 89(4):2481-93.

[6] Simons K, Toomre D. Lipid rafts and signal transduction. Nat Rev Mol Cell Biol. 2000; 1(1):31-9.

[7] Lafont F, Simons K. Raft-partitioning of the ubiquitin ligases Cbl and Nedd4 upon IgE-triggered cell signaling. Proc Natl Acad Sci U S A. 2001; 98(6):3180-4.

[8] Rajendran L, Simons K. Lipid rafts and membrane dynamics. J Cell Sci. 2005;118(Pt 6):1099-102

[9] de Almeida RF, Loura LM, Fedorov A, Prieto M. Lipid rafts have different sizes depending on membrane composition: a time-resolved fluorescence resonance energy transfer study. J Mol Biol. 2005; 4;346(4):1109-20.

[10] Visualizing detergent resistant domains in model membranes with atomic force microscopy. FEBS Lett. 2001; 13;501(1):92-6.

[11] Rinia HA, Boots JW, Rijkers DT, Kik RA, Snel MM, Demel RA, Killian JA, van der Eerden JP, de Kruijff B. Domain formation in phosphatidylcholine bilayers containing transmembrane peptides: specific effects of flanking residues. Biochemistry. 2002; 41(8):2814-24.

[12] Killian JA, von Heijne G. How proteins adapt to a membrane-water interface. Trends Biochem Sci. 2000; 25(9):429-34

[13] de Kruijff B, Killian JA, Ganchev DN, Rinia HA, Sparr E. Striated domains: self-organizing ordered assemblies of transmembrane alpha-helical peptides and lipids in bilayers. Biol Chem. 2006 Mar;387(3):235-41

[14] Killian JA. Synthetic peptides as models for intrinsic membrane proteins. FEBS Lett. 2003; 555(1):134-8

[15] Rinia HA, Kik RA, Demel RA, Snel MM, Killian JA, van Der Eerden JP, de Kruijff B. Visualization of highly ordered striated domains induced by transmembrane peptides in supported phosphatidylcholine bilayers. Biochemistry. 2000; 39(19):5852-8.

[16] van Meer G, Sprong H.Membrane lipids and vesicular traffic. Curr Opin Cell Biol. 200; 16(4):373-8.

[17] Hessa T, Kim H, Bihlmaier K, Lundin C, Boekel J, Andersson H, Nilsson I, White SH, von Heijne G. Recognition of transmembrane helices by the endoplasmic reticulum translocon. Nature. 2005; 433(7024):377-81

[18] Matsuzaki K. Why and how are peptide-lipid interactions utilized for self-defense? Magainins and tachyplesins as archetypes. Biochim Biophys Acta. 1999;1462(1-2):1-10

[19] Killian JA, von Heijne G. How proteins adapt to a membrane-water interface. Trends Biochem Sci. 2000; 25(9):429-34

[20] Powers JP, Hancock RE. The relationship between peptide structure and antibacterial activity. Peptides. 2003; 24(11):1681-91

[21] Shai Y. Mechanism of the binding, insertion and destabilization of phospholipid bilayer membranes by alpha-helical antimicrobial and cell non-selective membrane-lytic peptides. Biochim Biophys Acta. 1999; 1462(1-2):55-70

[22] carpet-like membrane destabilization

[23] Hasper HE, de Kruijff B, Breukink E.Assembly and stability of nisin-lipid II pores. Biochemistry. 2004; 43(36):11567-75.

[24] Sahl HG, Bierbaum G. Lantibiotics: biosynthesis and biological activities of uniquely modified peptides from gram-positive bacteria. Annu Rev Microbiol. 1998; 52:41-79.

[25] Hsu ST, Breukink E, Tischenko E, Lutters MA, de Kruijff B, Kaptein R, Bonvin AM, van Nuland NA. The nisin-lipid II complex reveals a pyrophosphate cage that provides a blueprint for novel antibiotics. Nat Struct Mol Biol. 2004; 11(10):963-7.

[26] Marra J, Israelachvili J Direct measurements of forces between phosphatidylcholine and phosphatidylethanolamine bilayers in aqueous electrolyte solutions. Biochemistry. 1985; 24(17):4608-18

[27] Hughes T, Strongin B, Gao FP, Vijayvergiya V, Busath DD, Davis RC. AFM visualization of mobile influenza A M2 molecules in planar bilayers. Biophys J. 2004; 87(1):311-22.

[28] Rigby-Singleton SM, Davies MC, Harris H, O'Shea P, Allen S. Visualizing the solubilization of supported lipid bilayers by an amphiphilic peptide. Langmuir. 2006; 22(14):6273-9

[29] Zasadzinski JA, Viswanathan R, Madsen L, Garnaes J, Schwartz DK. Langmuir-Blodgett films. Science. 1994; 263(5154):1726-33

[30] Brian, A. A., and H. M. McConnell. 1984. Allogenic stimulation of cytotoxic T cells by supported planar membranes. Proc. Natl. Acad. Sci. USA. 81:6159–6163

[31] Pompeo G, Girasole M, Cricenti A, Cattaruzza F, Flamini A, Prosperi T, Generosi J, Castellano AC. AFM characterization of solid-supported lipid multilayers prepared by spin-coating. Biochim Biophys Acta. 2005; 1712(1):29-36.

[32] Reviakine, I., and A. Brisson. 2000. Formation of supported phospholipid bilayers from unilamellar vesicles investigated by atomic force microscopy. Langmuir. 16:1806–1815

[33] Rinia HA, de Kruijff B. Imaging domains in model membranes with atomic force microscopy. FEBS Lett. 2001; 504(3):194-9

[34] Guo W, Kurze V, Huber T, Afdhal NH, Beyer K, Hamilton JA. A solid-state NMR study of phospholipid-cholesterol interactions: sphingomyelin-cholesterol binary systems. Biophys J. 2002; 83(3):1465-78

[35] Haris PI, Chapman D. The conformational analysis of peptides using Fourier transform IR spectroscopy. Biopolymers. 1995; 37(4):251-63

[36] Frias MA, Diaz SB, Ale NM, Ben Altabef A, Disalvo EA. FTIR analysis of the interaction of arbutin with dimyristoyl phosphatidylcholine in anhydrous and hydrated states. Biochim Biophys Acta. Jul 20, 2006

[37] Rossi C, Homand J, Bauche C, Hamdi H, Ladant D, Chopineau J. Differential mechanisms for calcium-dependent protein/membrane association as evidenced from SPR-binding studies on supported biomimetic membranes. Biochemistry. 2003 Dec 30;42(51):

[38] Janshoff A, Steinem C. Label-free detection of protein-ligand interactions by the quartz crystal microbalance. Methods Mol Biol. 2005;305:47-64

[39] Binnig G, Quate CF, Gerber C. Atomic force microscope. Phys Rev Lett. 1986; 56(9):930-933.

[40] Dufrene YF, Lee GU. Advances in the characterization of supported lipid films with the atomic force microscope. Biochim Biophys Acta. 2000; 1509(1-2):14-41

[41] Muller DJ, Janovjak H, Lehto T, Kuerschner L, Anderson K. Observing structure, function and assembly of single proteins by AFM. Prog Biophys Mol Biol. 2002; 79(1-3):1-43.

[42] Hansma HG. Surface biology of DNA by atomic force microscopy. Annu Rev Phys Chem. 2001; 52:71-92

[43] You HX, Yu L. Atomic force microscopy imaging of living cells: progress, problems and prospects. Methods Cell Sci. 1999; 21(1):1-17

[44] Muller DJ, Heymann JB, Oesterhelt F, Moller C, Gaub H, Buldt G, Engel A. Atomic force microscopy of native purple membrane. Biochim Biophys Acta. 2000; 1460(1):27-38

[45] Giocondi MC, Le Grimellec C. Temperature dependence of the surface topography in dimyristoylphosphatidylcholine/distearoylphosphatidylcholine multibilayers. Biophys J. 2004; 86(4):2218-30.

[46] Taatjes DJ, Quinn AS, Lewis MR, Bovill EG. Quality assessment of atomic force microscopy probes by scanning electron microscopy: correlation of tip structure with rendered images. Microsc Res Tech. 199; 44(5):312-26.

[47] Schneider J, Dufrene YF, Barger WR Jr, Lee GU Atomic force microscope image contrast mechanisms on supported lipid bilayers. Biophys J. 2000; 79(2):1107-18

[48] Tang J, Jiang J, Song Y, Peng Z, Wu Z, Dong S, Wang E. Conformation change of horseradish peroxidase in lipid membrane.Chem Phys Lipids. 2002; 120(1-2):119-29

[49] Fotiadis D, Scheuring S, Muller SA, Engel A, Muller DJ.Imaging and manipulation of biological structures with the AFM. Micron. 2002; 33(4):385-97.

[50] Hui SW, Viswanathan R, Zasadzinski JA, Israelachvili JN. The structure and stability of phospholipid bilayers by atomic force microscopy. Biophys J. 1995; 68(1):171-8.

[51] Dufrene YF, Boland T, Schneider JW, Barger WR, Lee GU.Characterization of the physical properties of model biomembranes at the nanometer scale with the atomic force microscope. Faraday Discuss. 1998;(111):79-94

[52] Lateral mobility of lipid analogues and GPI-anchored proteins in supported bilayers determined by fluorescent bead tracking. J Membr Biol. 1993; 135(1):83-92.

[53] Giocondi MC, Pacheco L, Milhiet PE, Le Grimellec C. Temperature dependence of the topology of supported dimirystoyl-distearoyl phosphatidylcholine bilayers. Ultramicroscopy. 2001; 86(1-2):151-7

[54] Rinia HA, Snel MM, van der Eerden JP, de Kruijff B. Visualizing detergent resistant domains in model membranes with atomic force microscopy. FEBS Lett. 2001; 501(1):92-6.

[55] Muller DJ, Heymann JB, Oesterhelt F, Moller C, Gaub H, Buldt G, Engel A. Atomic force microscopy of native purple membrane. Biochim Biophys Acta. 2000; 1460(1):27-38

[56] Muller DJ, Baumeister W, Engel A. Conformational change of the hexagonally packed intermediate layer of Deinococcus radiodurans monitored by atomic force microscopy. J Bacteriol. 1996; 178(11):3025-30

[57] Muller DJ, Fotiadis D, Scheuring S, Muller SA, Engel A. Electrostatically balanced subnanometer imaging of biological specimens by atomic force microscope. Biophys J. 1999; 76(2):1101-11.

[58] de Kruijff B, Killian JA, Ganchev DN, Rinia HA, Sparr E. Striated domains: self-organizing ordered assemblies of transmembrane alpha-helical peptides and lipids in bilayers. Biol Chem. 2006; 387(3):235-41.

[59] Mou J, Czajkowsky DM, Shao Z. Gramicidin A aggregation in supported gel state phosphatidylcholine bilayers.Biochemistry. 1996; 35(10):3222-6

[60] Berquand A, Mingeot-Leclercq MP, Dufrene YF.Real-time imaging of drug-membrane interactions by atomic force microscopy. Biochim Biophys Acta. 2004; 1664(2):198-205

[61] van Kan EJ, Ganchev DN, Snel MM, Chupin V, van der Bent A, de Kruijff B.The peptide antibiotic clavanin A interacts strongly and specifically with lipid bilayers. Biochemistry. 2003; 42(38):11366-72.

[62] Mou J, Czajkowsky DM, Zhang Y, Shao Z. High-resolution atomic-force microscopy of DNA: the pitch of the double helix. FEBS Lett. 1995; 371(3):279-82

[63] Silva LP.Imaging proteins with atomic force microscopy: an overview. Curr Protein Pept Sci. 2005 Aug;6(4):387-95.

[64] Hansma HG, Bezanilla M, Zenhausern F, Adrian M, Sinsheimer RL. Atomic force microscopy of DNA in aqueous solutions. Nucleic Acids Res. 1993; 21(3):505-12.

[65] Green JD, Goldsbury C, Kistler J, Cooper GJ, Aebi U.Human amylin oligomer growth and fibril elongation define two distinct phases in amyloid formation. J Biol Chem. 2004; 279(13):12206-12

[66] Green JD, Kreplak L, Goldsbury C, Li Blatter X, Stolz M, Cooper GS, Seelig A, Kistler J, Aebi U. Atomic force microscopy reveals defects within mica supported lipid bilayers induced by the amyloidogenic human amylin peptide. J Mol Biol. 2004; 342(3):877-87.

[67] Tao NJ, Lindsay SM, Lees S. Measuring the microelastic properties of biological material. Biophys J. 1992; 63(4):1165-9.

[68] Kienberger F, Ebner A, Gruber HJ, Hinterdorfer P.Molecular recognition imaging and force spectroscopy of single biomolecules.Acc Chem Res. 2006; 39(1):29-36

[69] Schneider J, Dufrene YF, Barger WR Jr, Lee GU. Atomic force microscope image contrast mechanisms on supported lipid bilayers. Biophys J. 2000; 79(2):1107-18

[70] Cui Y, Bustamante C.Pulling a single chromatin fiber reveals the forces that maintain its higher-order structure. Proc Natl Acad Sci U S A. 2000; 97(1):127-32.

[71] Merkel R, Nassoy P, Leung A, Ritchie K, Evans E.Energy landscapes of receptor-ligand bonds explored with dynamic force spectroscopy. Nature. 1999; 397(6714):50-3.

[72] Oberhauser AF, Badilla-Fernandez C, Carrion-Vazquez M, Fernandez JM.The mechanical hierarchies of fibronectin observed with single-molecule AFM. J Mol Biol. 2002; 319(2):433-47

[73] Marszalek, P. E., Oberhauser, A. F., Pang, Y. P. & Fernandez, J. M. Polysaccharide elasticity governed by chair-boat transitions of the glucopyranose ring. Nature 1998; 396, 661-664

[74] Berquand A, Xia N, Castner DG, Clare BH, Abbott NL, Dupres V, Adriaensen Y, Dufrene YF. Antigen binding forces of single antilysozyme Fv fragments explored by atomic force microscopy. Langmuir. 2005; 21(12):5517-23

[75] Dammer U, Hegner M, Anselmetti D, Wagner P, Dreier M, Huber W, Guntherodt HJ. Specific antigen/antibody interactions measured by force microscopy. Biophys J. 1996; 70(5):2437-41

[76] Allen S, Davies J, Davies MC, Dawkes AC, Roberts CJ, Tendler SJ, Williams PM. The influence of epitope availability on atomic-force microscope studies of antigen-antibody interactions. Biochem J. 1999; 341

[77] Oesterhelt F, Oesterhelt D, Pfeiffer M, Engel A, Gaub HE, Muller DJ. Unfolding pathways of individual bacteriorhodopsins. Science. 2000; 288(5463):143-6

[78] Muller DJ, Kessler M, Oesterhelt F, Moller C, Oesterhelt D, Gaub H. Stability of bacteriorhodopsin alpha-helices and loops analyzed by single-molecule force spectroscopy. Biophys J. 2002; 83(6):3578-88

[79] Lee GU, Chrisey LA, Colton RJ. Direct measurement of the forces between complementary strands of DNA. Science. 1994; 266(5186):771-3.

[80] Schumakovitch I, Grange W, Strunz T, Bertoncini P, Guntherodt HJ, Hegner M. Temperature dependence of unbinding forces between complementary DNA strands. Biophys J. 2002; 82(1 Pt 1):517-21

[81] Merkel R, Nassoy P, Leung A, Ritchie K, Evans E. Energy landscapes of receptor-ligand bonds explored with dynamic force spectroscopy. Nature 1999; 397(6714):50-3.

[82] Evans E., Ritchie K., Dynamic strength of molecular adhesion bonds. Biophys J. 1997; 72(4):1541-55.

[83] Bell GI. Models for the specific adhesion of cells to cells. Science. 1978; 200(4342):618–627

[84] Evans E., Energy landscapes of biomolecular adhesion and receptor anchoring at interfaces explored with dynamic force spectroscopy. Faraday Discuss. 1998;(111):1-16.

[85] Strunz T, Oroszlan K,Schumakovitch I, Guntherodt H, Hegner M Model energy landscapes and the force-induced dissociation of ligand-receptor bonds. Biophys J. 2000; 79(3):1206-12

[86] Yuan C, Chen A, Kolb, P. and Moy, V.T. Energy Landscape of Streptavidin-Biotin Complexes Measured by Atomic Force Microscopy Biochemistry; 2000; 39(33) pp 10219 - 10223;

[87] Schwesinger, F., Ros, R., Struntz, T., Anselmetti, D., Güntherodt, H-J., Honegger, A., Jermutus, L., Tiefenauer, L. and Pluckthun, A. Unbinding forces of single antibody-antigen complexes correlate with their thermal dissociation rates, Proc. Natl. Acad. Sci. USA 2000; 97, 9972-9977

[88] Zhang X, Wojcikiewicz E, Moy VT. Force spectroscopy of the leukocyte function-associated antigen-1/intercellular adhesion molecule-1 interaction. Biophys J. 2002; 83(4):2270-9

Chapter 2. Striated domain-forming propensities of transmembrane WALP peptides in lipid bilayers of different packing state.

Abstract

In this study we investigated the behaviour of supported lipid bilayers, mimicking a biological membrane. We demonstrated the possibility of the AFM technique to provide wealth of information for molecular organization of the investigated bilayers, formed from single lipid species. More specifically, we studied the patterns of phase separation in mixed bilayers, coexisting in gel/liquid disordered state. Imaging of the bilayers, formed in presence of cholesterol reveals common features of these liquid ordered bilayers as well as some pronounced differences in their mechanical properties. We get further insight in the studied model membrane system by following the self-assembling patterns of WALP peptides, which mimic the transmembrane part of membrane proteins. While in gel state bilayers of DPPC and SM a formation of peptide enriched striated domains were observed, no domain formation was detected in liquid ordered or liquid disordered bilayers. Our experiments demonstrate that the underlying driving force for the formation of characteristic peptide-enriched striated domains is the high order in gel state lipid bilayers.

Biological membranes are highly complex molecular systems, with backbones that consist of a variety of lipid molecules, assembled in a bilayer. A growing number of studies provide evidence for the existence of membrane domains, enriched in certain lipids [summarised in 1]. For instance treatment with nonionic detergents at low temperatures results in isolation of cholesterol and sphingomyelin (SM) enriched lipid fractions. This suggests that SM-cholesterol rich domains exist within biomembranes [2]. Also membrane proteins can be non-uniformly distributed, sometimes in association with lipid domains of specific composition [3]. A special class of domains can be distinguished in which membrane proteins together with specific lipids organise in highly ordered structures. The outstanding example is the purple membrane that consists of a highly organised assembly of bacteriorhodopsin (BR) and specific lipids [4]. The underlying mechanism, leading to the formation of such highly organised domains is not clear, but most probably involves lipid/lipid, lipid/protein and protein/protein interactions.

The importance of these interactions for domain formation can be systematically investigated provided that appropriate model systems are available. Lipid bilayers of different composition are commonly used model systems that closely resemble the organization of biological membranes. In particular, supported bilayers have been successfully used to study domain formation by Atomic Force Microscopy – AFM [5]. This technique allows imaging of biological samples with nanometer resolution at physiological hydrated conditions at ambient temperatures and thereby it allows to directly visualise the presence of domains in bilayers.

It was established by AFM that certain transmembrane model peptides induce formation of highly characteristic domains in dipalmitoylphosphatidylcholine (DPPC) bilayers under gel state conditions [6, 7]. These domains are named striated domains because of the very regular line pattern that is present in the domain. The peptides that give rise to striated domains consist of a core of alternating alanine (A) and leucine (L) residues and span the membrane as an alpha-helix. They are called WALP peptides when this hydrophobic membrane-spanning motif is flanked on both sides by two tryptophan (W) residues. These residues preferentially reside in the interfacial region of the bilayer and thereby stably anchor the peptide in a transmembrane configuration [8]. WALP peptides have been extensively studied as models for the intrinsic part of membrane proteins [9]. The pattern of the observed striated domains induced by WALP peptides consists of line-type depressions and elevations, equally spaced with a repeat distance of approximately 8 nm. Most of the domains are interconnected by line-type depressions in the bilayer (see forthcoming figure 2A). Striated domains are formed by a wide variety of non-charged analogues of the WALP family [7]. However, analogues with positively charged anchoring residues like lysine do not give rise to such domains [7]. The molecular organization in the striated domains can be explained by a model, in which the tilted packing of the DPPC molecules in the gel state is disturbed by the presence of the peptides. This results in the formation of domains in which the line-type depressions are viewed as ordered linear aggregates of WALP peptides surrounded by lipid molecules in a fluid state, while the elevated lines, separating the line-type depressions, are formed by less tilted lipid molecules [10]. Despite considerable insight into the molecular architecture of the striated domains and the role of the peptide component very little is known about the lipid specificity of domain formation. Almost all studies were carried out in DPPC under gel state conditions. However, domain formation is not unique to that lipid because also in distearoylphosphatidylcholine very similar domains were observed below the chain melting temperature [6].

In this study we focus on the importance of the packing state of the lipid for striated domain formation. In biomembranes different packing states can be distinguished. The well known disordered (also called fluid or liquid-crystalline) state is believed to occur in almost every membrane and is believed to be essential for many membrane

processes. Also the gel state with highly ordered chains is known to occur in different membranes, such as for example those found in bacteria [11]. The liquid-ordered phase, formed by cholesterol and saturated lipids like sphingomyelin, is intermediate in terms of packing between the disordered and gel state and is believed to occur in the form of small domains in membranes that are rich in sterols and saturated lipids, such as the plasma membrane.

In the present study these different states are modeled with appropriate lipid mixtures in supported bilayers and AFM is used to inspect domain formation induced by WALP peptides. We focus on phosphocholine head group containing phospholipids because of their abundance in membranes of mammalian cells and their well-understood properties. Since different phases in lipid mixtures can be identified by AFM because of their height difference, the localisation of the peptide can also be studied, either by its ability to induce striated domains or by using thiol analogues of WALP in conjunction with decoration by nanometer sized gold particles.

We demonstrate that the formation of striated domains is not restricted only to PC, since we observed a similar phenomenon in SM bilayers, which is also in the gel state at room temperature. However, no traces of peptide aggregation could be found in bilayers in the liquid-ordered or liquid-disordered state, or in bilayers with coexisting gel and liquid-disordered state domains. All obtained results indicate that the driving force for domain formation is the high order of the lipids in the gel state.

2. Materials and methods

Lipids 1,2 Dipalmitoyl-*sn*-glycero-3-phosphocholine (DPPC), 1,2 Dioleoyl-*sn*-glycero-3-phosphocholine (DOPC) and Egg sphingomyelin, consisting of a mixture of SMs with exclusively saturated, mainly (84%) 16:0 chains were obtained from Avanti Polar Lipids (Alabaster, AL). The minor SM species include $C_{18:0}$ (6%), $C_{22:0}$ (4%) and $C_{24:0}$ (4%). Cholesterol was obtained from Merck (Darmstadt, Germany). All lipids were dissolved at 20 mM in a mixture of methanol/chloroform (1:3 v/v).

Peptide preparation WALP peptides were prepared by solid phase synthesis and purified and handled as described [12]. The peptides used in this study were CH_3-CO-GWWL$(AL)_8$WWA-NH_2 (WALP23) and SH_2.CH_2CO-GWWL$(AL)_8$WWA-NH_2 (SH-WALP23). Purity of the peptide was ≥ 95%. Peptide identity was confirmed by Electrospray Ionization Mass Spectrometry. The peptide was dissolved at 0.5 mM concentration in TFE.

Preparation of Gold Particles. A suspension of colloidal gold particles was prepared, using the method of Baiker [13].

AFM sample preparation AFM samples were prepared as described previously [14]. Briefly, lipids or lipid and peptide mixtures (2 mol% peptide) in organic solutions were mixed and dried in a rotary evaporator, followed by overnight storage under high vacuum. The dry mixed lipid or lipid:peptide films were hydrated with 20 mM NaCl solution, resulting in a lipid concentration of 1 mM. After freeze–thawing, the suspension was sonicated at 45°C. Possible remaining large vesicles were pelleted by centrifugation (20800×*g* for 1 h at 4°C) and the supernatant containing small unilamellar vesicles (SUV) was used within 5 days. The AFM results were not dependent on the time of storage within this time period. Supported lipid bilayers were prepared by depositing 75 microliters SUV suspension onto freshly cleaved mica. After 1 h at room temperature, the sample was rinsed with the NaCl solution and heated for 1 h at 65°C. After cooling down to room temperature, the sample was rinsed again and then imaged by AFM.

AFM imaging

The supported bilayers were covered by 20 mM NaCl solution during the measurements. The samples were mounted on an E-scanner, which was calibrated on a standard grid, of a Nanoscope III AFM (Digital Instruments, Santa Barbara, CA, USA). A fluid cell without O-ring was fitted and the sample was scanned in contact mode, using oxide sharpened Si_3N_4 tips attached to a triangular cantilever with a spring constant of 0.06 N/m (NanoProbe, DI, Santa Barbara, CA, USA). All images were recorded at temperatures between 23 and 26°C and at a minimal force (< 500 pN) to ensure stable scans and well-resolved images.

Decoration of bilayers with gold particles. After visualization of a bilayer with striated domains, the AFM head was removed and 10 µl gold particle suspension was added to the NaCl solution, covering the sample. After an incubation time of 10 minutes, the sample was gently rinsed (3 times, each time with 75 µl NaCl solution) in order to remove unbound gold particles. Then the AFM head was mounted again and the labeled sample was imaged.

Results

In this study we used AFM to investigate striated domain formation in peptide-lipid mixed bilayers under different lipid packing conditions, including systems that undergo phase separation. To provide a frame of reference first the behaviour of bilayers of the pure lipid components will be described.

AFM analysis of bilayers formed by a single lipid

Striated domains were observed under gel state conditions [6, 7]. We therefore first analysed different pure lipid systems under gel state conditions. Representative images recorded under fully hydrated conditions are presented in figure 1A and 1B. In this type of AFM images, the brighter areas correspond to higher areas in the bilayer, and the darker areas are lower. Visualization of supported DPPC bilayers (e.g. fig 1A) regularly results in images, which are typical for the appearance of bilayers that are not phase-separated and that have a constant height profile. The thickness of the layer can be measured through naturally occurring defects down to the mica (the dark spot on the left hand side of the image) and was found to be 5.5-6.0 nm in good agreement with earlier observations [6]. This value corresponds to the combined thickness of the bilayer and the thin (~ 0.8-1 nm [15]) layer of water between the bilayer and the mica support. In general, the surface of the DPPC bilayer appears to be rather homogeneous and smooth. However, at high magnification and using the sharpest AFM tips, some linear defects can be visualised as relatively straight, darker (and hence - lower than the surrounding bilayer) lines, intersecting at defined angles of ~ 120 degrees (Figure 1 A). These line-type defects correspond to cracks in the gel state bilayer [16].

Bilayers of SM at room temperature are also in a gel state [17] and show up in AFM as flat structures, but the surface of the bilayer is more inhomogeneous than the surface of a DPPC bilayer. At close inspection the bilayer surface was found to be undulated in an irregular labyrinth-like pattern (Figure 1 B). The height difference between the undulations was ~ 0.2-0.3 nm. The lower areas account to ~ 10 percent of the total bilayer area. The height of the SM bilayer down to the mica was measured to range from 5.3 to 5.6 nm. Note that in this particular figure several defects in the bilayer down to the mica are present.

These results show that despite the similar head group and packing state the morphology of DPPC and SM differ in several aspects.

Supported bilayers of DOPC at room temperature are in the liquid-crystalline or disordered state and therefore are softer and can be penetrated upon increasing the scanning force. Yet, when precautions are taken and the force on the tip is minimized during the experiment, these bilayers can be successfully imaged. Resulting images of DOPC bilayers revealed a homogeneous surface without any signs of phase separation or cracks (Figure 1 C). Small areas of uncovered mica are observed, which allows us to measure the bilayer thickness, which is 4.0-4.5 nm. This is considerably smaller than the thickness of the supported gel state bilayers of DPPC and SM, reflecting together with its much more uniform appearance, the more fluid and non-ordered nature of the DOPC bilayer.

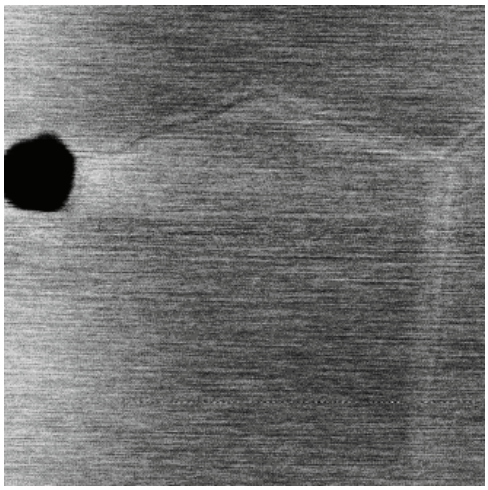

A

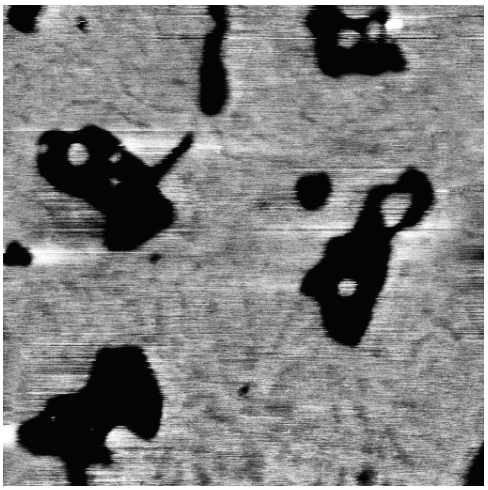

B

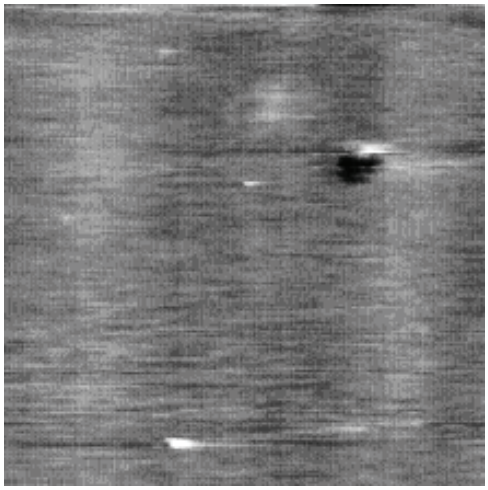

C

Figure 1. Images of bilayers, formed from pure lipids. Supported bilayer, formed from DPPC (A), spingomyelin (B) and DOPC (C). Image sizes are 1x1 micron and the z-scale is 3 microns.

Localisation of WALP in striated domains.

In order to study the localisation of the peptide molecules in these systems, we used a WALP analogue with a free SH-group at the N-terminus (SH-WALP), which then could be directly visualized by decoration of the supported bilayer with gold particles. To test whether the SH-WALP still had the ability to form striated domains, the SH-WALP peptide was incorporated into supported DPPC bilayers and inspected by AFM (Figure 2 A). The observed morphology is characteristic for WALP peptides [6,7, and forthcoming fig. 3A] and consists of smooth areas, in which line-type depressions are present. The depth of these line-type depressions is ~ 0.2-0.3 nm below the level of the bilayer surface. In addition striated domains are present. The domains consist of white (elevated) lines and dark (lower) lines, which are equally spaced and form domains with a characteristic striated pattern. The elevated lines in these domains are ~ 0.2 nm higher than the surrounding flat bilayer. After inspecting many images of both SH-WALP and the parent WALP peptide, we found that the main difference between these peptides is the higher curvature of the

lines forming the striated domains in the case of SH-WALP. The domains formed by SH-WALP also tend to be smaller, but more numerous than the domains induced by WALP. Such small variations in the pattern of the domains were also observed previously, when the length of WALP peptides or the nature of the flanking residues was varied. This demonstrates that the precise morphology of the domains depends, in a subtle manner, on the precise chemical nature of the peptide. The repeat distance of the line-type depressions in the domains is similar for both peptides (8 ± 0.5 nm for -WALP and 8.5 ± 1 nm for SH-WALP) and is comparable with the repeat distance previously measured for WALP peptides [7]. We therefore conclude that SH-WALP is a suitable model peptide to visualize the localization of the peptide with respect to the domains.

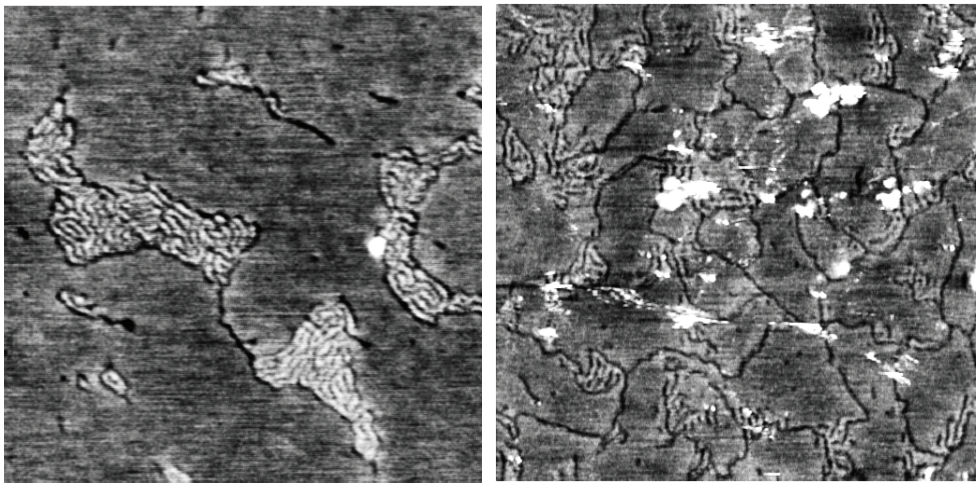

A B

Figure 2. Images of 2 mol% SH-WALP in a DPPC bilayer. A) Before Au-particle labelling. B) After labeling with Au particles. Image sizes are 0.5x0.5 microns and the z-scale is 3 microns.

Decoration of DPPC/SH-WALP bilayers with gold nanoparticles led to the AFM image shown in Fig.2B. The gold particles are visible as bright (higher) dots on the bilayer. We counted the number of gold particles at different positions on the supported bilayer. The total number of particles, which were counted on 9 different images, was 202. Of these particles 79 % were detected on the striated domains, 14% were present on the line-type depressions in the lipid bilayer, and 7% were detected on the flat bilayer, without an apparent connection to a domain or a line-type depression. This demonstrates that the WALP peptides are preferentially localised in striated domains and line-type depressions.

Next we wanted to find out whether domain formation is restricted only to DPPC bilayers, or whether it can be observed in bilayers formed from other lipids. To answer this question and to obtain insight into the driving force of domain formation, we studied the behaviour of WALP peptides in bilayers formed from single lipids and lipid mixtures.

WALP peptides induce striated domains in SM gel state bilayers, but not in DOPC liquid-crystalline bilayers. Incorporation of 2 mol % WALP peptide into gel state SM bilayers resulted in phase separation between domains containing line-type depressions and the rest of the bilayer. This resembles the formation of striated domains in the DPPC/WALP system but the morphology of the domains is notably different (compare fig 3B with figs 2A,

3A). As a whole, more single line-type depressions, not sequestered in striated domains were observed than in the case of DPPC. Furthermore, the line-type depressions within SM striated domains are more curved than those within the respective DPPC:WALP system (Compare the images in figure 3 A and B). The other important difference is the apparent lack of the elevated lines, observed in WALP-induced striated domains in DPPC. This results in the lack of a detectable height difference between the domain areas and the flat bilayer surface outside the striated domains. However, the depth of the line-type depressions appears to be 0.2-0.3 nm, the same value as in the DPPC:WALP system. The spacing of these line-type depressions within domains varies considerably, causing the pattern of the domains to look more disordered than the pattern of the striated domains, formed in DPPC bilayers. It should be noted that the observed undulation of the surface of the pure lipid SM bilayer could not be detected in the presence of the WALP peptides. The bilayer appears to be smooth outside the peptide-induced domains and line-type depressions.

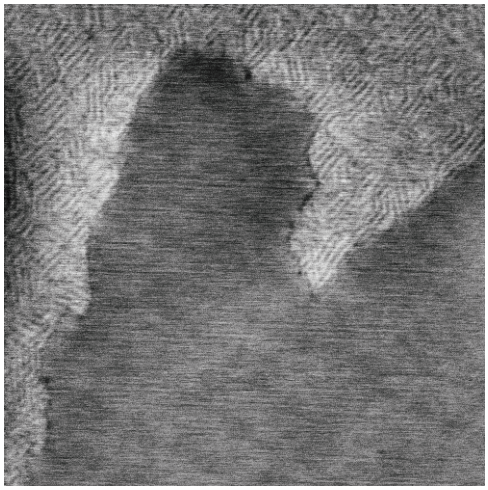

A

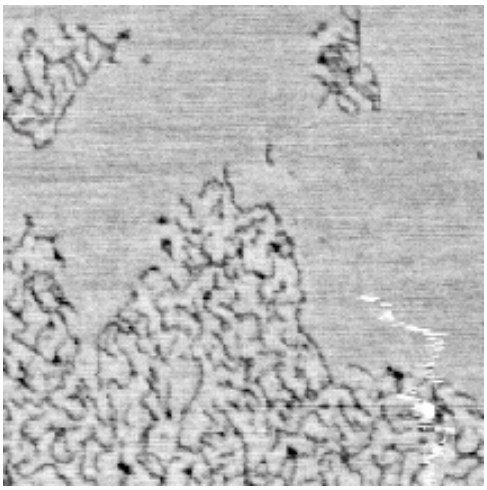

B

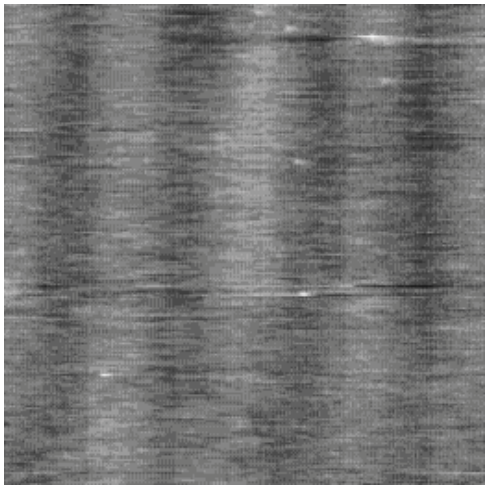

(C)

Figure 3. Images of supported bilayers formed from single lipid species in the presence of 2 mol % WALP peptide. DPPC bilayer (A), spingomyelin (B) and DOPC (C). Images are 1x1 microns and the z-scale is 3 microns.

With these experiments we demonstrated that the formation of peptide-enriched domains is not restricted to PC:WALP systems only, but that it is a more general phenomenon. The differences in appearance between peptide-containing SM and DPPC bilayers must originate from the differences in the properties of both lipid samples.

The incorporation of WALP peptides in supported bilayers from DOPC did not change the appearance of the bilayer. Even at close inspection of all images, no traces of peptide induced structures, such as domains or line-type depressions could be found (Figure 3 C). Apart from some holes down to the mica (not shown in this image), the only feature on the surface of the bilayer is a wave of periodic darker and lighter bands, superimposed over the flat bilayer surface. However, this is not a real feature of the bilayer, but a commonly encountered artifact in AFM imaging.

Effects of WALP incorporation on binary lipid mixtures which show gel-fluid phase separation.

We first designed systems that allowed us to follow partitioning of WALP peptides in coexisting lipid areas in different states. We selected lipid bilayers formed from DPPC:DOPC mixtures at different molar ratios in the absence of peptide. At a 1:1 molar ratio, circular domains with irregular boundaries are observed, 0.8-1.0 nanometer higher than the surrounding flat bilayer, and hence presumably representing gel phase DPPC domains (Figure 4 A). The surrounding bilayer of liquid-crystalline DOPC has a thickness of ~ 4.2-4.5 nm. At close inspection a level with a thickness, intermediate between those of higher domains and flat bilayer is observed (the arrow in figure 4 A). This intermediate level usually surrounds concentrically the highest domains and is ~ 0.5 nm higher than the flat bilayer, suggesting that at these positions the domains are not coupled and are present only in one of the lipid monolayers. Increasing the molar ratio of the gel-state forming lipid DPPC to 9:1 causes merging of the higher domains in a continuous bilayer, in which lower domains (denoted by arrow) with irregular shape are present. The thickness of the bilayer is 5.5-6.0 nm, and the domains are ~ 0.8 nm lower than the surrounding bilayer (Figure 4 B), suggesting that these domains represent lipids in the fluid phase. Only two different levels were observed, in contrast to the non-coupled areas in bilayers formed from the 1:1 DPPC:DOPC mixture. Thus, in these experiments we demonstrated that bilayers formed from DPPC and DOPC exhibit phase separation, and that we can control the type of formed domains – DOPC domains in a continuous DPPC bilayer or vice versa - by varying the ratio of the lipids.

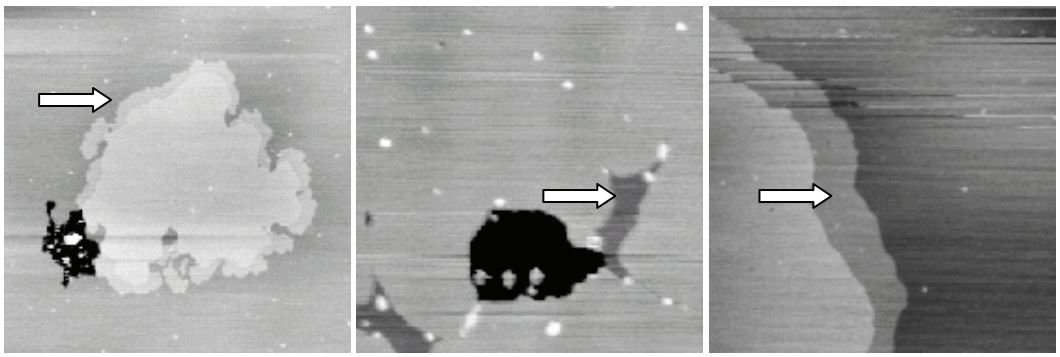

A B C

Figure 4. Images of mixed DOPC:DPPC lipid bilayers. A) Lipid bilayer, formed from a DOPC:DPPC mixture at a molar ratio 1:1, no peptide present. B) Lipid bilayer at a DOPC:DPPC 1:9 molar ratio, no peptide present. C) DOPC:DPPC 1:1, 2 mol % WALP peptide. The scan size in (A) and (B) is 3x3 microns, in (C) 1x1 – micron. The z-scale is 5 nm.

Incorporation of WALP peptides in these bilayers resulted in images, which visually could not be distinguished from the respective lipid mixtures in the absence of peptide [data not shown]. No traces of the peptide could be detected even at magnifications, where line-type depressions and domains, induced by WALP peptides in gel state bilayers are clearly resolved. This is obvious from the high magnification images of a boundary of an elevated phase-separated DPPC domain (Figure 4 C). No traces of the peptide can be detected on each of the three bilayer levels. This lack of detectable peptide aggregation in striated domains or line-type depressions was also observed at a 1:9 DOPC:DPPC molar ratio (data not shown). These results suggest that all peptide molecules are located in the liquid-crystalline DOPC areas.

Effects of WALP incorporation on binary lipid mixtures that form liquid-ordered domains.

Next, we investigated the morphology of pure and peptide-containing bilayers of the saturated lipids SM and DPPC with cholesterol. It is established that these bilayers have different packing conditions and exist in a so-called liquid-ordered state, which has properties intermediate between those of liquid-crystalline and gel states. In an SM:Cholesterol 1:1 mixture in the absence of peptide, no phase separation was observed, in contrast to the phase separation in DOPC:DPPC mixtures. In all imaged samples the formed bilayer contains large areas of bare mica, not covered with a bilayer (Figure 5 A). Sometimes even disconnected bilayer patches instead of a continuous bilayer were observed. Upon visualization of many of the samples, numerous spherical features with a diameter app. 60-80 nm (corresponding to the size of the SUV, used for bilayer formation) and a height between 20-50 nm were observed (For an overview image see Figure 5 B; the spherical structures are concentrated around the outer contour of the image). These features can be flattened upon scanning at a slightly increased imaging force (~ 0.5-1 nN). This flattening results in formation of circular bilayer patches, often not fused with the surrounding bilayer. No traces of phase separation were detectable and in all samples only a homogeneous bilayer was visualized, with a thickness of ~ 5.0 - 5.4 nm. These experiments indicate that there is some barrier against adsorption and proper spreading for SM:Cholesterol vesicles, processes which are required for formation of an intact supported bilayer.

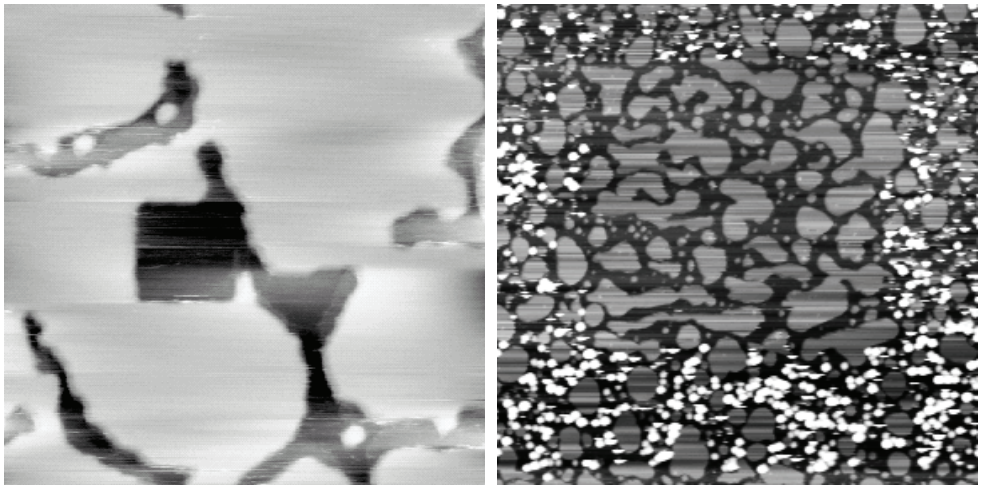

A B

Figure 5. Images of a mixed SM:cholesterol 1:1 bilayer in the absence of peptide. Image sizes are 1x1 microns (a) and 3x3 microns (b). The z-scales are 5 nm (A) and 50 microns (B).

Supported bilayers formed from the DPPC:Cholesterol 1:1 mixture resembled the behaviour of SM:Cholesterol bilayers in that they did not exhibit phase separation. Only flat bilayers (again with visible signs of an artificial ”wave” on the surface due to imaging artifacts) were routinely visualized (Figure 6). However, in contrast to SM:Cholesterol bilayers, the DPPC:Cholesterol bilayer covers almost completely the mica substrate. No spherical elevations, as in the case of SM:Cholesterol were observed. The thickness of the bilayer was found to be 6.5-7.0 nm. The differences in the behaviour of SM:Cholesterol and DPPC:Cholesterol bilayers demonstrate that AFM imaging can reveal variations in lipid:lipid interactions, which we can assume are responsible for the different behaviour of SM:Cholesterol and DPPC:Cholesterol bilayers.

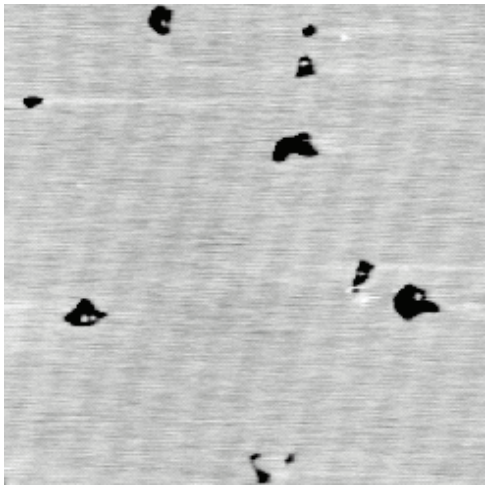

Figure 6. Image of DPPC:Cholesterol 1:1 bilayer in the absence of peptide. The image size is 3x3 microns, the z-scale is 5 nm.

Upon addition of peptide, the appearance of these bilayers remained very similar (Figure 7). The thicknesses of the bilayers are ~ 5.1-5.4 and 6.5-7.0 nm respectively. The WALP:SM:Cholesterol bilayers, similarly to SM:Cholesterol bilayers, include many defects down to the mica. In some bilayer preparations only bilayer patches were observed. Elevated spherical features, which could be flattened upon increasing the scanning force, were also present in this system. In both SM:Cholesterol and DPPC:Cholesterol bilayers no peptide aggregation could be visualized. Even at close inspection, the surface of the bilayers is perfectly homogeneous and no traces of line-type depressions or striated domains can be detected.

The results demonstrate that aggregation of the peptide in line-type depressions and striated domains can be observed only in gel state bilayers.

Discussion

In this chapter we studied by AFM the structural features and behaviour of bilayers, formed from pure lipids and lipid mixtures. We also obtained insight into the importance of acyl chain packing for striated domain formation. In the discussion we will propose the underlying forces that govern the localization and aggregation of WALP peptide molecules in a bilayer. We also will discuss the molecular mechanisms, leading to formation of different surface features, observed in our experiments.

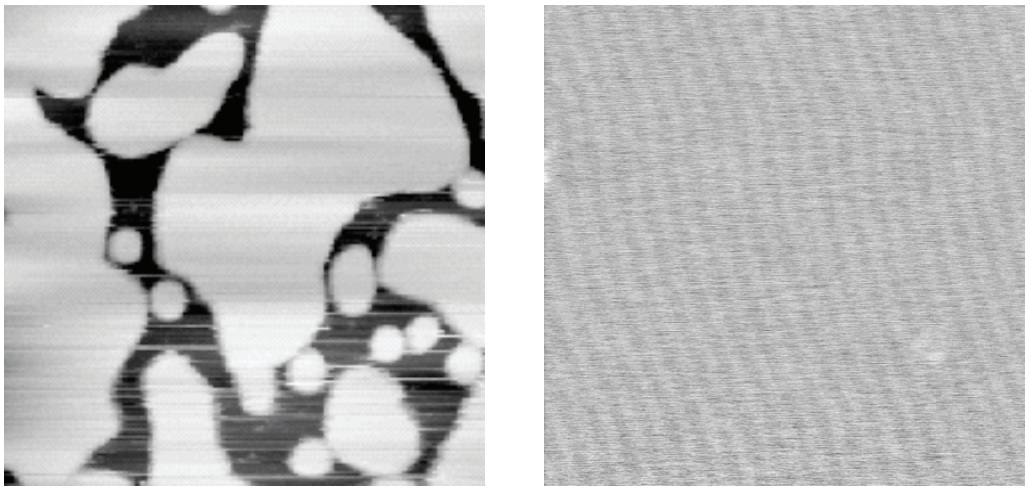

A B

Figure 7. Images of a SM:cholesterol 1:1(A) bilayer and a DPPC:cholesterol 1:1 bilayer (B) in the presence of 2 mol % WALP peptide. The image size is 1x1 micron, and the z-scale is 3nm In the AFM experiments with bilayers, formed from a single lipid species, we demonstrated that we could easily differentiate between liquid-crystalline and gel state bilayers. Whereas no structural features on the DOPC liquid-crystalline bilayer could be resolved, on both DPPC and SM bilayers we imaged specific surface features, which give us some indications for the molecular organization of these bilayers. First we will discuss the differences between the surface features of SM and DPPC bilayers. The straightness of the line-type defects in DPPC bilayer and the persistence of angle of intersection (~120^{o}) suggest that these defects reflect the hexagonal symmetry of the acyl chain packing in gel state DPPC bilayers [18]. Therefore we postulate that these defects occurred at boundaries where two crystallizing fronts in the bilayer meet each other. If the molecular tilt of the two meeting fronts is in different directions, this would prevent a proper "stitching" of the bilayer and thus a crack would occur.

However, no cracks were found in the SM gel state bilayers. Labyrinth-like undulations on the surface of the bilayer were observed instead. This suggests that some kind of phase separation take place in these bilayers. This could look surprising since one does not expect a phase separation in a bilayer formed from a single lipid. However, the SM used is in fact mixture of SMs with different chain lengths, including a species with longer 22:0 and 24:0 chains.

To explain the observed differences in the behaviour of the two gel state bilayers we first need to outline the main differences between SM and DPPC bilayers. Unfortunately little is known about the structure of SM bilayers at the atomic level [19]. However, few important differences which could explain the observed behaviour of SM bilayers are known. First, the SM molecule has almost identical cross sectional areas of the head-group and the hydrocarbon chain region, in contrast to the saturated PC lipids. This results in differences in the spontaneous curvature for both bilayers. For SM this curvature is close to zero, while the misbalance between the head-group and acyl chain areas for PC molecules leads to larger spontaneous curvature for PC bilayers [20]. This suggests that the SM molecules, in contrast to PC molecules, are not tilted in planar bilayers [21], since molecular tilt in PC bilayers is suggested to be a mechanism, which relives their higher spontaneous curvature.

The main molecular species in used SM has saturated 16:0 acyl chain [22]. We propose that upon crystallization the predominant saturated SM species form a gel-state bilayer, squeezing out SM molecules with longer chains due to mismatch of their hydrophobic lengths. These squeezed-out molecules form the observed labyrinth-like pattern in the

bilayer. It seems contradictory that the minor components with longer acyl chains form lower areas (judged by the percentage of higher and lower areas in the bilayer). A possible explanation could be found in several studies [23, 24], in which interdigitation in such bilayers due to a mismatch between longer acyl chain and sphingosine backbone was observed. Based on this observation we postulate that in pure SM bilayers the lower labyrinth-like pattern is formed by interdigitated SM molecule. A possible explanation for the lack of cracks in SM bilayers is that non-tilted SM molecules from different crystallization sites could "stitch" together in a bilayer without defects (cracks), or if defects are formed, their widths are below the resolution limit of AFM.

The addition of cholesterol to both gel-state bilayer forming lipids that were investigated, causes a major change in the bilayers morphology. The most obvious feature in both cholesterol containing bilayers is the lack of resolvable structural details on the surface of the bilayers. The straight intersecting cracks, observed in a pure DPPC bilayer, as well as the labyrinth-like pattern of higher and lower areas in a pure SM bilayer disappeared completely. We propose that this is due to the formation of bilayers in a liquid ordered state when cholesterol is added. This specific state is characterized by a higher fluidity than the gel state [25]. We demonstrated that the surface of the fluid DOPC bilayer lacks any structural features. Obviously, the more fluid nature of the formed liquid-ordered bilayers, similarly to the liquid-disordered ones, and the decreased packing order (which is the proposed driving force for the appearance of cracks and labyrinth-like pattern) causes the disappearance of any structural feature on the surface of the bilayers in liquid ordered state.

However, there is also a pronounced difference in the formation and behaviour of both bilayers. DPPC:Cholesterol mixtures readily form bilayers, which are defect-free on a micrometer scale. In contrast, in SM:Cholesterol mixtures the formation of a continuous bilayer was hindered and large areas of bare mica were observed. Moreover, we observed spherical features, which could be flattened upon increasing the scanning force. The monodispersity and the fact that the flattening of these features results in a formation of a bilayer patch on the same spot suggest that these features are intact vesicles – adsorbed, but unopened. A similar observation of unopened vesicles was reported previously [26]. This rather unusual behaviour of the SM bilayer (the presence of unopened vesicles and the presence of large uncovered areas of mica) suggests that there is some barrier upon adsorption and opening of the absorbed vesicles. Generally it is believed that these processes are governed by the balance between the favourable energy of adhesion of the vesicle and unfavourable energy of deformation of the adsorbed vesicle [27]. It is known that the cholesterol containing bilayers have significantly higher bending elasticity, which hinders the deformation of the vesicles [28]. This prevents their proper adsorption and spreading. This increased resistance against deformation of the vesicles also allows imaging of intact vesicles at minimized scanning force, a phenomenon, already observed in some recent studies on different lipid systems [29].

Incorporation of the WALP peptide in DPPC and SM bilayers also reveals some common features in both system, as well as certain differences. In both systems the peptide self-organizes in line-type depressions that segregate into domains at higher peptide concentration. However, the appearance of these domains differs in certain respects for both systems. We know that the line-type depressions, induced by WALP peptide in DPPC bilayer consist of a single line of peptides with alternate orientation [30]. When segregated in striated domains, these linear peptide aggregates are surrounded by lipid molecules in a more disordered state. These boundary lipids decrease the thickness of the bilayer, trying to match the hydrophobic thickness of the WALP peptide molecules, which is less than the hydrophobic thickness of a gel state DPPC bilayer [31].

The elevated lines in striated domains in DPPC:WALP system were supposed to be formed from lipid molecules, which lost their tilt. Why these elevated lines, separating line-type defects in DPPC bilayer are not detected in SM:WALP bilayers? The simplest explanation is provided by the assumption that the hydrocarbon chains in SM are not tilted. In this scenario the SM species (those with longer chains) that do not fit in the bilayer are squeezed together with the peptide molecules in the peptide rich domains. Under the influence of the linear peptide aggregates these longer SM species are fluidized and together with the peptide aggregates form the dark line-type depressions, observed by AFM. Since all SM molecules outside these peptide rich domains preserve their initial non-tilted conformation, no higher lines would appear.

Another difference between SM and PC bilayers is the loss of order in the peptide enriched domains in SM bilayers. Any attempt for rigorous explanation of this difference is hindered by the lack of detailed information for structure of SM bilayers. However, we could speculate that more disordered peptide enriched domains are due to lack of hexagonal packing in SM bilayers. This could be caused by the ability of SM molecules to form both intra- and inter-molecular hydrogen bonds, in contrast to the PC molecules [32], and the different hydration state of the lipid molecules in both bilayers [33].

Our hypothesis that the expulsion of the peptide from ordered gel state bilayers forms characteristic peptide enriched domains, resolvable by AFM explains the behaviour of DOPC:WALP, DPPC:Cholesterol:WALP and SM:Cholesterol:WALP bilayers. Indeed, in this liquid disordered and liquid ordered bilayers no driving force for peptide segregation is present. This suggests that the peptide is ideally intermixed in the surrounding bilayer, leading to disappearance of the line-type defects and striated domains and the inability of the AFM to detect the peptide in these bilayers.

The behaviour of phase-separated lipid mixtures reveals some characteristic features of the lipid bilayers in different states and gives us information about preferred localization of peptide in different bilayer areas. In our experiments we can identify (based on the thickness of the bilayer and on the experiments with varying DPPC:DOPC ratio) the higher circular domains in 1:1 DOPC to be DPPC gel state areas. They phase separate in surrounding lower DOPC liquid crystalline lipid bilayer. Interesting observation is the intermediate level between DOPC and DPPC areas. This is a clear indication that leaflets within bilayer are not always coupled. Whereas the obtained data do not allow us to determine unequivocally the reason for this behaviour, still we could propose a tentative hypothesis. It is known that the mica support could influence the distribution of molecules in a supported bilayer [34]. This suggests the possibility that the distribution of lipids in both leaflets is asymmetrical and that this is the underlying reason for the observed non-coupled bilayer areas. Obviously, the long range diffusion of lipid molecules within the continuous liquid crystalline DOPC bilayer is not hindered and DPPC molecules arrive to the crystallization site (higher gel-state domain) from all directions. This explains the concentric character of the intermediate level (non-coupled bilayer). Based on the obtained data, we could not determine the reason for the lack of non-coupled areas in case of 1:9 mixture, but we could speculate that this is connected with the hindered diffusion of molecular species in a gel-state DPPC bilayer, possibly coupled with the different mechanism of annealing of the continuous DPPC bilayer.

Addition of WALP peptide to either of the investigated DOPC:DPPC bilayers causes no detectable changes in the morphology of the mixed bilayers. We already established that whenever WALP peptide is incorporated in a gel state bilayer, it self-assembles in linear aggregates and striated domains. The absence of such features in gel state domains in mixed bilayers indicates that no peptide is present there. Having in mind the higher affinity of the WALP peptide

for lipids with a shorter (more fluid) acyl chains, we conclude that all peptide molecules are predominantly located in the liquid crystalline DOPC areas. This conclusion is supported by a recent study [35].

Finally, using gold nanoparticles, we demonstrated that modified SH-WALP peptide can be labeled when incorporated in a bilayer. This indicates that the SH group of SH-WALP is available for reaction with gold. This opens the possibility to measure the strength of incorporation of WALP peptides in a bilayer, using gold covered tip and implementing AFM as sensitive force sensor.

[1] Edidin M. The state of lipid rafts: from model membranes to cells. Annu Rev Biophys Biomol Struct. 2003;32:257-83.

[2] Brown DA, London E.Structure of detergent-resistant membrane domains: does phase separation occur in biological membranes? Biochem Biophys Res Commun. 1997; 240(1):1-7

[3] Lucero HA, Robbins PW.Lipid rafts-protein association and the regulation of protein activity. Arch Biochem Biophys. 2004; 426(2):208-24

[4] Muller DJ, Heymann JB, Oesterhelt F, Moller C, Gaub H, Buldt G, Engel A.Atomic force microscopy of native purple membrane. Biochim Biophys Acta. 2000; 1460(1):27-38.

[5] Rinia HA, de Kruijff B.Imaging domains in model membranes with atomic force microscopy. FEBS Lett. 2001; 504(3):194-9

[6] Rinia HA, Kik RA, Demel RA, Snel MM, Killian JA, van Der Eerden JP, de Kruijff B.Visualization of highly ordered striated domains induced by transmembrane peptides in supported phosphatidylcholine bilayers.Biochemistry. 2000; 39(19):5852-8.

[7] Rinia HA, Boots JW, Rijkers DT, Kik RA, Snel MM, Demel RA, Killian JA, van der Eerden JP, de Kruijff B.Domain formation in phosphatidylcholine bilayers containing transmembrane peptides: specific effects of flanking residues.Biochemistry. 2002; 41(8):2814-24

[8] Killian JA, von Heijne G. How proteins adapt to a membrane-water interface. Trends Biochem Sci. 2000 Sep;25(9):429-34

[9] de Kruijff B, Killian JA, Ganchev DN, Rinia HA, Sparr E. Striated domains: self-organizing ordered assemblies of transmembrane alpha-helical peptides and lipids in bilayers. Biol Chem. 2006; 387(3):235-41.

[10] Sparr E, Ganchev DN, Snel MM, Ridder AN, Kroon-Batenburg LM, Chupin V, Rijkers DT, Killian JA, de Kruijff B.Molecular organization in striated domains induced by transmembrane alpha-helical peptides in dipalmitoyl phosphatidylcholine bilayers.Biochemistry. 2005; 44(1):2-10

[11] Stoeckenius W, Bogomolni RA.Bacteriorhodopsin and related pigments of halobacteria. Annu Rev Biochem. 1982; 51:587-616

[12] Ganchev DN, Rijkers DT, Snel MM, Killian JA, de Kruijff B.Strength of integration of transmembrane alpha-helical peptides in lipid bilayers as determined by atomic force spectroscopy. Biochemistry. 2000; 43(47):14987-93

[13] Jan-Dierk Grunwaldt, Christoph Kiener, Clemens Wögerbauer and Alfons Baiker Preparation of Supported Gold Catalysts for Low-Temperature CO Oxidation via “Size-Controlled” Gold Colloids *1999,*Journal of Catalysis*, 181 (2), 223-232*

[14] Rinia HA, Demel RA, van der Eerden JP, de Kruijff B. Blistering of langmuir-blodgett bilayers containing anionic phospholipids as observed by atomic force microscopy. Biophys J. 1999; 77(3):1683-93.

[15] 15. Tamm, L. K., and Shao, Z. (1998) in *Biomembrane Structures*, (Harris, P. I., and Chapman, D., Eds.) pp 169-185, IOS Press, Amsterdam.

[16] Grandbois M, Clausen-Schaumann H, Gaub H. Atomic force microscope imaging of phospholipid bilayer degradation by phospholipase A2. Biophys J. 1998; 74(5):2398-404.

[17] Nyholm T, Nylund M, Soderholm A, Slotte JP.Properties of palmitoyl phosphatidylcholine, sphingomyelin, and dihydrosphingomyelin bilayer membranes as reported by different fluorescent reporter molecules Biophys J. 2003; 84(2 Pt 1):987-97

[18] Cevc, G., Marsh, D. 1987 Phospholipid Bilayers. Wiley, New York

[19] Neuringer LJ, Sears B, Jungalwala FB, Shriver EK Difference in orientational order in phospholipid and sphingomyelin bilayers. FEBS Lett. 1979;104(1):173-5

[20] Bystrom T, Lindblom G. Molecular packing in sphingomyelin bilayers and sphingomyelin/phospholid mixtures. Spectrochim Acta A Mol Biomol Spectrosc. 2003; 59(9):2191-5

[21] McIntosh TJ. Differences in hydrocarbon chain tilt between hydrated phosphatidylethanolamine and phosphatidylcholine bilayers. A molecular packing model. Biophys J. 1980; 29(2):237-45.

[22] Product Data Sheet, Avanti Polar Lipids.

[23] Ramstedt B, Slotte JP. Membrane properties of sphingomyelins.FEBS Lett. 2002; 531(1):33-7

[24] Niemela PS, Hyvonen MT, Vattulainen I. Influence of chain length and unsaturation on sphingomyelin bilayers. Biophys J. 2006; 90(3):851-63

[25] Kahya N, Scherfeld D, Bacia K, Poolman B, Schwille P.Probing lipid mobility of raft-exhibiting model membranes by fluorescence correlation spectroscopy. J Biol Chem. 2003; 278(30):28109-15

[26] Liang X, Mao G, Simon Ng KY. Probing small unilamellar EggPC vesicles on mica surface by atomic force microscopy. Colloids Surf B Biointerfaces. 2001; 34(1):41-51.

[27] Leonenko ZV, Carnini A, Cramb DT.Supported planar bilayer formation by vesicle fusion: the interaction of phospholipid vesicles with surfaces and the effect of gramicidin on bilayer properties using atomic force microscopy. Biochim Biophys Acta. 2000; 1509(1-2):131-47

[28] Song J, Waugh RE.Bending rigidity of SOPC membranes containing cholesterol. Biophys J. 1993; 64(6):1967-70

[29] Richter RP, Brisson AR. Following the formation of supported lipid bilayers on mica: a study combining AFM, QCM-D, and ellipsometry. Biophys J. 2005; 88(5):3422-33.

[30] Sparr E, Ganchev DN, Snel MM, Ridder AN, Kroon-Batenburg LM, Chupin V, Rijkers DT, Killian JA, de Kruijff B.Molecular organization in striated domains induced by transmembrane alpha-helical peptides in dipalmitoyl phosphatidylcholine bilayers. Biochemistry. 2005; 44(1):2-10

[31] Morein S, Koeppe II RE, Lindblom G, de Kruijff B, Killian JA.The effect of peptide/lipid hydrophobic mismatch on the phase behavior of model membranes mimicking the lipid composition in Escherichia coli membranes. Biophys J. 2000; 78(5):2475-85.

[32] Talbott CM, Vorobyov I, Borchman D, Taylor KG, DuPre DB, Yappert MC.Conformational studies of sphingolipids by NMR spectroscopy. II. Sphingomyelin. Biochim Biophys Acta. 2000; 1467(2):326-37.

[33] Jendrasiak GL, Smith RL.The effect of the choline head group on phospholipid hydration. Chem Phys Lipids. 2001; 113(1-2):55-66

[34] Kasbauer M, Junglas M, Bayerl TM.Effect of cationic lipids in the formation of asymmetries in supported bilayers. Biophys J. 1999; 76(5):2600-5

[35] McIntosh TJ. The 2004 Biophysical Society-Avanti Award in Lipids address: roles of bilayer structure and elastic properties in peptide localization in membranes Chem Phys Lipids. 2004; 130(2):83-98

Chapter 3. The strength of integration of transmembrane α-helical peptides in lipid bilayers as determined by Atomic Force Spectroscopy

Abstract

In this study we address the stability of integration of proteins in membranes. Using Dynamic Atomic Force Spectroscopy we measured the strength of incorporation of peptides in lipid bilayers. The peptides model the transmembrane parts of -helical proteins and were studied in both ordered peptide-rich and unordered peptide-poor bilayers. Using gold-coated AFM-tips and thiolated peptides we were able to observe force events which are related to the removal of single peptide molecules out of the bilayer. The data demonstrate that the peptides are very stably integrated into the bilayer and that single barriers within the investigated region of loading rates resist their removal. The distance between the ground state and the barrier for peptide removal was found to be 0.75 ± 0.15 nm in different systems. This distance falls within the thickness of the interfacial layer of the bilayer. We conclude that the bilayer interface region plays an important role in stably anchoring transmembrane proteins into membranes.

One out of three cellular proteins is a membrane protein because its sequence contains one or more stretches of hydrophobic amino acids that span the membrane as an α-helix. This motive allows for energetically favorable hydrogen bonding of the peptide backbone within the hydrophobic interior of the membrane. The hydrophobic helix in combination with flanking aromatic amino acids such as tryptophan ensures stable integration of intrinsic proteins into the lipid bilayer [1,2]. The bilayer is a complex and dynamic structure consisting of a hydrocarbon layer that is separated from the aqueous medium by a broad, water-rich interfacial region consisting of the head groups, the glycerols and esterbonds [1].

Estimates on the membrane affinity of the hydrophobic helix are available [1]. But precisely how stable are proteins integrated into membranes and what is the determinating factor for their stable integration? These are unanswered and fundamental questions in membrane biology that we address in this study.

To get insight into these questions a range of techniques such as optical tweezers [3] and biomembrane force probes [4] are available. Among these Atomic Force Microscopy (AFM) is unique because it can combine spatial information with force measurements. Ideally one would like to measure the strength of integration of a membrane protein in its natural surroundings. This has been done for bacteriorhodopsin and has resulted in insight into the unfolding pathway of this protein [5]. However, interpretation of such studies in terms of contributions of specific parts of the protein and its relation to its surrounding is hampered by the complexity of such systems. Therefore, in this study we analyzed the strength of integration of transmembrane peptides consisting of a single α-helix that spans the bilayer. Such peptides can be designed to model the transmembrane parts of proteins and are commonly used in membrane research [6].

The peptides used here are well characterized [6-8] and consist of a simple stretch of hydrophobic amino acids (alanine-leucine) of defined length, flanked on either side by two tryptophans. These peptides incorporate as transmembrane α-helices into bilayers. We functionalized these peptides on their N-terminus with a thio-group and incorporated them into supported bilayers of phosphatidylcholine, an abundant natural membrane lipid. We studied peptides dispersed in fluid bilayers as well as peptides organized in highly organized peptide-rich domains [8]. In these domains the peptides interact with each other and the surrounding lipids, thus mimicking multi-span membrane proteins. We probed the strength of integration of the peptides into the bilayers by pulling at them with a gold-covered AFM tip and we observed distinct events corresponding to the removal of single peptides from the bilayer.

The results provide for the first time information on the strength of integration of α-helical peptides incorporated into lipid bilayers and lead to the conclusion that the bilayer interface region plays an important role in stable integration of transmembrane α-helices in membranes.

Experimental Procedures

Materials

1,2 Dipalmitoyl-*sn*-glycero-3-phosphocholine (DPPC) and 1,2 dioleoyl-*sn*-glycero-3-phosphocholine (DOPC) were obtained from Avanti Polar Lipids (Alabaster, AL).

Peptides were prepared by solid phase synthesis and purified and handled as described [8] with some modifications as will be described elsewhere to introduce an N-terminal free SH-group. The peptides used in this study were [SH-CH_2-CO]GWWL(AL)$_8$WWA-NH_2 (SH-WALP23), [CH_3-CO]GWWL(AL)$_8$WWA-NH_2 (Ac-WALP23) and CWWL(AL)$_{10}$WWA-NH_2 (Cys-WALP27). Purity of the peptides was ≥ 95%. Their identity was confirmed by Electrospray Ionization Mass Spectrometry.

Preparation of supported bilayers

Peptide-containing supported bilayers on mica were prepared via the vesicle fusion method as described in [8]. Small unilamellar vesicles (SUV) were prepared by hydrating a mixed peptide/lipid film of desired composition with a 20 mM NaCl solution (1 mM lipid), containing 0.05 mM dithiothoreitol (DTT), followed by ten freeze-thaw cycles and sonication in a bath sonicator at maximum power for 30 min. at 45 °C, followed by a 1h, 20.800 g spin at 4 °C. 75 μl of the SUV-containing supernatant was deposited onto freshly cleaved mica, followed by a 1h incubation at room temperature to allow absorption of the vesicles. Subsequently, the sample was rinsed 3 times with 75 μl of the NaCl/DTT solution, heated for 1h at 65 °C, cooled down to room temperature and washed again 3 times with the solution. The resulting supported bilayer was covered with the solution during the AFM measurements.

AFM imaging

The samples were mounted on an E-scanner, which was calibrated on a standard grid of a nanoscope III AFM (Digital Instrument, Santa Barbara, California). A fluid cell without O-ring was fitted and the sample was scanned in contact mode, using either oxide sharpened Si_3N_4 tips attached to a triangular cantilever with a spring constant of 0.06 N/m (Nano Probe Digital Instruments) or with gold-covered tips mounted on a rectangular cantilever with a spring constant of 0.027 or 0.006 N/m (Olympus Bio-Lever BL-RC 150 VB). Images were recorded at a minimal force (100 - 200 pN) where the scans were stable and at temperatures between 23 - 28 °C.

AFM force measurements

After visualization of the image with a tip speed of 10 μm/s the gold-coated tips were positioned on the spot of interest whereafter force-distance curves were recorded in the retraction cycle. By varying the vertical velocity of the scanner and by using gold-coated cantilevers of different spring constants, different loading rates were applied. These tips were calibrated using the Hutter method [9] yielding values of the spring constant of 0.025 and 0.007 N/m which was close to the values quoted for these tips of respectively 0.027 and 0.006 N/m. The maximum force exerted by the tip (with a measured spring constant of 0.025 N/m) on the bilayer was lower than 1 nN and in the case of the softer cantilever this force was below 400 pN. Data sets were obtained with different tips but in each case at least two loading rates were investigated per tip.

From the statistical distribution of the unbinding events (at least hundred measured per condition) the most probable unbinding force was plotted versus the natural logarithm of the loading rate. In this analysis only force-distance curves were included in which the nominal loading rate as determined from the slope of the curve prior to the rupture [10] was within 20% of the loading rate applied.

Because of the inherent uncertainty in determining the cantilever spring constant (~20%) the points obtained with different AFM tips were normalized on a single curve and the slope of this curve was determined. Then the X-intercept was determined from the best of the experimental points.

Results

Ordered peptide-rich domains as system for force spectroscopy

Transmembrane peptides with aromatic flanking residues and a core of alternating leucines and alanines spontaneously form highly ordered domains with lipids when incorporated in gel state dipalmitoyl

phosphatidylcholine (DPPC) bilayers and inspected by AFM [8]. This is also the case for the peptides analyzed in this study. Fig. 1A shows as an example an AFM image of the SH-WALP peptide incorporated at 2 mol% in DPPC and scanned with a conventional AFM tip. The image shows the smooth surface corresponding to gel state DPPC and domains that consist of regularly spaced dark lines (repeat distance 8 ± 0.5 nm) separated by lighter areas. The domains are typically connected by cracks (dark lines). Scanning the system with a gold-coated tip yielded similar images (Figure 2). The image visualizes a supported bilayer in which line-type depressions and striated domains are present. The black hole at the bottom of the image is a defect in the bilayer (hole down to the mica), through which we could confirm the presence of the intact supported bilayer with a thickness of ~ 6 nm. The resolving power of the Au-covered tip is less than that of the Si_3N_4 tip most likely because it is more blunt.

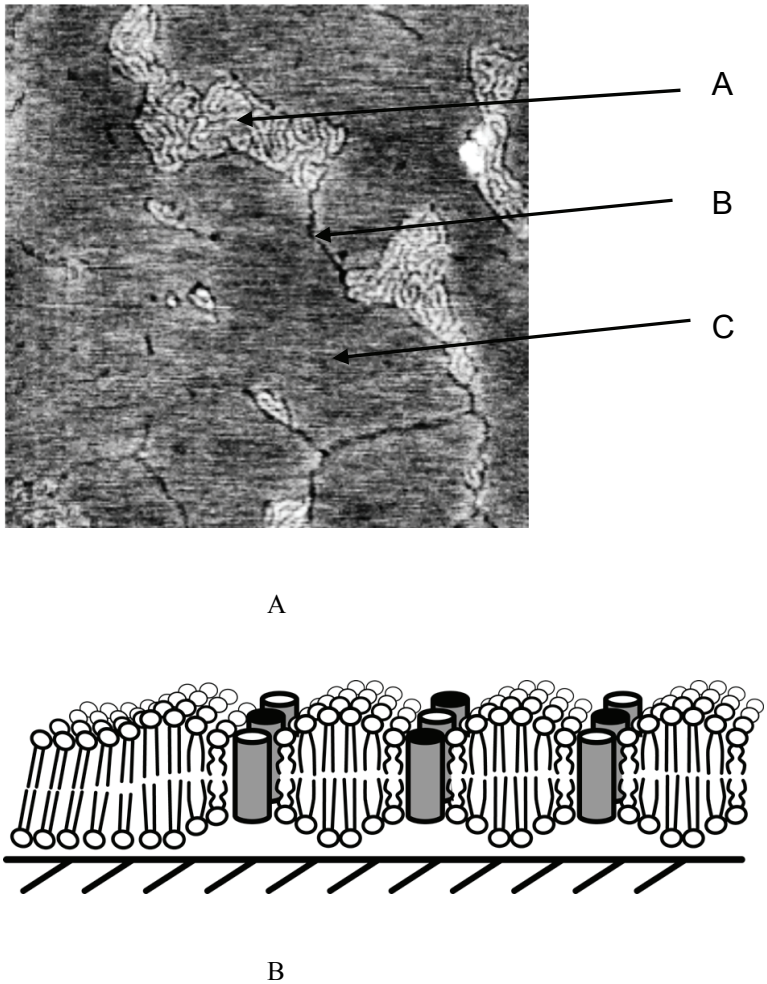

Figure 1 (A) An AFM image of striated domains in 2 mol% SH-WALP23 containing DPPC bilayers, showing striated domains (arrow A), cracks (arrow B) and the flat bilayer surface (arrow C). Image size 500 x 500 nm, Z-scale is 3 nm. (B) A schematic illustration of the molecular organization of striated domains. See text for further details.

The molecular organization of these so-called striated domains based on [8] is illustrated in fig. 1B. The domains consist of regularly spaced linear assemblies of anti-parallel transmembrane peptides. In these assemblies the peptides interact with each other and with the surrounding lipids which are disordered because of the peptide-lipid interaction. The lipids inbetween the rows of peptides have lost the tilt that the acyl chains of DPPC have outside the domains.

The organization of the domains and its lipid-protein ratio of 8 is independent of the protein concentration. The striated domains of the thiopeptide can be specifically decorated with 8 nm sized gold particles (not shown) demonstrating that the SH-group is accessible to a gold surface approaching the bilayer.

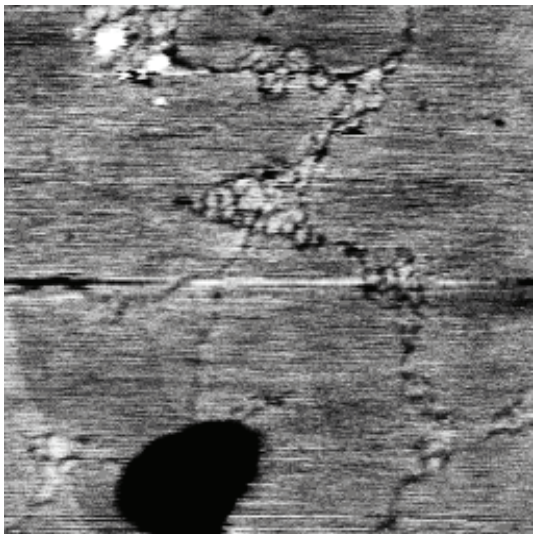

Figure 2. An AFM image of striated domains in 2 mol% SH-WALP23 containing DPPC bilayers, visualized with an Au-covered tip.

We consider the striated domains to be a very useful system for peptide pulling experiments because the localization of the peptide is known and its surroundings mimic the situation encountered for α-helices in complex multi-span proteins where also both peptide-peptide and peptide-lipid contacts occur.

Peptide-pulling in striated domains

When the gold-covered AFM tip is positioned onto the striated domains of a 2 mol% SH-WALP23 containing bilayer, upon pulling in more than 75% of the cases one or more negative peaks preceding the horizontal line in the force-distance (f-d) curves are observed, demonstrating tip-sample interactions [11]. In about 70% of the cases one peak is observed such as shown for curves 2a-c in fig. 3. In 25% of the cases two peaks are observed (curve 3) and in rare cases (~ 5% incidence) three or more peaks are observed (curve 4).

When the gold-covered AFM tip is positioned onto the bilayer but outside the striated domains and retracted, force-distance (f-d) curves as shown in fig. 3 (curve 1) are observed. These curves, which were observed in more than 99% of the cases, are typical for a tip that does not interact with the sample.

The tip-sample interactions observed are specific because (i) when the tip is placed over domains formed by the thiofree control peptide Ac-WALP23 in less than 5% of the cases an interaction is observed and (ii) when a conventional (non gold-coated) tip is placed over the domains in less than 1% of the cases an interaction is observed.

A histogram of the distribution of registered force for SH-WALP23 over striated domains is shown in fig. 4. For the SH-WALP23 a pronounced peak around 100 pN is observed in the force distribution whereas for the control the much less numerous force events did not show a pronounced peak. The data strongly indicate that upon pulling with the gold-coated tips we extract thiopeptides from the bilayer. It is very unlikely that we measure the breaking of the gold-thio bond because under these conditions this bond has a much higher rupture strength of 1.4 nN [12].

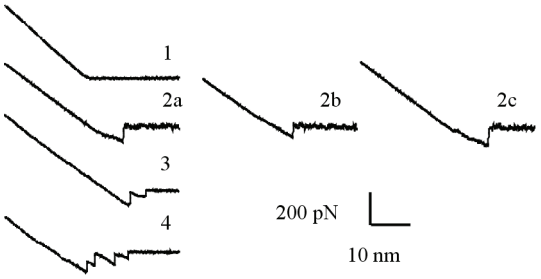

Figure 3. Representative retraction force-distance curves recorded on different areas of a 2 mol% SH-WALP23 containing DPPC bilayer using a gold-covered AFM tip. Curve 1 is representive for the peptide-free DPPC domains whereas curves 2 - 4 are obtained on the striated domains.

How can we derive quantitative information from the pulling experiments? Breaking non-covalent bonds between biomolecules depends on the rate at which the external force is applied [13,14]. In the AFM pulling experiment we load the system at a certain rate. This loading rate r (in pN/s) is the speed by which the cantilever moves away from the sample multiplied by the spring constant of the cantilever. In this case [13] the most probable force measured F depends on r according to:

$$F = (kT/X_b)\ln(r/(kT/X_b).K_{off})$$

in which X_b is the distance between the ground and transition state, kT is the thermal energy and K_{off} is the natural off-rate of the complex.

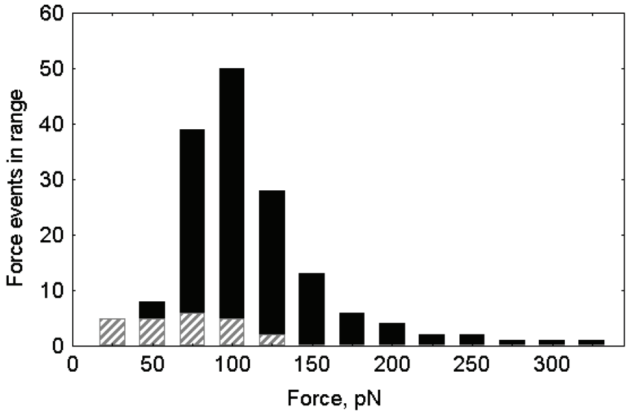

Figure 4. Distribution of force events registered with a gold-covered AFM tip over striated domains present in 2 mol% SH-WALP23 (solid bars) or AC-WALP23 (striped bars) containing DPPC bilayers. A loading rate of 45 nN/s was used. In f-d curves with more than one peak only the last peak was evaluated because it reflects the strength of the last bond between the tip and the sample.

By analyzing the relation between the force events measured and the loading rate we obtain information on the occurrence of the energy barriers and the thermal off-rates at these barriers.

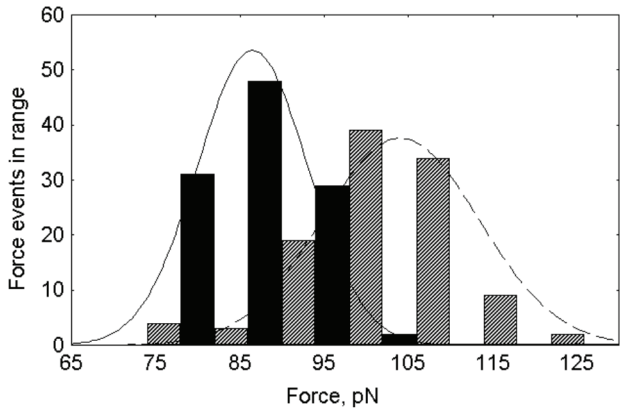

Figure 5. Distribution of force events registered on striated domains present in 2 mol% SH-WALP containing DPPC bilayers at loading rates of 4.8 nN/s (solid bars) and 45 nN/s (striped bars). The curves are Gaussian fits of the data.

We probed the strength of the registered interaction of the gold-coated tips with SH-WALP23 domains at loading rates ranging from 0.1 to 45 nN/s. As examples histograms for the measured force distribution at two different loading rates are shown in fig.5. The Gaussian fit of the data points yield values of 78 ± 6 and 96 ± 9 pN for loading rates of 4.8 and 45 nN/sec respectively and demonstrate that the unbinding force increases with an increase in loading rate as expected from theory. The average unbinding forces plotted as a function of the logarithm of the loading rate yield a straight line which indicates a single barrier for peptide extraction (fig. 6). From the slope the position of this barrier relative to the ground state can be calculated to be X_b = 0.75 ± 0.15 nm. From the X-intercept a K_{off} of 10^{-4} - 10^{-5} s^{-1}can be estimated. Pulling experiments on striated domains of 2 mol% containing Cys-WALP27 which has a 4 amino acid longer membrane spanning domain gave qualitatively similar results (data not shown). Interestingly, for this peptide a lower value of X_b = 0.5 ± 0.1 nm and a K_{off} of 10^{-4} s^{-1} were measured.

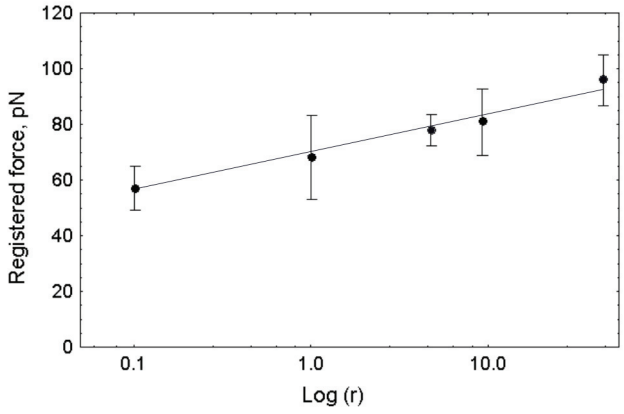

Figure 6. Loading rate dependency of the mean force events registered over striated domains present in 2 mol% SH-WALP23 containing DPPC bilayers. Each point is the value and its standard deviation obtained from the Gaussian fit of the distribution of force events recorded.

These data demonstrate that quantitative information on the strength of integration of a peptide in the ordered peptide-rich domains can be determined by Atomic Force Spectroscopy.

Peptide pulling in fluid bilayers

Many proteins span the membrane with single hydrophobic α-helices that are embedded in and interact with the fluid bilayer.

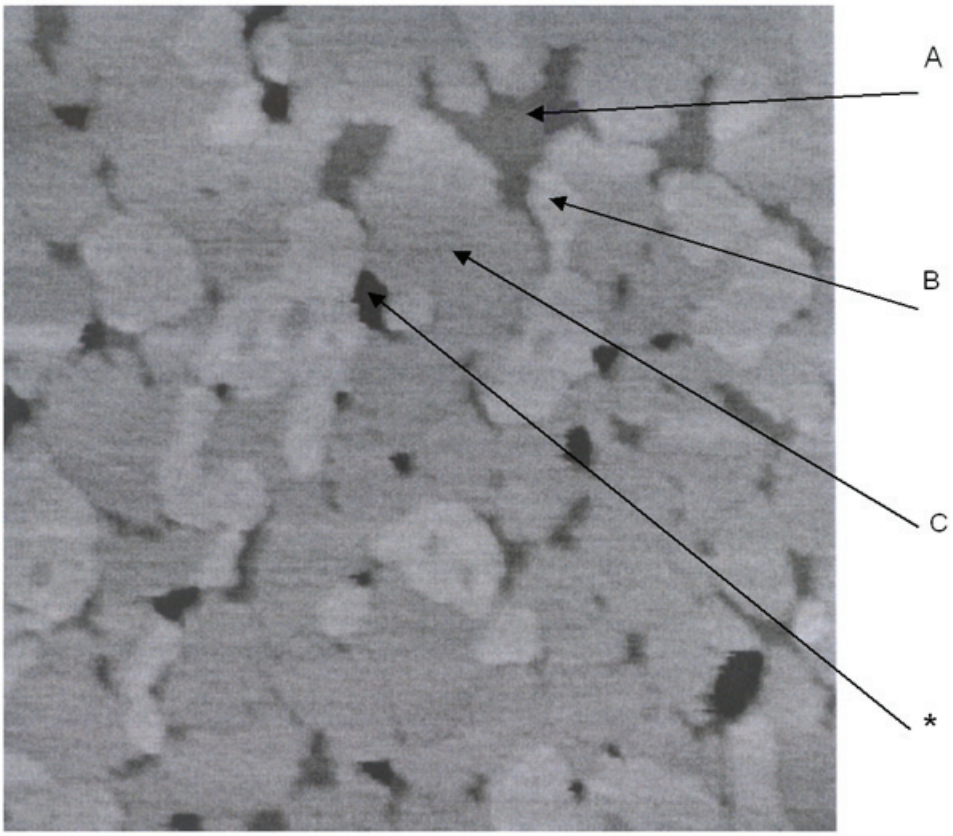

Fig. 7B

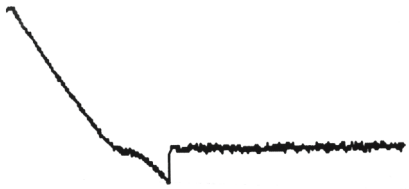

Figure 7. Peptide extraction from fluid DOPC domains. (A) An AFM image (size 500 x 500 nm, Z-scale 15 nm) of a supported bilayer of 0.5 mol% SH-WALP23 in DOPC/DPPC (1:9) showing bilayer domains of DOPC (arrow A), DPPC (arrow B) or domains with a monolayer of DOPC and DPPC (arrow C). The asterix indicates a defect in the bilayer down to the mica. (B). A typical force event recorded during retraction of the gold-covered tip from a DOPC bilayer domain. In rare cases multiple events such as shown in curves 3 - 4 of figure 3 were observed. (C). Loading rate dependency of the mean force events registered on DOPC bilayer domains. Each point is the value and its standard deviation of the Gaussian fit of the distribution of force events recovered. The data were obtained with a single AFM tip.

To model such a situation we can incorporate SH-WALP23 in DOPC that forms fluid bilayers at room temperature. In this system the peptide is homogenously distributed as individual transmembrane α-helices [6].

To confine the peptide in an area that can be localized by AFM, we created fluid bilayer domains of DOPC within supported bilayers of gel state DPPC. An AFM image of such a system is shown in fig. 7A. The dark (low) areas (see arrow A) correspond to DOPC bilayer domains that are surrounded by either areas of DPPC bilayers (arrow B) that are 1 nm higher (lighter) due to acyl chain ordering or by areas of bilayers with intermediate darkness that consist of a monolayer of DOPC and a monolayer of DPPC (arrow C).

In such systems the SH-WALP23 peptide is expected to be localized in the fluid DOPC [15]. Indeed, when the gold-covered AFM tip is positioned on such a DOPC domain upon pulling force-distance curves typical of an interaction between the tip and the sample are observed (fig. 7B). Analysis of force-distance curves of this system at different loading rates (fig. 7C) revealed a value of X_b of 0.7 nm and a value for K_{off} of 6 x 10^{-4}. These values are strikingly similar to these observed for the peptide in the very different striated domains and suggest that removal of a transmembrane helix from a membrane occurs through a common mechanism.

Discussion

In our pulling experiments on transmembrane α-helical peptides in different bilayers we observed specific force events. We first discuss the nature of these events. It is unlikely that they relate to lifting of the bilayer or creating a lipid tether [16] because in these cases the retract part of the force-distance curves after the last peak would not coincide with the approach part of the curve, as we observed. Furthermore, the striated domains with their high content of peptide and embedding into gel state DPPC bilayers are expected to strongly resist lifting or bending of the supported bilayer. Finally, the very similar behavior observed for the ordered and disordered bilayer systems also strongly argue against these possibilities. We therefore conclude that the events we observe in the pulling experiments reflect the removal of the peptide out of the bilayer. Given the large number of cases in which single events were observed, we most often register the removal of single peptides that are attached to the tip. That this is true even for the peptide-rich striated domains can be understood from the alternating out-in organization in which two SH-group-containing N-termini are separated by approximately 2 nm (see fig. 1B). In cases of rare multiple force events most likely two or more peptides are simultaneously attached to the tip and removed from the bilayer upon retraction. In theory, it is possible that the C-termini of the peptides are interacting with the mica and that we measure the detachment of the peptide from the mica. We exclude this possibility because the C-terminus of the peptide is uncharged, thereby excluding favorable electrostatic interactions. Moreover, it is known that these peptides are localized with their tryptophans in the ester carbonyl region of the phospholipids [17]. Since in case of SH-WALP there is only a single alanine present C-terminal to these tryptophans the C-terminus will reside within the phospholipid head group region which is separated by about 1 nm of water from the mica. Finally, for bacteriorhodopsin (BR) present in a supported purple membrane it was found that the forces associated with the removal of helices out of the membrane were similar for membranes absorbed onto mica, graphite or onto another purple membrane [18]. This demonstrates that even the more extended loops in BR connecting the transmembrane helices are not stably interacting with the mica. Therefore, we conclude that the removal of the peptide out of the bilayer is not influenced by the peptide-mica interaction.

It is of interest to compare the most probable unbinding forces of the different WALP-containing systems at loading rates used in literature on related systems.

For this comparison we selected a loading rate of 45 mN/s. By intra- and extrapolation of our data we obtain comparable most probable unbinding forces of 90 pN for extraction of both WALP23 and WALP27 out of striated domains, demonstrating that increasing the length of the helix does not significantly affect the force it takes to remove it out of the bilayer. It takes similar values of 100 - 200 pN to extract the helices of BR out of the membrane [5,18]. Given the large differences between these systems (multi-span versus single span, different composition of helices and lipid environment) this suggests that removal of a helix out of a membrane occurs through a common mechanism, not very dependent of the chemistry of the system. For the DOPC domains it takes slightly less force (60 pN) to remove the WALP23 out of the bilayer which can be understood from the more fluid character of these domains. For comparison, to remove a di-C18:0 lipid out of stearoyl/oleoyl phosphatidylcholine bilayer requires only 20 - 40 pN [4], demonstrating that transmembrane helices are much more stably integrated in a bilayer than a diacyl membrane lipid.

From the analysis of the loading rate depending of the force to extract a peptide from the bilayer we could estimate the thermal off rate of spontaneous detachment of the peptide from the bilayer. For striated domains K_{off} values of 10^{-4} - 10^{-5} s^{-1} were observed which corresponds with lifetimes of the peptide in the bilayer in the order of hours or days. For DOPC domains a slightly larger value of K_{off} was estimated. These values are several orders of magnitude lower than that reported for di-C16:0 lipids [4] and are only an order of magnitude higher than the value reported for the extremely stable biotin-avidine complex [10]. This again demonstrates that the strength of integration of a transmembrane peptide is very high and belongs to the most stable non-covalent biological interactions reported so far [10,19-20].

We detected single barriers for removal of the α-helices out of the bilayer. For the WALP23 peptide which has a hydrophobic length that closely matches the hydrophobic thickness of the bilayer, this barrier was determined to be localized 0.75 ± 0.15 nm from the ground state in the striated domain. Surprisingly, a very similar value was observed for the peptide present in the DOPC domains. These systems differ very much in architecture. In one case the peptide resides in a highly ordered peptide-rich bilayer in which the peptide interacts with both neighboring peptides as well as with lipids. In the other case the system is fluid and the peptide interacts only with the surrounding lipids. This suggests that the value of 0.75 nm must correspond to a specific and fundamental property of the bilayer. What could this be? One obvious possibility is that it relates to the anchoring function of the tryptophans. The tryptophans are positioned near the boundary between the hydrocarbon and interfacial region of the bilayer and anchor the hydrophobic helix at that position. Although the tryptophans will resist to be pulled into the hydrocarbon layer or into the interfacial region [17], this resistance is expected to be relatively weak, because tryptophans flanking a hydrophobic α-helix can readily move across a bilayer [21] and their polarity gives them a possibility to move into the interface. Therefore, the barrier must be a property related to moving the hydrophobic α-helix out of the hydrophobic core of the bilayer into the water-rich interfacial region. This interfacial region is a broad and dynamical zone that harbors all polar atoms of the membrane lipids. In the WALP23 system there is no significant hydrophobic mismatch between the length of the peptide and the thickness of the hydrophobic region of the surrounding fluidized lipid molecules, both being ~ 3 nm. This implies that pulling on the peptide molecule out of the bilayer gradually will expose growing part of the hydrophobic helix will be expressed to the water-rich interfacial region. The barrier appears on a distance of 0.75 nm from the equilibrium position, which corresponds to exposure of 4-5 residues (a

complete turn of the helix) to the aqueous environment. Hydrogen bonding of the peptide backbone to water will destabilize the helix, leading to unfolding and complete withdrawal from the bilayer. This model for the removal of the peptide from the bilayer is visualized in figure 8 and is further described in its legend.

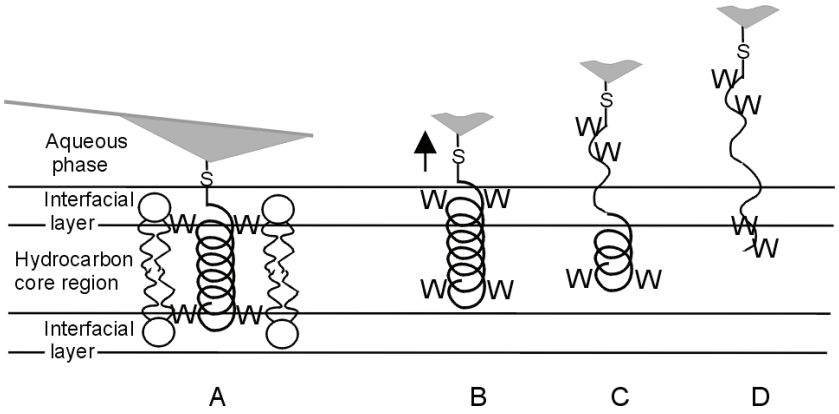

Figure 8. Schematic representation of the model describing the mechanical removal of an α-helical transmembrane peptide (WALP23) out of the bilayer. The domains of the peptide-lipid interface and hydrocarbon core region are approximately to scale. The gold-coated AFM tip that is chemically attached to the SH-group of the peptide is not to scale. The tryptophans (W) are indicated. The peptide in the ground state is anchored in the bilayer by the tryptophans on both the cis-side and the trans-side, and buries its hydrophobic helix into the hydrocarbon layer (A). When sufficient force is applied to the peptide such that it is displaced ~ 0.75 nm from its ground state, it exposes part of the hydrophobic helix to the interface (B). Because of the water present in the interface the helix will be destabilized and become unfolded upon pulling. At the same time, the displacement of the helix from its ground state results in negative mismatch at the side facing the support, which will make incorporation of the remainder of the peptide in the bilayer less favorable (C). No further major energy barriers are expected upon further pulling and the peptide is removed from the bilayer (D).

The model nicely explains our observation that the energy barrier resisting extraction of the longer WALP27 is only 0.5 nm away from the equilibrium position. The larger peptide has a positive hydrophobic mismatch and sticks already a part of its hydrophobic α-helix in the interface [22]. The barrier for removal is therefore more readily approached.

The disordered lipids surrounding the peptide are expected to fill the gap in the bilayer caused by removal of the peptide. However, the possibility that some boundary lipids cover the hydrophobic helix upon its extraction, thus protecting it from the aqueous environment, cannot be completely excluded. Yet, this is not very probable, since the removal of the helices of BR out of the purple membrane was proposed to follow a similar helix-unfolding pathway [5] with similar forces needed to extract all helices. In the tightly packed purple membrane there is very small amount of lipids around the BR molecules and covering all extracted helices with a lipid material seems highly improbable.

In conclusion, we have demonstrated that the hydrophobic α-helix of membrane proteins is very stably anchored within the lipid bilayer in a way that is remarkably insensitive to the precise chemical surroundings. It is the bilayer interface that is the barrier resisting mechanical removal of the peptide from the bilayer. This implies that the bilayer interfacial region plays an important role in stable anchoring of proteins in membranes.

Acknowledgments

The inspiring discussions with prof. E. Evans, University of British Columbia, are greatly appreciated. The authors are grateful to Kees van der Werf, Twente University, The Nederlands for the assistance with the tip calibrations.

References

1. White S.H. (2003) Translocons, thermodynamics, and the folding of membrane proteins, FEBS Letters 555, 116-121.

2. Killian, J.A. and Von Heijne, G. (2000) How proteins adapt to a membrane-water interface, TIBS 25, 429-434.

3. Kellermayer, M.S.Z., Smith, S.B., Granzier, H.L. and Bustamante, C. (1997) Folding-unfolding transitions in single titin molecules characterized with laser tweezers, Science 276, 1112-1116.

4. Evans, E. and Ludwig, F. (2000) Dynamic strengths of molecular anchoring and material cohesion in fluid biomembranes J. Phys.: Condens. Matter 12, A315-A320.

5. Oesterhelt, F., Oesterhelt, D., Pfeiffer, M., Engel, A., Gaub, H.E. and Müller, D.J. (2000) Unfolding pathways of individual bacteriorhodopsins, Science 288, 143-146.

6. De Planque, M.R.R. and Killian, J.A. (2003) Protein-lipid interactions studied with designed transmembrane peptides: role of hydrophobic matching and interfacial anchoring (Review), Mol. Membr. Biol. 20, 271-284.

7. De Planque, M.R.R., Goormaghtigh, E., Greathouse, D.V., Koeppe, R.E., Kruijtzer, J.A.W., Liskamp, R.M.J., De Kruijff, B. and Killian, J.A. (2001) Sensitivity of single membrane-spanning α-helical peptides to hydrophobic mismatch with a lipid bilayer: effects on backbone structure, orientation, and extent of membrane incorporation, Biochemistry 40, 5000-5010.

8. Rinia, H.A., Kik, R.A., Demel, R.A., Snel, M.M.E., Killian, J.A., van der Eerden, J.P.J.M. and De Kruijff, B (2000) Visualization of highly ordered striated domains induced by transmembrane peptides in supported phosphatidylcholine bilayers, Biochemistry 39, 5852-5858.

9. Hutter, J.L. and Bechhoefer, J. (1993) Calibration of atomic-force microscope tips, Rev. Sci. Instrum. 64, 1868-1873.

10. Dettmann, W., Grandbois, M., Andre, S., Benoit, M., Wehle, A.K., Kaltner, H., Gabius, H-J. and Gaub, H.E. (2000) Differences in zero-force and force-driven kinetics of ligand dissociation from beta-galactoside-specific proteins (plant and animal lectins, immunoglobulin G) monitored by plasmon resonance and dynamic single molecule force microscopy. Arch. Biochem. Biophys. 2, 157-170.

11. Hoh, J.H., Cleveland, J.P., Prater, C.B., Revel, J.-P. and Hansma, P.K. (1992) Quantitized adhesion detected with the atomic force microscope. J. Am. Chem. Soc. 114, 4917-4918.

12. Grandbois, M., Beyer, M., Rief, M., Clausen-Schaumann, H. and Gaub, H. (1999) How strong is a covalent bond? Science 283, 1727-1730.

13. Evans E. (1998) Energy landscapes of biomolecular adhesion and receptor anchoring at interfaces explored with dynamic force spectroscopy, Faraday discuss. 111, 1-16.

14. Evans E. and Ritchie, K. (1997) Dynamic strength of molecular adhesion bonds Biophys. J. 72, 1541-1555.

15. Van Duyl, B., Rijkers, D.T.S., De Kruijff, B.and Killian J.A. (2002) Influence of hydrophobic mismatch and palmitoylation on the partitioning of transmembrane □-helical peptides into detergent resistant domains, FEBS Letters 523, 79-84.

16. Maeda, N., Senden, T.J. and Di Meglio, J.-M. (2002) Micromanipulation of phospholipid bilayers by atomic force microscopy.Biochem. Biophys. Acta 1564, 165-172.

17. De Planque, M.R.R., Bonev, B.B., Demmers, J.A.A., Greathouse, D.V., Koeppe II., R.E., Separovic, F., Watts, A. and Killian, J.A. (2003) Interfacial anchor properties of tryptophan residues in transmembrane peptides can dominate over hydrophobic mismatch effects in peptide-lipid interactions.Biochemistry 42, 5341-5348.

18. Müller, D.J., Kessler, M., Oesterhelt, F., Möller, C., Oesterhelt, D. and Gaub, H. (2002) Stability of bacteriorhodopsin alpha-helices and loops analyzed by single-molecule force spectroscopy, Biophys. J. 83, 3578-3588.

19. Schwesinger, F., Ros, R., Struntz, T., Anselmetti, D., Güntherodt, H-J., Honegger, A., Jermutus, L., Tiefenauer, L. and Pluckthun, A. (2000) Unbinding forces of single antibody-antigen complexes correlate with their thermal dissociation rates, Proc. Natl. Acad. Sci. USA 97, 9972-9977.

20. Merkel, R. (2001) Force spectroscopy on single passive biomolecules and single biomolecular bonds, Physics Reports 346, 343-385.

21. Ridder, A.N.J.A., Morein, S., Stam, J.G., Kuhn, A., De Kruijff, B. and Killian, J.A. (2000) Analysis of the role of interfacial tryptophan residues in controlling the topology of membrane proteins. Biochemistry 39, 6521-6528.

22. Demmers, J.A.A., Van Duijn, E., Haverkamp, J., Greathouse, D.V., Koeppe II, R.E., Heck, A.J.R. and Killian, J.A. (2001) Interfacial positioning and stability of transmembrane peptides in lipid bilayers as studied by hydrogen/deuterium exchange and mass spectrometry. J. Biol. Chem. 276, 34501-34508.

Appendix: Strength of integration of a model transmembrane peptide in a lipid bilayer as measured by the Biomembrane Force Probe technique.

Abstract

In this study we used the Biomembrane Force Probe (BFP) technique as a complementary method to analyze the strength of integration of the transmembrane model peptide WLP in a bilayer. The results obtained are similar to those obtained via AFM in supported bilayers of a related system. This suggests that the forces measured are independent of the technique used and reflect an intrinsic and fundamental property of lipid-protein interactions.

Introduction

Currently, several single molecule techniques for measuring intermolecular forces in biological systems are used. These are Atomic Force Microscopy (AFM), the technique of choice throughout this thesis, the use of laser tweezers and the Biomembrane Force Probe technique (BFP). In the ideal case a system, studied by one technique, such as AFM, should be cross-examined with either one of those complementary techniques to exclude the possibility that the measured forces are influenced by the used technique. From these two techniques, BFP is superior in measuring forces in the order of ~ 0.1 nN, which is the expected range for the strength of the peptide integration in a bilayer [1] . Moreover, this technique is technically less complicated than laser tweezers. Therefore, in this appendix we used BFP as a complimentary technique to verify our data on the stability of integration of transmembrane peptide within a lipid bilayer, obtained by Atomic Force Microscopy (chapter 3).

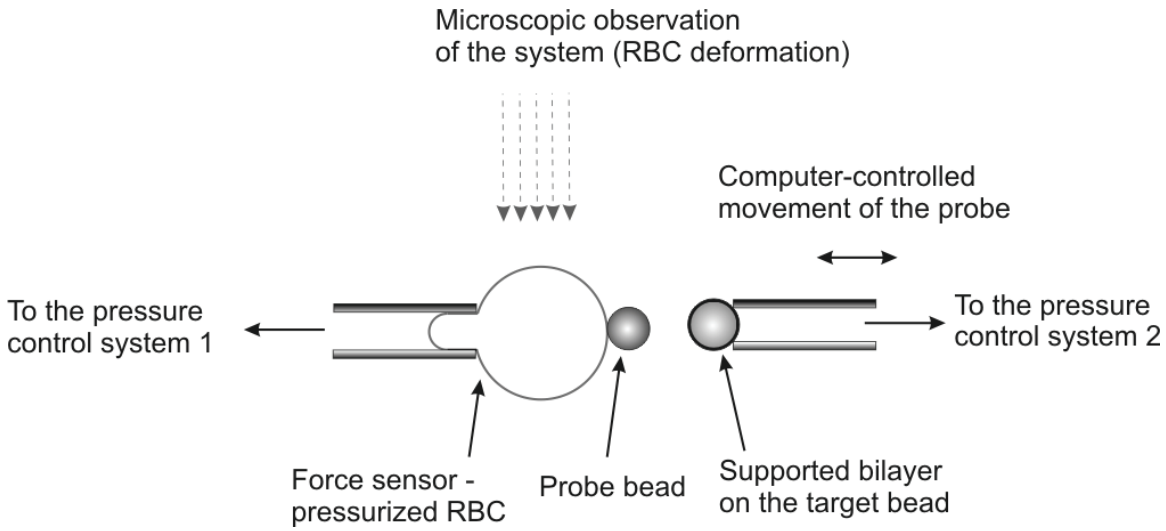

Figure 1. Scheme of the Biomembrane Force Probe set-up.

Briefly, the principle of BFP is as follows. In this technique the force sensor is a streptavidin-functionalized red blood cell (RBC), aspirated by a pressure control system at the end of a capillary with known diameter (~2 microns) (See Figure 1). Knowing the diameters of the capillary and the red blood cell, as well as the aspiration pressure, one can determine the effective spring constant of the red blood cell. For a detailed description of BFP, see [2]. A biotin-functionalized silica bead (or probe bead) is attached on the apex of the RBC through a streptavidin/biotin linkage by

gently touching the surface of the RBC with the bead. This probe bead also carries His-tag antibodies for recognition of the target molecule. The target molecule, in this case a transmembrane peptide WLP23, functionalized with a His-tag, is incorporated in a supported bilayer, deposited on another glass bead. This so-called supported vesicle is immobilized by aspiration on the end of a second capillary. The capillary with the target bead can move such that the supported bilayer can be brought into contact with the probe bead with a predetermined force of contact. Afterwards, the target bead is retracted at a controlled speed. If the His-tag on the WLP peptide forms a bond with the anti-His-tag on the surface of the probe bead, then the RBC will be deformed upon separation of the two beads. This deformation is measured and converted to a force as described [2, 3]. In this way the maximal strength of the formed bond can be determined from the maximal deformation of the RBC just before the probe bead is set free and the RBC restores its spherical shape.

Materials and methods

Chemicals

1-stearoyl-2-oleoylphosphatidylcholine (SOPC) was purchased from Avanti Polar Lipids and dissolved in chloroform at a 12 mM concentration. The fluorescent lipid N-(Lissamine Rhodamine B sulfonyl) -1,2-dihexadecanoyl-sn-glycero-3- phosphoethanolamine, triethylammonium salt (Rhodamine DHPE) was from Invitrogen and was dissolved in chloroform at a 1.2 mM concentration.

Anti-histidine antibody was purchased form Qiagen Inc. Maleimide-PEG12-NHS N-Hydroxy-succinimide was from Quanta BioDesign. His6-NH_2 was from NeoMPS. Both Maleimide-PEG12-NHS and His6-NH_2 were dissolved in 50 mM phosphate buffer at pH 6.9 just prior the functionalization of target beads.

Cys-WLP23 peptide (CWWL17WWA-NH_2) was prepared as described [1] and dissolved in TFE at a 0.1 mM concentration.

The buffer used for vesicle preparation and BFP experiments was 150 mOsm 1-Piperazineethane sulfonic acid, 4-(2-hydroxyethyl)-monosodium salt (HEPES) at pH 6.9.

Technique

The Biomembrane Force Probe experiments and data interpretation were performed as previously described [2, 3], but with some modifications to obtain a target bead covered with a lipid bilayer with incorporated modified Cys-WLP. A fluorescent Rhodamine DHPE at a 0.1 mol % concentration was incorporated in the bilayer and prior to each experiment the presence of the intact lipid bilayer on the bead was verified, using fluorescence microscopy. In the lipid bilayer surrounding the bead, the investigated Cys-WLP 23 peptide was incorporated at a molar ratio of 1:500. In the framework of the project we functionalized the Cys-WLP23 peptide through maleimide based chemistry [4] to include a His-tag, and thus to be recognizable by the anti-HIS-tag antibody on the surface of the probe bead

The functionalization of the target bead with a lipid/peptide bilayer (supported vesicles) was performed as follows, following the protocol, described in [5]. First one ml of SOPC 1 mol % Rhodamine-DHPE (total lipid concentration of 0.58) mM lipid vesicles, containing 0.2 mol % Cys-WLP23 were prepared as described [1]. Then the vesicles are mixed for 3 hours with 4.1 μl His6-NH_2 at a concentration of 85 μM and 5.2 μl NHS-PEG12-Maleimide at a concentration of 85 μM in order to functionalize the peptide with a His-tag. The resulting functionalized peptide structure was His6-NHS-PEG12-Maleimide-Cys-WLP23. Finally the vesicles, containing the functionalized peptide were mixed for 1 hour with washed silica beads at room temperature. The resulting supported lipid/peptide vesicles were used as the target beads in the BFP experiments.

Results and discussion Before performing the actual measurements of strength of integration of WLP peptide, we determined the strength of the Anti-His-tag/His-tag binding. To do this we measured the unbinding strength between a probe bead and a target bead functionalized respectively with anti-His tag and His-tag functionalities. The rupture strength of this couple should be higher than the expected strength of peptide incorporation, otherwise this will be the weak link in the experimental set-up, which strength will be measured. The most probable unbinding force for this couple turned out to be more than 100 pN (data not shown), which is more than the ~ 60 pN (at similar loading rates) measured earlier by us for the strength of incorporation of WALP 23 in a lipid bilayer (chapter 3). From this experiment we conclude that the experimental system we designed for the BFP measurements will allow us to analyze the measured forces in terms of the strength of incorporation of the WLP-peptide in a bilayer.

As a control we monitored the interaction between the probe bead and the test bead, when the test bead is covered only with a SOPC bilayer (no peptide present). In this case, force events were detected in very rare cases (less than 2 percent of all contacts). However, when the WLP peptide was present in the bilayer, the number of the curves, showing interaction was significantly higher, totaling 10-15 % in each experiment. Therefore, we concluded that the measured interaction force was due to the WALP removal from the bilayer and not due to the non-specific interaction between the probe bead and the SOPC bilayer.

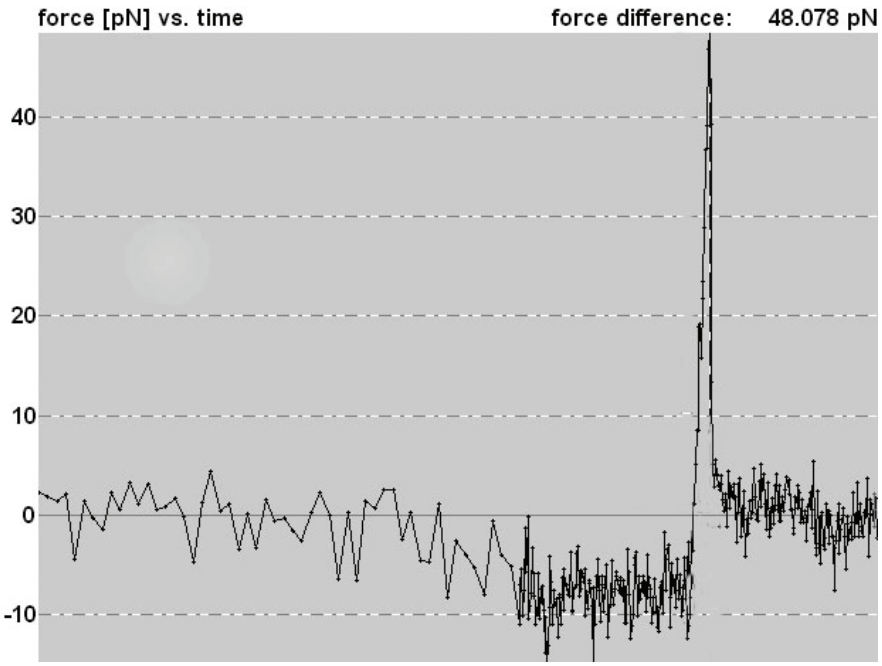

Figure 2 A force-retraction curve during an approach/retract cycle, at which interaction between the probe bead and the target bead was registered.

A force-extension curve from an actual approach/retract cycle, where interaction is detected, is presented in figure 2. In this figure the values around 0 pN represents non deformed RBC before and after contact with the test bead, plateau at approximately -10 pN represents the exerted force during the contact. The height of the peak after the contact represents the strength of the registered interaction. More than 100 force curves were recorded and analyzed

for three loading rates. Histograms of the force distributions at loading rates of 60 pN/sec, 600 pN/sec and 6000 pN/sec are presented in figures 3, 4 and 5, respectively. The most probable unbinding forces for the investigated loading rates were ~ 30 pN at 60 pN/sec, 40 pN at 600 pN/sec and 60 pN at 6000 pN/sec. All force distributions are broader than expected according to the theory.

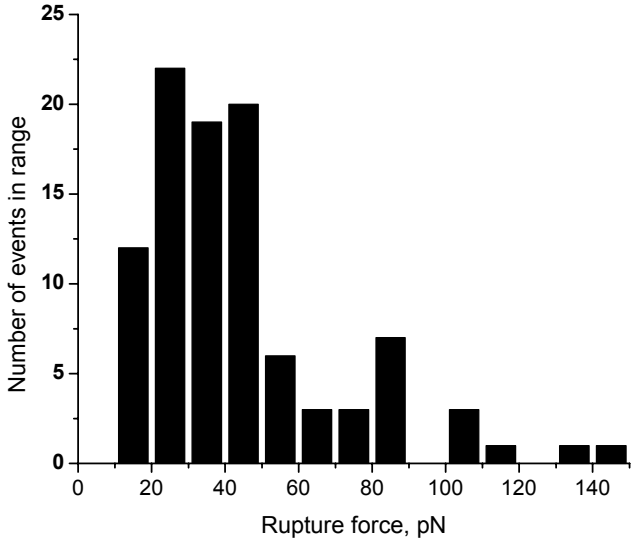

Figure 3. Force distribution at a loading rate of ~ 60 pN/sec

Several conclusions can be drawn from the data. First, as expected from the theory of strength of thermally activated bonds, the most probable measured strength of incorporation increases with the increase in the loading rate. Secondly, the measured values correlate well with the values, which we observed in the WALP/DOPC system, using AFM [1].

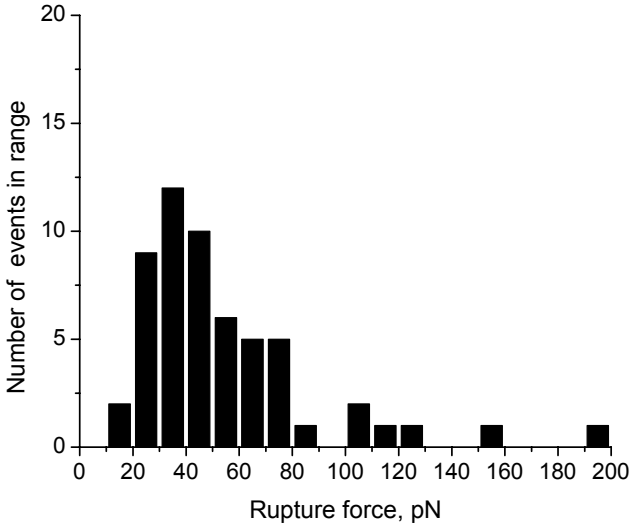

Figure 4. Force distribution at a loading rate of ~ 600 pN/sec

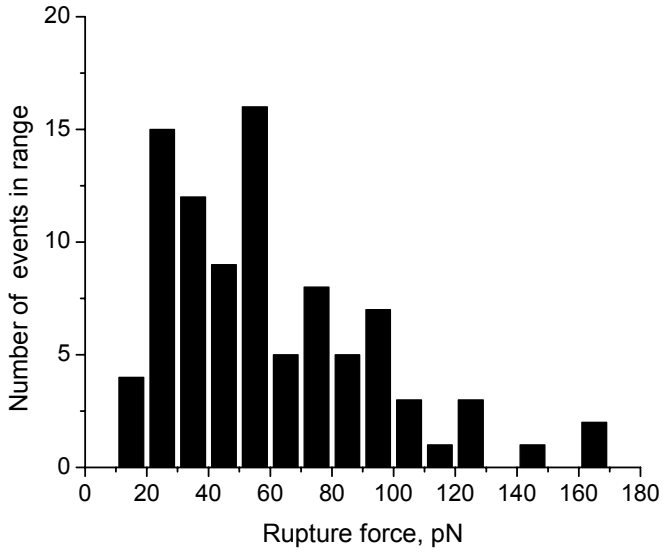

Figure 5. Force distribution at a loading rate of ~ 6000 pN/sec.

From the presented histograms of force distributions one can see that the distribution of the registered unbinding events is broader than the Gaussian distribution, as expected according to the theory [2, 3]. In the case of the BFP experiments, force distributions are much broader than the respective distributions from AFM experiments. A possible explanation for this deviation from the theoretical predictions can be proposed based on the design of the BFP experiments. While in the AFM experiments we are pulling a peptide out of a planar bilayer, supported on an atomically flat surface (mica), in BFP experiments we are pulling it out of a closed vesicle, supported on the surface of silica bead, aspirated on the end of a capillary. The aspiration pressure, applied on the target vesicle/bead assembly is not precisely controlled and could vary from experiment to experiment. Since different aspiration pressures result in a different lateral tension in the bilayer, this would cause the observed broadening of the force distributions.

The broader distributions of the most probable rupture force F at each of the tested loading rates r hindered the rigorous interpretation of the F(log(r)) dependency. Nevertheless the data allowed us to get an estimate of the distance of the position of the energy barrier with respect to the ground state. The obtained value varied in the range between 0.2 and 1.0 nm. Previously obtained by AFM value of 0.7 nm in DOPC/SH-WALP 23 system falls within this range.

The registered strengths of integration for a variety of WALP peptides in chapter 3 of this thesis are similar to the obtained values for WLP peptide in this study. This indicates that the increased hydrophobicity of the transmembrane α helix does not influence significantly the strength of integration of the peptide in the bilayer.

In conclusion, in the performed study we confirmed the validity of the data and the model, previously described by us on WALP/DOPC bilayers [1]. We also demonstrated that the strength of integration of the model α-helical peptide in a bilayer is relatively independent on the precise chemical composition of the system.

1. D.N. Ganchev, D. T. S. Rijkers, M. M. E. Snel, J. A. Killian, and B. de Kruijff Strength of Integration of Transmembrane α-Helical Peptides in Lipid Bilayers As Determined by Atomic Force Spectroscopy. Biochemistry 2004 43(47) 14987 - 14993

2. E. Evans, K. Ritchie, and R. Merkel Sensitive force technique to probe molecular adhesion and structural linkages at biological interfaces. Biophys. J. 1995 68(6) 2580–2587.

3. E. Evans Energy landscapes of biomolecular adhesion and receptor anchoring at interfaces explored with dynamic force spectroscopy. Faraday Discuss. 1998 (111) 1-16

4. Hermanson, G.T. (1996). Bioconjugate Techniques, Academic Press

5. T. M. Bayerl and M. Bloom Physical properties of single phospholipid bilayers adsorbed to micro glass beads. A new vesicular model system studied by 2H-nuclear magnetic resonance. Biophys J. 1990 58(2) 357–362.

Chapter 4. Size and orientation of the Lipid II head group as revealed by AFM imaging

Abstract

In this study we investigated the size and orientation of bacterial Lipid II (L II) head group when the L II molecule is present in liquid-crystalline domains of DOPC in a supported DPPC bilayer. Using Atomic Force Microscopy we detected that L II causes the appearance of a 1.9 nm thick layer, situated over the DOPC head group region. At increased scanning force this layer can be penetrated by the AFM tip down to the level of DOPC bilayer. Using different L II precursor molecules we demonstrated that the detected layer consists of the head groups of L II and that the MurNAc-pentapeptide unit of the head group is responsible for the measured 1.9 nm height of that layer. Monolayer experiments provided information about the in-plane dimensions of the L II head group. Based on these results and considerations on the molecular dimensions of L II head group constituents, we propose a model for its orientation of the L II head group in the membrane. In this model the pentapeptide of the L II head group is rather extended and points away from the bilayer surface, which could be important for biological processes, in which L II is involved.

The cell wall is an essential structure in bacteria and plays an important role in determining bacterial shape and protects against osmotic stress. It consists of a cross-linked polysaccharide-peptide complex, called peptidoglycan, the building blocks of which are synthesized inside the cell as a part of a specific carrier molecule, called Lipid II (Figure 1 A) [1]. Lipid II (LII) is a complex molecule (Figure 1 B) containing a long polyisoprenyl (bactoprenyl) chain connected via a pyrophosphate to a large hydrophilic group, consisting of a disaccharide-pentapeptide unit, which is the building block for the peptidoglycan synthesis. The biosynthesis route of L II includes attachment to the phosphorylated bactoprenyl chain of a N-acetylmuramic acid (MurNAc) carrying a pentapeptide, resulting in the formation of Lipid I. Hereafter an additional sugar, N-acetylglucosamine (GlcNAc), is attached to form a complete L II molecule. After the assembly on the cytosolic leaflet of the membrane, L II is translocated to the periplasmic side by an unknown mechanism, where the disaccharide-pentapeptide is incorporated in the cell wall. The phosphorylated bactoprenyl chain returns to the cytosolic leaflet for a new cycle of synthesis. The L II pool in an average cell turns out to be very low, the number of molecules being in the order of several hundreds to thousands per cell [2], but because of its high turnover this amount suffices to allow the peptidoglycan layer of bacteria to grow rapidly.

The bacterial cell wall is a structure, specific for bacteria, and not present in higher organisms. This makes the cell wall and the molecules, involved in its synthesis, ideal targets for bactericides. It was established that several antibiotics target specifically the L II molecule. Some of these antibiotics, such as mersacidin and vancomycin, prevent the synthesis of the cell wall by interacting with L II [3, 4]. Others like the lantibiotic nisin use L II as a receptor for targeted pore formation [5, 6]. Nisin and L II assemble into pores of defined composition [6, 7] that permeabilize the membrane thereby killing the bacteria.

The importance of the role of the lipid II in the cell wall synthesis and as a target of antibiotics strongly contrasts with the lack of knowledge on this intriguing biomolecule. This applies in particular to the orientation of the head group of L II when this molecule is present in a membrane. The head group of L II is crucially important for specific recognition by certain antibiotics [8]. It was demonstrated that vancomycin binds to the last two residues in the pentapeptide [9] whereas the pyrophosphate moiety is essential for specific docking of nisin [10]. This suggests that orientation of the L II head group plays a significant role in this specific recognition. The proper utilization and incorporation of the head group in the peptidoglycan layer also will require a certain orientation of the carbohydrate-pentapeptide building block with respect to the membrane. Therefore, insights in the organization of L II head group at the membrane will provide a better understanding on the processes of specific antibiotic recognition and cell wall synthesis. However, the complex structure of the L II polar head group, which includes a pentapeptide with an unusual amino acid composition (d-γ Glu on a position 2 and two d-Ala on positions 4 and 5), makes this structure rather difficult to characterize via direct structure determining techniques such as NMR and X-ray diffraction.

AFM has proven to be a suitable technique to image and mechanically manipulate membranes and bilayers with nanometer resolution and in aqueous environment [11, 12]. In this study we applied AFM to supported lipid bilayers, containing L II and L II precursors in order to get insight into the surface organization of this molecule. To be able to facilitate imaging of L II we made use of a bilayer of gel state lipids in which small domains of liquid crystalline lipids are present. These domains are expected to contain fluid lipids such as L II and they are readily identified by their lower height [13].

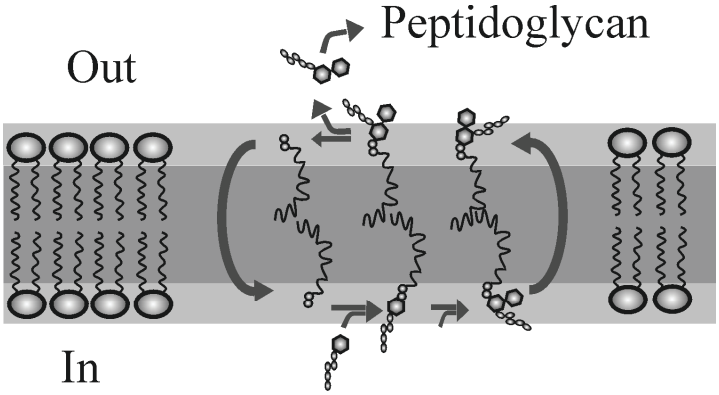

A

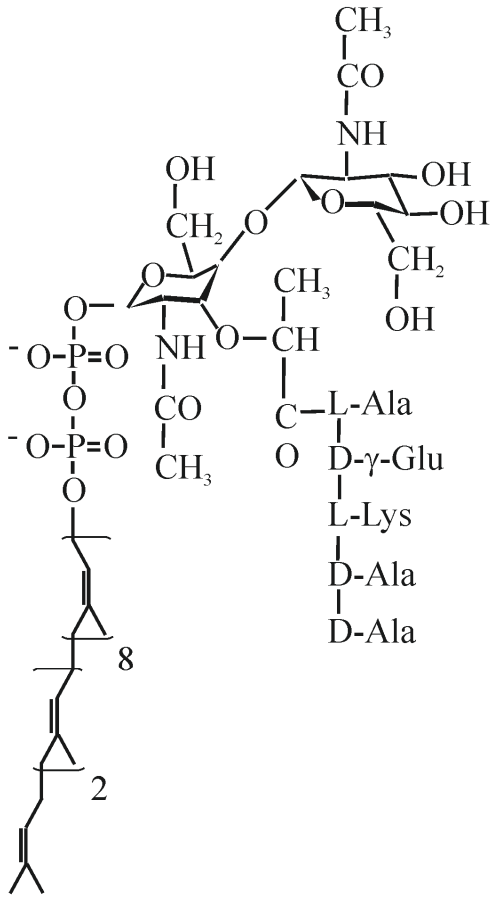

B

Figure 1 A) Schematic representation of L II synthesis and function in a peptidoglycan synthesis. Different precursor molecules of L II, i.e. bactoprenyl phosphate, bactoprenyl pyrophosphate and Lipid I are depicted. B) The chemical structure of Lipid II.

The data provide for a first time quantitative information about the size and orientation of the L II head group at the bilayer interface. We demonstrate that the Lipid II head group protrudes ~ 1.9 nm over the head group region of the DOPC bilayer, where the L II is located. This corresponds to a conformation with the pentapeptide pointing away from the bilayer surface.

Materials and methods

Lipids. 1,2 Dipalmitoyl-*sn*-glycero-3-phosphocholine (DPPC) and 1,2 Dioleoyl-*sn*-glycero-3-phosphocholine (DOPC) were obtained from Avanti Polar Lipids (Alabaster, AL) and were dissolved at 20 mM in a mixture of methanol/chloroform (1:3 v/v). Synthesis of Lipid II, Lipid I and bactoprenylpyrophosphate (a generous gift from E. Swiezewska) was described elsewhere [6]. The lysine form of UDP-MurNAc-pentapeptide was labelled with NBD-chloride at the lysine of the pentapeptide moiety residue in an identical way as described for the labelling of UDP-MurNAc-pentapeptide with pyrenesulfonylchloride [6].

Nisin A was produced by batch fermentation, isolated, and purified as described [14]. It was dissolved in a buffer solution (50 mM NaCl and 50 mM Na_3PO_4, pH 6.8, adjusted with HCl) at 10 μM concentration.

Preparation of Small Unilamellar Vesicles (SUV). SUV were prepared as described previously [15]. Briefly, a mixture of lipids in the desired molar ratio was dried in a rotary evaporator and the mixed films were stored overnight under high vacuum. All films were hydrated with a buffer, containing 50 mM NaCl and 50 mM Na_3PO_4, adjusted to pH 6.8 with HCl. This buffer was used throughout the study. The final lipid concentration was 1 mM. Ten freeze – thawing cycles were performed in order to obtain a suspension of large multilamellar vesicles. Subsequently, this suspension was sonicated in an ultrasound bath sonicator (Branson, Danburry, Connecticut) at maximum power for 30 min, at 45° C. Possible remaining large vesicles were spun down for one hour at 20800 g, at 4° C. The SUV suspension was used within 3 days and the AFM results were not dependent on the time of storage.

Preparation of supported lipid bilayers. The preparation of supported lipid bilayers was performed as earlier described [16]. Briefly, we deposited 75 μl SUV suspension onto freshly cleaved mica (ϕ = 10 mm). The vesicles were left to adsorb on the mica for one hour at room temperature. Subsequently, the sample was rinsed with 75 μl of the buffer solution (3 times) and heated for 1 hour at 65° C. After cooling down to room temperature, the sample was rinsed again with 75 μl of the buffer solution (3 times).

Incubation with nisin. In these experiments we gently applied 75 μl 10 μM nisin solution over the preformed bilayer. This first volume was replaced with another 75 μl nisin solution, ensuring in this way a final concentration of the nisin over the bilayer to be ~ 10 μM. The sample was left for 15 minutes at room temperature and then rinsed 3 times with 75 μl of the buffer solution in order to remove the non-adsorbed nisin.

AFM imaging. The supported bilayers were covered by the buffer solution during the measurements. The samples were mounted on an E-scanner, which was calibrated on a standard grid, of a Nanoscope IIIa AFM (Digital Instruments, Santa Barbara, California). A fluid cell without O-ring was fitted and the sample was scanned in contact mode, using oxide sharpened Si_3N_4 tips attached to a triangular cantilever with a spring constant of 0.06 N/m (NanoProbe, DI, Santa Barbara, California). Imaging was performed at a minimal force (< 0.5 nN) where the scans were stable and clear, and at temperatures between 23-28^o C. In some cases images were recorded at increased scanning force.

Surface Pressure-Area isotherms. Surface pressure-area (π-A) isotherms were obtained by compression of a spread lipid monolayer on a surface of a computer driven Langmuir trough. Compression is performed by moving a Teflon barrier over the surface of the trough. The speed of the barrier was 3 cm/min, dimensions of the trough were 17.3 cm. (width)x35 cm. (length). As a subphase 50 mM NaCl and 50 mM Na_3PO_4 buffer, adjusted to pH 6.8 was used. The surface tension of the buffer was 71.2 mN/m. 20 nmol L II from organic solvent (methanol:chloroform 1:1)

was carefully deposited on 4-5 different spots on the surface of the trough. Before the start of the compression cycle we waited 15 minutes for evaporation of the solvent. The initial surface pressure, at which the compression started, was 0 mN/m. Experiments were performed at room temperature, ~ 22^{o} C.

Results

Imaging the effect of L II incorporation on DOPC domains in DPPC bilayer.

We initially selected the 5 mol % DOPC in DPPC mixed bilayer as experimental system in our studies. The small liquid-crystalline domains of DOPC with a packing similar to biological membranes can be readily distinguished from the surrounding gel state DPPC bilayer because they are 0.76 nm ± 0.11 nm lower and therefore show up as darker in the AFM images (See series of images in figure 2 A). When half of the DOPC in these samples is replaced with L II again the typical phase-separation pattern is observed as in the binary mixture (Figure 2 B). However, in contrast to the DOPC:DPPC mixture, the domains are now 1.16 ± 0.14 nm higher than the surrounding DPPC bilayer and show up as lighter areas in the AFM images. The thickness of the DPPC bilayer as measured at defects down to the mica (shown for instance in the bottom right panel of figure 2) was 5.5-6.0 nm in all cases. These data suggest that L II is preferentially localized in DOPC domains and increases its thickness with ~ 1.9 nm when scanned at low force (~ 0.5 nN). Further to describe the surfaces of the investigated bilayers, we made cross sections of the DOPC:DPPC and LII:DOPC:DPPC bilayers, using the AFM software. Typical height profiles are presented in figure 3. To verify the localization of L II we incubated the samples with the lantibiotic nisin that specifically interacts with L II. In the absence of L II no changes were detected in the morphology of the sample (data not shown). However, in the L II containing sample the DOPC:L II containing domains were substantially perturbed (Figure 4). The overall contour of the domain was preserved, but the bilayer within the domain acquired a particulate structure with large local fluctuations in the height, reaching heights up to 10-15 nm with respect to the DPPC. Apparently, the nisin-L II interaction causes major reorganization within the L II containing bilayer. We observed (data not shown) that part of the nisin is loosely bound to the domains because consecutive scanning results in removal of the higher aggregates in the DOPC: L II domain, most likely because some loosely adsorbed nisin was removed. These experiments demonstrate that L II is localized in the DOPC domains and that the presence of L II causes an increase in height of these domains.

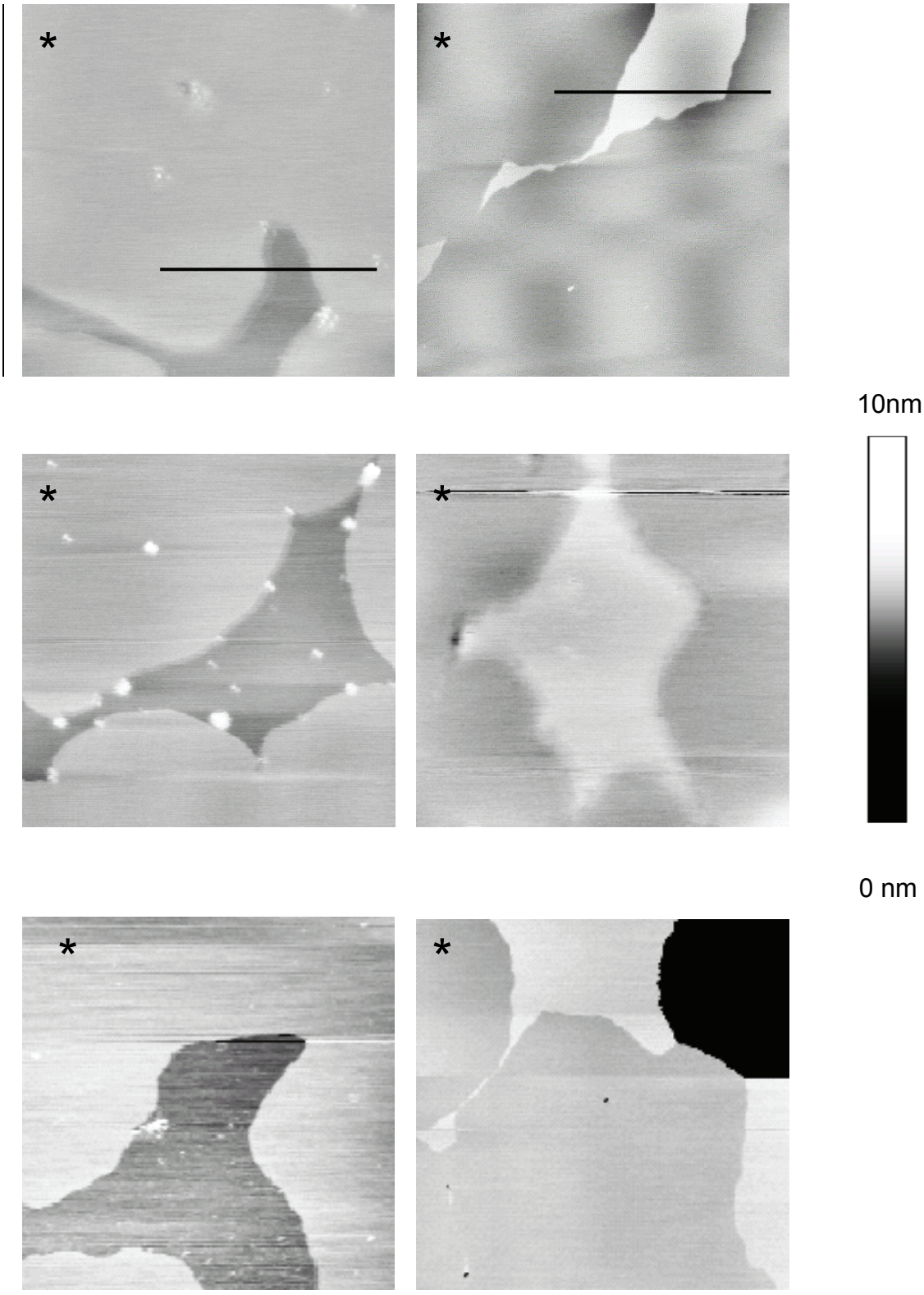

Figure 2 A series of typical AFM images of domains present in supported mixed DOPC:DPPC (5:95 molar ratio) bilayer in the absence (column A) and presence of Lipid II (column B). Images are taken from different bilayer preparations to demonstrate the reproducibility of the results. The composition of L II containing sample is L

II:DOPC:DPPC 2.5:2.5:95. All images are recorded at low scanning force (< 0.5 nN). The scan size in all cases is 2x2 microns and the z-scale is 10 nm. In all images the DPPC bilayer was marked by an asterisk

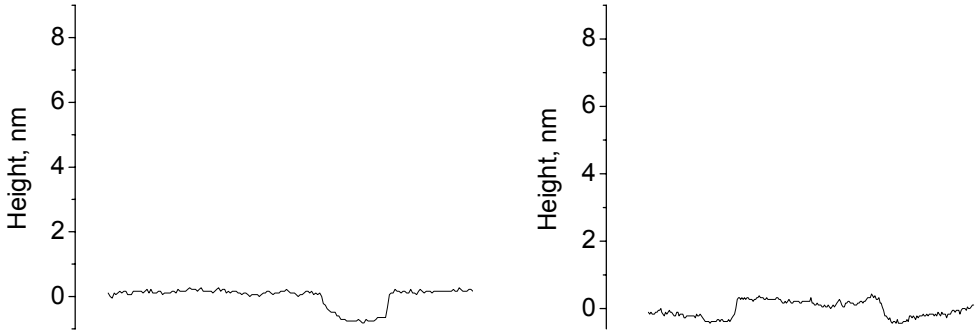

A B

Figure 3 Figure 3 Height profiles of the bilayer surface of the images in column 1 of figure 2, taken across the black lines in the images. A) A height profile of DOPC/DPPC bilayer. B) A height profile of LII:DOPC:DPPC bilayer at low imaging force.

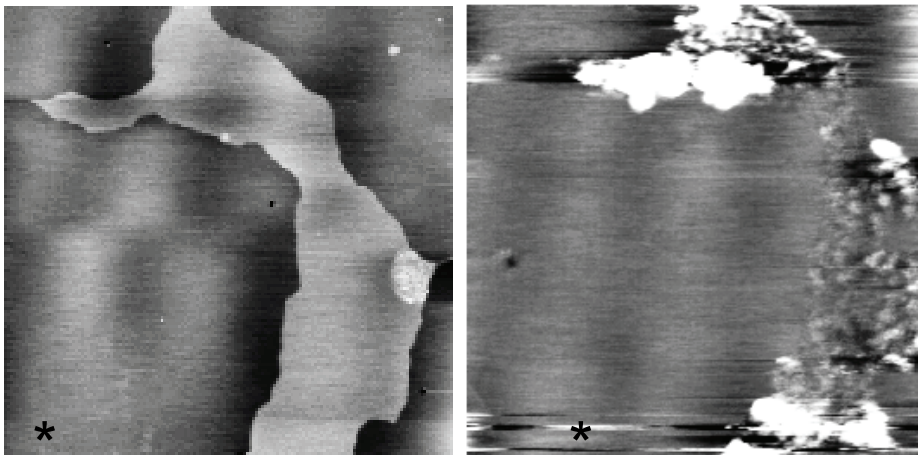

A B

Figure 4 AFM images of domains in L II:DOPC:DPPC bilayer at molar ratio 2.5:2.5:95, before incubation with nisin (A) and after the incubation (B). The same domain is visualized in both images. The scanning force is minimized (~ 0.5 nN), the scan size is 5x5 microns and the Z scale is 10 nm.

The L II:DOPC domains are sensitive to the applied scanning force.

The force, which is applied on the AFM tip during scanning, usually is minimized down to ~ 0.5 nN to avoid damaging of the sample. However, we could increase this force in a controlled fashion in order to mechanically manipulate the sample. We exploited this ability of the AFM in order to further characterize the studied system.

Therefore we imaged both the DOPC:DPPC and L II:DOPC:DPPC bilayers at elevated scanning force. The AFM images of DOPC domains in DOPC:DPPC bilayers recorded at 10 fold increase in the applied force were found to be similar to the images, recorded at low force (compare fig 5 A with fig. 2 A, top panel). Only some debris was removed by the tip during scanning. However, the behaviour of L II:DOPC:DPPC bilayer at increased scanning force is strikingly different. At approximately a 10-fold increase in the applied force the L II:DOPC domains are visualized 0.81 ± 0.15 nm lower than the surrounding DPPC bilayer (Fig. 5 B, compare the same domain in fig. 2 B, top panel) instead of ~ 1.16 nm higher. A height profile of the penetrated domain is presented in figure 6. This process is completely reversible and when the scanning force is decreased back to 0.5 nN, the domains reappear and could be visualized again 1.16 ± 0.14 nm higher than the DPPC areas (data not shown). This procedure could be performed consecutively several times over one and the same spot without lipid material being carried away by the tip during these manipulations. These results demonstrate that in the DOPC/L II (1:1) domains the presence of L II causes the appearance of a ~ 1.9 nm thick layer, situated over the DOPC head group region, which could be reversibly penetrated by the AFM tip down to the level of the surface of the DOPC bilayer.

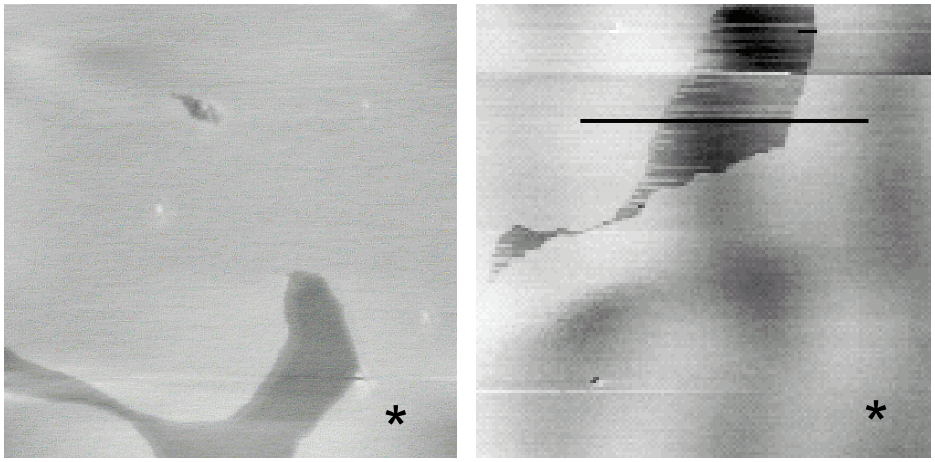

A B

Figure 5 AFM images of domains in DOPC:DPPC and L II:DOPC:DPPC bilayers recorded at high scanning force (5 - 6 nN). A) DOPC domains. B) L II:DOPC domains, the scan size in both cases is 2x2 microns, the z-scale is 10 nm. Note that the same areas as in figure 2, first row, are visualized.

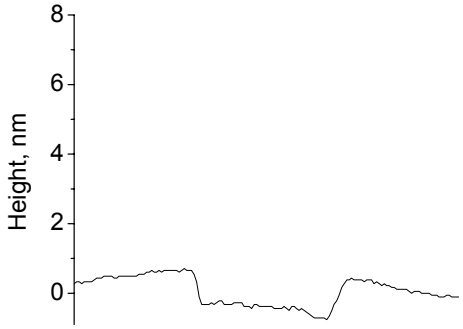

Figure 6 Height profile of a bilayer surface of a LII:DOPC:DPPC bilayer, taken across the black line in the image in figure 5 B at an elevated imaging force.

Next, we were interested to determine at which L II concentration the 1.9 nm thick layer would start to appear. Therefore we varied the L II/lipid ratio and increased the DOPC:DPPC ratio to 1:9 in order to facilitate the detection of the L II:DOPC domains. At all investigated molar ratios the thickness of the continuous DPPC bilayer is 5.5 – 6.0 nm. At L II:DOPC molar ratios of 1:4.5 and 1:9 very similar behaviour was found as described for a molar ratio 1:1. L II:DOPC domains appeared 1.15 ± 0.20 nm higher than the DPPC bilayer and they are stable upon scanning at a minimized force (data not shown). Increasing the scanning force resulted in tip penetration through the layer and subsequent visualization of lower domains (0.7 ± 0.2 nm.). Tip penetration is completely reversible and minimizing the force allows higher domains to be visualized. At a L II:DOPC ratio of 1:14 it is still possible to visualize elevated domains, but only at minimal scanning force (below 1 nN) (Fig 7 A). At a still lower ratio of 1:19 elevated areas can be detected, but visualizing complete elevated domains is rather difficult since even at a slight increase in the force during scanning (due to a thermal drift in the AFM) the domains are imaged as lower areas with respect to the DPPC level (see the change in contrast in the domain, visualized in figure 7 B). Upon lowering the L II amount below 1:49 molar ratio results in images in which the L II:DOPC domains have the typical appearance as in the absence of L II. We were unable to visualize elevated areas even at the lowest possible force, allowing stable imaging. A typical image of L II:DOPC domains at a 1:99 ratio is shown in figure 7 C. These experiments demonstrate that a certain L II:DOPC ratio of approximately 1:14 is needed in order to form elevated domains that can be stably imaged at low force but which are penetrated by the AFM tip down to the DOPC bilayer level at increased force.

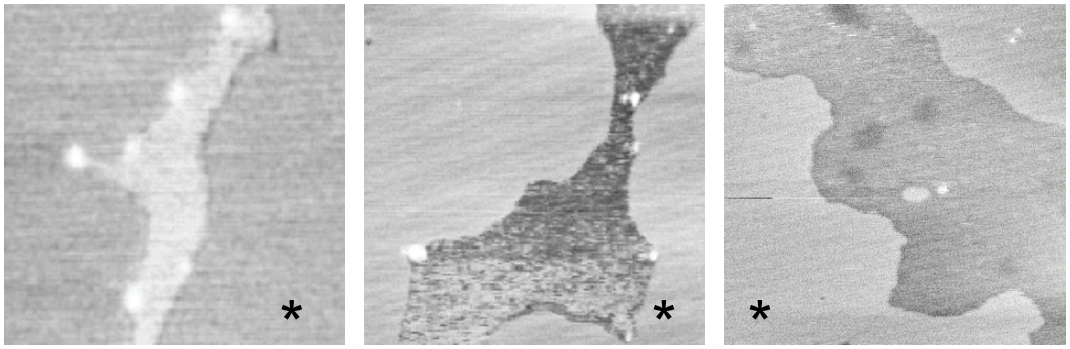

A B C

Figure 7 AFM images of L II:DOPC:DPPC domains at different L II:DOPC ratios. The ratio (L II+DOPC):DPPC in all cases was 10:90. A) L II:DOPC 1:14. B) L II:DOPC 1:19 C) L II:DOPC 1:99. All images were recorded at force of ~ 0.5 nN. The scan size in all cases is 2x2 microns and the z-scale is 10 nm.

The head group of L II is responsible for the measured 1.90 nm increase in the bilayer heights.

We next tried to determine which part of the L II molecule causes the observed increase height of the DOPC domains. We systematically decreased the size of the L II group and studied L II precursors, incorporated in DOPC:DPPC bilayers. The used molar ratio of precursor:DOPC:DPPC was 1:9:90. All investigated precursor

molecules contain the bactoprenyl chain, to which either one phosphate (11 P) or two phosphates (11 PP) are attached. Lipid I differs from L II by missing the last sugar (GlcNAc) in its hydrophilic head group (see figure 1).

The behaviour of L I:DOPC domains follows the pattern established for L II containing domains. At minimized scanning force the domains are 1.21 ± 0.13 nm higher then the 5.5-6.0 nm thick DPPC bilayer (Fig 8 A). Upon increase in the scanning force they are visualized as 0.74 ± 0.12 nm lower then the DPPC level, which amounts to 1.95 nm thickness of the layer, present above DOPC head group level. This process is reversible and minimizing the scanning force allows visualization of higher domains.

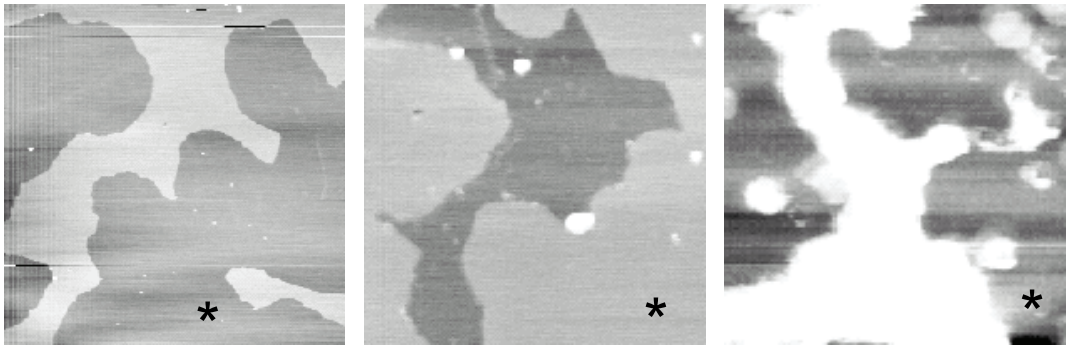

A B C

Figure 8 AFM images of domains in L I:DOPC:DPPC 1:9:90 bilayer (A) and 11 PP:DOPC:DPPC 1:9:90 bilayer before (B) and after (C) incubation with nisin. All images were recorded at minimal scanning force (<0.5 nN). The scan size in both cases is 5x5 microns and the z-scale is 10 nm.

When we imaged systems containing only the bactoprenyl chain with attached phosphate or pyrophosphate groups (11 P or 11 PP), we were not able to detect higher domains in respect to the DPPC bilayer. In all experiments only lower domains were observed, even at the minimal force, needed for stable scanning (Figure 8 B). The thickness of the DPPC bilayer remained 5.5-6.0 nm, the 11 P (or 11 PP):DOPC domains were ~ 0.77 ± 0.16 nm lower than the surrounding DPPC bilayer. Experiments with nisin decoration were performed over both L I:DOPC:DPPC and 11 PP:DOPC:DPPC bilayers. Nisin, which is positively charged, was shown to aspecifically interact with negatively charged lipids [18]. After the incubation with nisin, irregular in height elevations were observed in both cases (Fig 6 C depicts a 11 PP:DOPC domain after nisin incubation), instead of lower areas, which confirms the presence of the respective precursor molecules in the observed domains.

The differences in height between the L II (precursor):DOPC domains and the surrounding DPPC bilayer are summarized in table 1.

The performed experiments demonstrated that the increase in height of L II:DOPC domains is presumably caused by the N-acetyl muramic acid-pentapeptide part of the L II head group

The increased height is not an artefact caused by electrostatic interactions between AFM tip and the lipid head group.

In principle it is possible that the charged lysine residue in the pentapeptide of L II head group interacts electrostaticaly with the AFM tip. This could affect the height differences which we measure for L II in DOPC domains. To check this possibility we imaged supported bilayers, containing a L II analogue, in which the charged lysine was blocked with an NBD group. The used L II-NBD:DOPC:DPPC molar ratio was 1:9:90. Phase-separated domains, 1.22 ± 0.16 nm higher than the surrounding DPPC bilayer were imaged at minimized scanning force (Table 1). These domains are sensitive to an increase in the scanning force, following in their behaviour the pattern, similar to that observed for the parent molecule. Upon imaging at an increased force, the tip scans over the DOPC head group level, 0.76 ± 0.14 nm below the DPPC bilayer (table 1). These experiments demonstrate that the charge of the lysine residue does not influence the measured height differences and this makes it unlikely that electrostatic interactions between the AFM tip and the sample play a role in causing the increased height of the DOPC:L II domains.

The head group of L II has a limiting area of ~ 1.5 nm^2.

So far we determined the height of the L II head group with respect to the surface of the bilayer. In order to completely characterize the size of the head group, we need to know the area, which a L II molecule occupies in a bilayer. We can estimate this area by determining the limiting area of a L II in a monolayer, spread on a buffer surface. We performed monolayer compression experiments in a Langmuir trough and determined the limiting area per molecule and collapse pressure for a pure L II monolayer, spread on a buffer surface. In separate runs we obtained reproducible π-A isotherms with limiting areas of ~ 1.5 nm^2 and a collapse pressure of 43.5 mN/m (Figure 9).

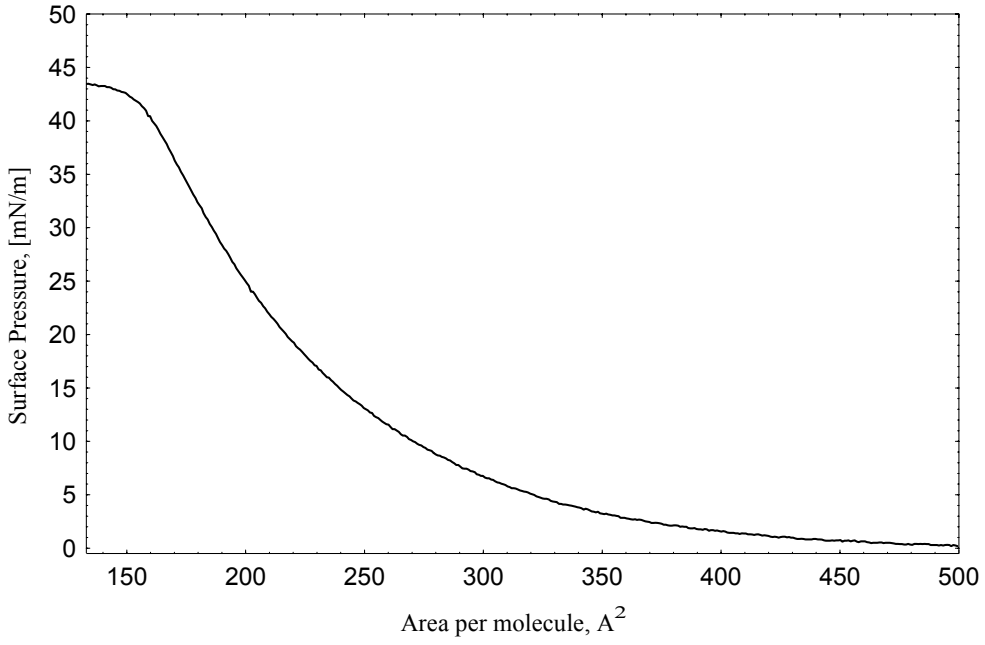

Figure 9 Pressure-Area isotherms for a L II monolayer spread over buffer solution in a Langmuir trough.

Discussion

The aim of this study was to provide information about the size and orientation of the head group of Lipid II. We used a combination of AFM imaging and force manipulation to fully characterize the dimensions of the head group. The obtained results revealed that the L II head group protrudes app. 1.9 nm from the DOPC level bilayer and forms a layer that is stable at minimized scanning force. Using L II precursor molecules (L I and 11 PP) we demonstrated that this height increase is due to the N-acetyl muramic acid-pentapeptide part of the L II head group. We fully described the size of the L II head group, by determining the limiting area per molecule in a spread monolayer to be 1.5 nm^2.

Here we will discuss the imaging mechanism, which determines the observed heights of L II:DOPC domains at minimized and increased scanning force, and after discussing the possible effect of electrostatic interaction on the measurements, we will describe the orientation of L II head group, using the data for the head group dimensions.

In our experiments we demonstrated that the fluid state bactoprenyl chain of the Lipid II co-separates in the liquid crystalline DOPC domains, most probably due to the squeezing out of the fluid L II acyl chain from the highly ordered gel state bilayer. Therefore we postulate that over the DOPC domains the tip scans over the head group region of the L II and when the force increases, it penetrates through it down to the DOPC head group level (see Figure 10). In the presented cross sections we could see that the surface of both non-penetrated and penetrated L II domains could not be distinguished from the surfaces of the conventional DOPC or DPPC areas. Interestingly, in contrast to the irreversible damaging of the lipid bilayers at increased scanning force [17], in our experiments the imaged L II containing domains restore their initial height once the scanning force is minimized. This demonstrates that L II molecules are not removed by the tip at increased scanning force, which is an indication for their stable anchoring within DOPC bilayer.

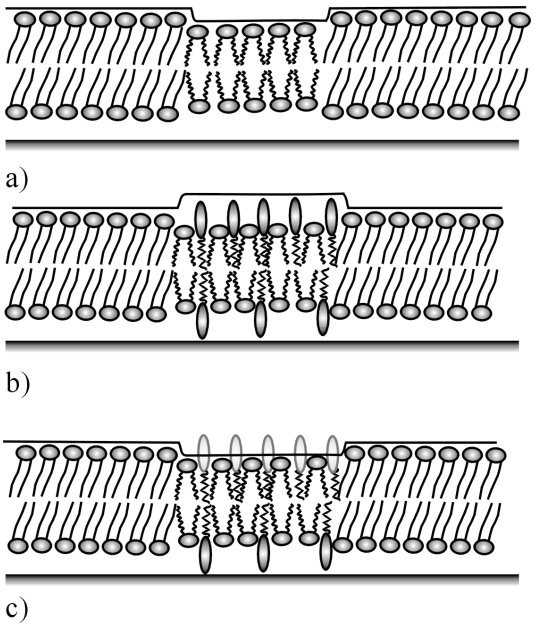

Figure 10. Position of the AFM tip over domains of different composition in L II:DOPC:DPPC supported bilayers. The height profile (position of the tip)is shown with a thick line. A) Pure DOPC domains – scanning at minimal force. B) L II:DOPC:DPPC domains imaged at low force – the tip scans over the L II head groups. C) At increased scanning force the tip penetrates through the L II head group region and scans over the DOPC head groups.

Another characteristic feature, observed in our experiments is the fact that after the penetration through the L II head group level, the tip scans over the DOPC head group level. What is the explanation of this unusual behaviour? Obviously, there is a difference between the scanning forces, which each of the head group layers could withstand. At 1:1 L II:DOPC molar ratio a force of ~ 4-5 nN is sufficient to penetrate through the L II head group level, and this force decreases with the decrease in the L II molar ratio.

In literature there are several reports on the forces needed to penetrate through a supported bilayer which range from 5-20 nN for different liquid crystalline bilayers to 20-30 nN for the more ordered gel state bilayers [18-21]. If we assume that the tip radii are similar in all cases, then we can conclude that our value of ~5 nN to penetrate the L II layer down to the DOPC head group level is in good agreement with these studies. Why is it easier to penetrate through the Lipid II head group layer than through a DOPC head group bilayer? The simplest explanation is that the L II head group layer is much looser. The L II head groups are charged and thereby will repel each other, resulting in a decreased cohesion and a layer that is easier to penetrate. This latter interpretation is supported by studies which showed that bilayers of charged lipids are more easily penetrated than non-charged bilayers [18].

The "penetration depth" defined as the height difference between non-penetrated and penetrated L II:DOPC domains is a measure of some characteristic dimension of the large Lipid II head group. Here we discard the possibility that some part of the L II hydrocarbon chain could contribute to the measured height differences due to the fact that the position of phosphate groups in a bilayer, determined for other lipids is quite well defined [22]. Moreover, exposure of the hydrocarbon area to the polar environment of the interface would require a large unfavorable energy, which is found to be between 20-40 kcal/mol.$Å^2$ [23, 24]. This reasoning supports our hypothesis (evidences for which we provided with our precursor experiments) that the measured height increase is caused by the L II head group alone.

In principle it could be argued that the positively charged lysine (the third amino acid residue in the pentapeptide) could interact with the negatively charged tip, influencing in this way the measured height differences. However, we can safely exclude this possibility because blocking the charge on the lysine with NBD did not affect the height difference. Furthermore, the presence of negative charges on 11 P and 11 PP within DOPC domains did not change the observed ~ 0.7 - 0.8 nm height difference between DPPC and the DOPC domains in which these molecules are localized. The absence of an electrostatic contribution to the measured height may be explained by the high ionic strength of the buffer solution used. The presence of 50 mM sodium chloride and 50 mM sodium phosphate screens to a large extent the electrostatic interactions.

These considerations lead us to conclude that the measured 1.9 nm is caused by the Lipid II head group. What could be the conformation of the L II head group that is consistent with this dimension? An important indication is provided by a comparison between height measurements of L II and L I. Since we observed very similar heights for these lipids we can conclude that the 1.9 nm height difference is due to the pentapeptide and the MurNAc to which the peptide is attached.

The estimated vertical dimension of the L II head group (1.9 nm) suggests that it is not very probable that the pentapeptide is oriented with its backbone lying flat over the bilayer surface because the average diameter of the peptide backbone and the side chains can be estimated to be much less than 1.9 nm. Therefore we propose that the head group adopts a configuration, in which the pentapeptide in an extended conformation points away from the bilayer. If we assume a rise per residue of 0.35 nm (as in a β sheet conformation) a total length of ~ 1.4 nm can be estimated for the pentapeptide. To this number we can add the contributions due to the MurNAc and the –O-CH-CO-

motif which connects the pentapeptide to this sugar, which together can be roughly estimated to contribute between 0.3-0.6 nm to the total height. This gives us a height of the L II head group of 1.7-2.0 nm, which closely matches the value of 1.9 nm, measured by AFM.

The π-A isotherms give us the area, occupied by the L II molecule in a monolayer. Not surprisingly, having in mind the bulky head group of the L II, this area of 1.5 nm^2 is more than twice the area, occupied by the PC molecule in a liquid crystalline bilayer [25]. The collapse pressure is comparable to the collapse pressures, reported for other lipids [26]. No phase transition was observed and the monolayer remains in a liquid expanded state during the whole compression cycle. Interestingly, the surface pressure starts to rise at area per lipid molecule of ~ 4.5 nm^2, which indicates a long-range interaction. The origin of this interaction could be either the electrostatic repulsion between the head groups (suppressed by the salt ions in the buffer, but still detectable in this type of experiments), or an entropic contribution from the highly disordered bactoprenyl chain. We did not investigate this issue further since this is out of the scope of this study.

A rough estimation of the size of the two sugar rings (assuming 0.15 nm between C atoms, forming the C-C bond) is ~ 0.1 nm^2 per sugar ring. This value is close to the values, which could be inferred from relevant studies on glycolipids, containing different number of sugar rings [27 – 29]. In these studies the limiting area per molecule for different glycolipids was found to increase ~ 0.05 – 0.15 nm^2 for each sugar ring. For the case of glycolipid GD3, containing four sugar rings in its head group, the limiting area per molecule was found to be ~ 0.9 nm^2 [30], while lactosylceramide occupies an area, slightly smaller than a SM molecule with the same length of acyl chains [31]. These studies also suggest that the sugar rings can have different orientation with respect to the surface of the bilayer, which results in differences in the area per each ring. Obviously, in our case, the area of both sugars (assuming that they lie flat on the bilayer surface and thus occupy a maximal possible area) could not account for the 1.5 nm^2 limiting area per molecule. Therefore, we postulate that the pentapeptide determines the large area, occupied by the L II molecule. The measured limiting area per molecule suggests a radius of the pentapeptide at a cross-section, determining this area to be ~ 0.7 nm. We observed that below a L II-DOPC ratio of approximately 1:14 the AFM tip starts to penetrate the L II-DOPC domains at lower forces. It can be calculated from the cross sectional areas of L II and DOPC (0.45 nm radius [31]) that at this concentration there are not enough L II molecules to form a tightly packed L II head group layer, even when it is assumed that all L II molecules are in the leaflet, facing the tip. So we could speculate that tight packing (or nearly tight packing) of L II head groups is needed to withstand the pressure, exerted by the scanning AFM tip at minimized force.

In summary we would like to point out that we provided for a first time information on the size and the orientation of the Lipid II head group when this molecule is incorporated within a membrane-mimicking liquid crystalline bilayer. Based on the obtained data we proposed that the pentapeptide of the L II head group adopts a configuration pointing away from the bilayer surface and is rather extended. This could be important in the specific recognition by antimicrobial peptides and for the peptidoglycan synthesis.

Lipid mixture	Frames analyzed	Height difference, nm (mean ± SD)
DOPC/DPPC – low force	10	-0.76 ± 0.11
L II:DOPC:DPPC - low force	20	1.16 ± 0.14
L II:DOPC:DPPC - high force	20	-0.81 ± 0.15
L I:DOPC:DPPC - low force	10	1.21 ± 0.13
L I:DOPC:DPPC - high force	10	-0.74 ± 0.12
11 PP/DOPC/DPPC – low force	20	-0.77 ± 0.16
L II-NBD:DOPC:DPPC - low force	5	1.22 ± 0.16
L II-NBD:DOPC:DPPC - high force	5	-0.76 ± 0.14

Table 1. Effect of L II and some analogues on the height differences between the DOPC domains where they reside and the surface of the gel state DPPC bilayer. The data are obtained from the experiments described in figures 2-6. At least three different samples were analyzed for each system.

References

[1] van Heijenoort, J. (1994) in *Bacterial Cell Wall*, Elsevier, Amsterdam.

[2] Kramer N.E., Smid E.J., Kok J., de Kruijff B., Kuipers O.P., Breukink E. (2004) Resistance of Gram-positive bacteria to nisin is not determined by lipid II levels,
FEMS Microbiol. Lett. 239(1), 157-161.

[3] Brötz, *H.,* Bierbaum, *G.,* Leopold, *K.,* Reynolds, P. E. and Sahl H-G. (1998) The Lantibiotic Mersacidin Inhibits Peptidoglycan Synthesis by Targeting Lipid II. *Antimicrobial Agents and Chemotherapy 42***,** 154-160

[4] Sheldrick G. M., Jones P. G., Kennard O., Williams D. H., Smith G. A. (1978) Structure of vancomycin and its complex with acetyl-D-alanyl-D-alanine, *Nature 271*, 223 - 225

[5] Breukink, E., Wiedemann, I., van Kraaij, C., Kuipers, O. P., Sahl, H.-G., de Kruijff, B. (1999) Use of the cell wall precursor lipid II by a pore-forming peptide antibiotic. *Science 286(5448),* 2361-2364.

[6] Breukink E, van Heusden HE, Vollmerhaus PJ, Swiezewska E, Brunner L, Walker S, Heck AJ, de Kruijff B. (2003) Lipid II is an intrinsic component of the pore induced by nisin in bacterial membranes, *J. Biol. Chem. 278*, 19898-19903.

[7] Hasper HE, de Kruijff B, Breukink E (2004) Assembly and stability of nisin-lipid II pores, *Biochemistry 43,* 11567-11575.

[8] Hoffmann, A., Pag, U., Wiedemann I., and Sahl H-G. (2002) Combination of antibiotic mechanisms in lantibiotics, *Il Farmaco 57,* 685-691

[9] Bonev B.B., Breukink E., Swiezewska E., de Kruijff B., Watts A. (2004) Targeting extracellular pyrophosphates underpins the high selectivity of nisin, *FASEB J. 18(15),* 1862-1869.

[10] Hsu S.T., Breukink E., Tischenko E., Lutters M.A., de Kruijff B., Kaptein R., Bonvin A.M., van Nuland N.A. (2004) The nisin-lipid II complex reveals a pyrophosphate cage that provides a blueprint for novel antibiotics, *Nat. Struct. Mol. Biol. 11*, 963-967

[11] Müller, D.J., Kessler, M., Oesterhelt, F., Möller, C., Oesterhelt, D., and Gaub H. (2002) Stability of Bacteriorhodopsin α-Helices and Loops Analyzed by Single-Molecule Force Spectroscopy, *Biophys. J. 83*, 3578-3588

[12] Dufrene Y.F., Boland T., Schneider J.W., Barger W.R., Lee G.U. (1998) Characterization of the physical properties of model biomembranes at the nanometer scale with the atomic force microscope, *Faraday Discuss. 111*, 79-94

[13] Ganchev D.N., Rijkers D.T.S., Snel, M.M.E., Killian J.A., and de Kruijff B. (2004) Strength of Integration of Transmembrane α-Helical Peptides in Lipid Bilayers As Determined by Atomic Force Spectroscopy *Biochemistry 43*, 14987 - 14993

[14] Kuipers, O.P., Rollema, H.S. Yap, W.M., Boot, H.J., Siezen, R.J., de Vos, W.M .(1992) Engineering dehydrated amino acid residues in the antimicrobial peptide nisin, *J. Biol. Chem. 267*, 24340-24346.

[15] Mou, J., Czajkowsky, D.M., and Shao, Z. (1996) Gramicidin A aggregation in supported gel state phosphatidylcholine bilayers. *Biochemistry 35*, 3222-3226

[16] Rinia, H.A., Kik, R.A., Demel, R.A., Snel, M.M.E., Killian, J.A., van der Eerden, J.P.J.M., and de Kruijff, B. (2000) Visualization of Highly Ordered Striated Domains Induced by Transmembrane Peptides in Supported Phosphatidylcholine Bilayers *Biochemistry 39*, 5852-5858

[17] Rinia, H.A., Demel, R.A., van der Eerden, J.P.J.M., and de Kruijff, B. (1999) Blistering of langmuir-blodgett bilayers containing anionic phospholipids as observed by atomic force microscopy, *Biophys. J.* 77, 1683-93

[18] Künneke, S., Krüger, D., and Janshoff A. (2004) Scrutiny of the Failure of Lipid Membranes as a Function of Headgroups, Chain Length, and Lamellarity Measured by Scanning Force Microscopy, *Biophys. J. 86*, 1545-1553.

[19] Franz, V., Loi, S., Müller, H., Bamberg, E., and Butt, H.-J. (2002)Tip penetration through lipid bilayers in atomic force microscopy *Coll. and Surf. B: Biointerfaces, 23 (2-3)*, 191-200

[20] Loi S., Sun G., Franz V., Butt H.-J. (2002) Rupture of molecular thin films observed in atomic force microscopy. II. Experiment, *Phys. Rev. E 66*, 031602-1 - 031602-6.

[21] Grant, L.M., and Tiberg, F. (2002) Normal and Lateral Forces between Lipid Covered Solids in Solution: Correlation with Layer Packing and Structure *Biophys. J. 82,* 1373-1385

[22] White S.H, Wimley, W.C. (1999) Membrane protein folding and stability: physical principles. *Annu Rev Biophys Biomol Struct. 28,* 319-65

[23] Reynolds, J.A., Gilbert, B.D. and Tanford, C. (1974) Empirical Correlation between Hydrophobic Free Energy and Aqueous Cavity Surface Area
PNAS 71, 2925-2927

[24] Hermann R.B., (1977) Use of Solvent Cavity Area and Number of Packed Solvent Molecules around a Solute in regard to Hydrocarbon Solubilities and Hydrophobic Interactions *PNAS 74,* 4144-4145.

[25] Smaal, E.B., Mandersloot, J.G., Demel, R.A., de Kruijff B., and de Gier, J. (1987) Consequences of the interaction of calcium with dioleoylphosphatidate-containing model membranes: calcium-membrane and membrane-membrane interactions, *Biochim. Biophys. Acta: Biomembranes 897,* 180-190

[26] Dynarowicz-Łątka, P., and Hąc-Wydro, K. (2004) Interactions between phosphatidylcholines and cholesterol in monolayers at the air/water interface *Coll. and Surf.B: Biointerfaces 37,* 21-25

[27] Filek, M., Gzyl, B., Laggner, P., and Kriechbaum M. (2005) Effect of indole-3-acetic acid on surface properties of the wheat plastid lipids, *J. of Plant Physiology 3,* 245-252

[28] Heywang, C., Mathe, G., Hess D., and Sackmann E. (2001) Interaction of GM_1 glycolipid in phospholipid monolayers with wheat germ agglutinin: effect of phospholipidic environment and subphase, *Chem. Phys. Lipids 113,* 41-53

[29] Maggio, B**.** (2004) Favorable and unfavorable lateral interactions of ceramide, neutral glycosphingolipids and gangliosides in mixed monolayers *Chem. Phys. Lipids 132(2),* 209-224

[30] Diociaiuti, M., Ruspantini, I., Giordani, C., Bordi F., and Chistolini P. (2004) Distribution of GD3 in DPPC monolayers: a thermodynamic and atomic force microscopy combined study, *Biophys. J. 86,* 321-328

[31] Li, X.-M., Momsen, M.M., Brockman, H.L., and Brown R.E. (2002) Lactosylceramide: Effect of Acyl Chain Structure on Phase Behavior and Molecular Packing, *Biophys. J. 83,* 1535-1546

Chapter 5. Summary and perspectives

The biological membrane plays a crucial role in sustaining the integrity of each living cell and in differentiating cellular organelles in eukaryotes. Moreover, the proteins, present in the membranes perform vital functions of mass transport, specific recognition and signaling. Therefore it is of prime importance to study in detail the organization of the biological membrane as well as the interactions between its constituents, since these interactions are essential for proper functioning of the membrane as a whole.

Structural studies on membranes revealed their spatial non-homogeneity with respect to the lipids. Moreover, recently a great interest was generated in the so-called lipid rafts. The proposed location of certain membrane proteins in these rafts suggests the importance of lipid/peptide interactions which could be the basis for the proposed co-separation of certain lipids and proteins in rafts. The size of these domains was proposed to be from a few nanometers up to a few hundred nanometers [1, 2]. Therefore, to study the nanoscale organization of the membrane requires implementation of techniques, capable of providing detailed information in the nanometer and sub-nanometer scale. Moreover, the used technique ideally should be able to provide information on the interaction between membrane components. One such technique is AFM, which can be used to obtain morphological information on hydrated biological samples. Moreover, recently it was demonstrated that AFM successfully can be used to probe intra- and intermolecular interactions and to mechanically manipulate samples in a well controlled manner.

In the present thesis we implemented these possibilities of the AFM technique to study lipid and lipid/peptide supported bilayers. These types of bilayers are a suitable model systems for biological membranes, and hence they are used quite often in membrane research [3, 4]. We applied the possibilities of both imaging and force manipulation by AFM techniques to characterize studied systems on a molecular level. First, we imaged the spatial organization of lipid and lipid/peptide bilayers and were able to obtain information on their molecular organization. Next, we performed force measurements on the same system, determining the strength of integration of a transmembrane peptide in the bilayer. Finally, we used AFM to determine the molecular dimension and orientation of the head group of Lipid II, a biologically important molecule in bacteria.

In the second chapter of this thesis we systematically varied the composition of lipid bilayers and followed their phase separation behaviour. The localisation of a model WALP peptide in these bilayers was also studied. With the performed experiments we demonstrated the possibilities of the AFM to distinguish different characteristic features in the investigated supported bilayers, from which we extracted information on their molecular organization. We studied the interesting phenomenon of peptide self-assembly in striated domains and argued that the high order of lipid molecules within gel state bilayers is the driving force for this self-assembly. The detailed study of the behaviour of lipid mixtures in the absence and presence of model transmembrane peptides further revealed possible principles of membrane organization in biological membranes.

The ongoing research in the membrane field provides more and more examples of how important the interactions are between the building blocks of the membrane. The correct functioning of the cellular protein “machines” depends to a large extent on fine-tuning with the surrounding lipid environment and hence on protein/lipid, lipid/lipid and protein/protein interactions. We could argue that these interactions are crucial in a majority of the processes, taking place within or through the membrane. AFM is one of the techniques, which provides the possibility to get some insight in these interactions. Exploiting this possibility, in chapter 3 we succeeded for the first time to determine the force, needed to extract a single transmembrane α-helical peptide out of a model membrane. Intriguingly, it turns out that this force did not vary significantly with the changes in the exact chemistry of the system. This led us to the

conclusion that in our experiments we probed a fundamental property of the bilayer and we proposed that the bilayer interface plays a determining role in the stability of peptide incorporation.

In the last chapter of the present thesis we again used AFM to mechanically manipulate the sample, but now in order to characterize Lipid II, a biologically important molecule, which is involved in trafficking of bacterial cell wall components through the membrane and, importantly, is the prime target of several classes of antimicrobial peptides [5]. By fine-tuning of the applied scanning force we succeeded to selectively penetrate only through the L II head group layer, while still scanning over the DOPC head group level. The collected data allowed us to propose (by combining the AFM data with pressure/area isotherms) a model for the size and orientation of the L II head group in a bilayer, which model could further enhance our understanding of the processes of bacterial cell wall synthesis and the antimicrobial action of peptides, that specifically target L II.

Overall, with the performed experiments we gained insight into the factors that govern the spatial organization of lipids and proteins within supported lipid bilayers –model systems, closely resembling biological membranes. We used phase separation phenomena in these bilayers in a variety of experiments, where we determined the organization of lipid bilayers, the forces between their ingredients and the molecular dimensions of some specific lipid molecules. We revealed how changes of the lipid composition govern the overall behaviour and properties of the bilayers, including the size and shape of the phase-separated domains that are formed. Moreover, we followed the self-assembly properties of a model transmembrane peptide in bilayers in different states, as well as its partitioning in bilayers of coexisting areas in different states. We used the knowledge, obtained in these experiments, as a basis to further study in detail the lipid/peptide interactions and to determine the stability of incorporation of an α-helical peptide in the bilayer. Previously, we observed the intriguing phenomenon of peptide self-aggregation in striated domains in DPPC bilayers. This system is important not only from a fundamental viewpoint (what are the underlying forces for the peptide self-assembly and separation?), but it also resembles the ordering of certain membrane proteins in specialized membranes [6]. Therefore, in this thesis we further investigated this important system and provided further insight in the factors, governing the peptide self-assembly. We identified the high order of the gel state bilayer as the main driving force for striated domain formation. Moreover, in our force measurements we determined that the interface layer of the bilayer provides much of the stability of peptide integration in a bilayer. These findings will contribute to our understanding of membrane processes, involving proteins.

In this study we demonstrated the potential of the AFM technique applied on lipid bilayers to provide insight down to a molecular level. Many researchers realized that potential and AFM studies on lipid bilayers become more and more common (for recent reviews, see [7, 8]). AFM also provides the possibility to observe in situ the time evolution of different membrane processes. Some noteworthy examples are the visualization of the interaction of membranes with antibiotics and different drugs [9, 10]. The effect of amyloid fibrils on a bilayer also was followed in time [11].

The mechanical manipulation of lipid bilayers, as applied by us, can be further developed, for instance for using functionalized AFM tips to probe specific properties of the bilayer or to incorporate biologically relevant molecules in the bilayer. An example of such an approach can be found in [12], where by controlling the chemistry of the tip by attaching a weak acid, a classical analytical titration was performed. In this case the titration was performed on the surface of a membrane-mimicking bilayer and at a nanometer scale. This example demonstrates the possibility of the AFM tip to act as a real "nanosensor" with a controllable chemical composition on its surface. A related approach makes use of enzymes, attached on an AFM tip [13]. These developments promise further insight on a single molecular level in the biochemical processes taking place in the membrane.

Another rapidly evolving experimental approach in membrane studies is the combination of AFM with another complimentary technique. Recent examples are simultaneous investigation of lipid bilayers by AFM and fluorescence microscopy [14] or Quartz Crystal Microbalance [15]. These complementary techniques provide more general (averaged) information, while the AFM reveals the nanoscale (and molecular) organization of the bilayer. This dual approach promises further interesting findings, as the combination of AFM technique with a complementary one will become more widespread. As an attempt to make a prognosis for the technical development in this field we can foresee still other techniques, coupled with AFM. Suitable candidates seem to be MALDI-TOF MS and FTIR spectroscopy.

The ingenious way in which nature provides a simple way for the formation of membrane structures through lipid self-assembly inspired many studies in this field. Scientist realized that the properties of lipids to assemble in different structures can be used for variety of purposes. The spherical closed lipid bilayers, or liposomes, were already successfully studied as possible carriers for drugs [16], and are commercially implemented in cosmetic products. The future promises more applications and we can imagine that liposomes, of which the surface is functionalized with specific molecules can recognize a target cell with high specificity. After recognition between the functionalized surface of the vesicle and the target, the cargo of the vesicle will be released locally, killing for instance tumor cells [17] or pathogenic microorganisms. In this way the efficiency of the treatment could be immensely increased and the toxic effect of certain drugs on normal cells will be reduced.

A planar bilayer, deposited on the target surface also has immense potential for practical applications. The inherent biocompatibility of lipids is one example of a potential application. The functionalization of the surface of biomaterials with a lipid bilayer would alleviate the severe problem of the response of the immune system to the foreign body. Therefore, lipid bilayer functionalization of different implants promises fewer problems [18].

Another possible application of lipid bilayers in bioengineering is the design of highly sensitive biosensors. In this type of application the surface of a chip would be covered with a lipid bilayer in which specific biomolecules are incorporated, for instance (modified) ion channels [19]. In principle it would be possible to detect even single molecules if binding of the analyzed molecules leads to the transport of more than one ion or molecule across the bilayer [20]. This exceptional sensitivity, combined with a high specificity of detection makes this type of devices highly promising. However, to be implemented in practice, further investigations are needed. More specifically, the functionalization of the surface of the sensor with an intact closed bilayer and incorporation in this bilayer of functional sensitive molecules, such as (modified) ion channels or signal transducers is still a challenge. Another problem is that while the lifetime of such devises allows laboratory experiments and demonstrations, still they are not stable for commercial purposes [19].

Summarizing the results from this study we would like to point out that we demonstrated the possibility to image, manipulate and characterize lipid bilayers and their components. Here we briefly outlined the perspectives in the involved scientific fields. Having in mind the importance of potential areas of application of (functionalized) lipid bilayers and the possibilities of the AFM technique we hope that this study will be followed by other exciting studies in this promising area.

References

[1] Schutz G.J., Kada G., Pastushenko V.P., Schindler H. Properties of lipid microdomains in a muscle cell membrane visualized by single molecule microscopy. *EMBO J.* 2000; 19: 892–901

[2] Gaus K., Gratton E., Kable E.P., Jones A.S., Gelissen I., Kritharides L., Jessup W. Visualizing lipid structure and raft domains in living cells with two-photon microscopy. *Proc. Natl. Acad. Sci. USA* 2003; 100: 15554–15559

[3] Simons K., Vazz V.L.C. Model systems, lipid rafts, and cell membranes. *Annu. Rev. Biophys. Biomol. Struct.* 2004;33:269-95

[4] de Kruijff B., Killian J. A., Ganchev**,** D.N**.,** Rinia, H.A., Sparr E**.,** Striated domains: self-organizing ordered assemblies of transmembrane alpha-helical peptides and lipids in bilayers. *Biol Chem.* 2006 387 (3): 235-41.

[5] Breukink E., Wiedemann I., van Kraaij C., Kuipers O.P., Sahl H., de Kruijff B.Use of the cell wall precursor lipid II by a pore-forming peptide antibiotic. *Science*. 1999, 286 (5448): 2361-2364.

[6] Müller D.J., Schoenenberger C.-A., Schabert, F., Engel, A. Structural changes in native membrane proteins monitored at subnanometer resolution with the atomic force microscope: a review J Struct Biol. 1997;119 (2):149-57

[7] Janshoff A., Steinem C. Scanning force microscopy of artificial membranes. Chembiochem. 2001;2(11):798-808

[8] Connell S.D., Smith D.A.The atomic force microscope as a tool for studying phase separation in lipid membranes. Mol Membr Biol. 2006; 23(1): 17-28.

[9] Berquand A., Mingeot-Leclercq M.P., Dufrene Y.F. Real-time imaging of drug-membrane interactions by atomic force microscopy. Biochim Biophys Acta. 2004; 1664(2): 198-205

[10] Berquand A., Fa N., Dufrene Y.F., Mingeot-Leclercq M.P.Interaction of the macrolide antibiotic azithromycin with lipid bilayers: effect on membrane organization, fluidity, and permeability. Pharm Res. 2005 (3): 465-75.

[11] Green J.D., Kreplak L., Goldsbury C., Li Blatter X., Stolz M., Cooper G.S., Seelig A., Kistler J., Aebi U. Atomic force microscopy reveals defects within mica supported lipid bilayers induced by the amyloidogenic human amylin peptide. J Mol Biol. 2004; 342(3): 877-87.

[12] Garcia-Manyes S., Gorostiza P., Sanz F. Titration force microscopy on supported lipid bilayers. Anal Chem. 2006; 78(1): 61-70.

[13] Wang X., Zhou D., Sinniah K., Clarke C., Birch L., Li H., Rayment T., Abell C. Electrostatic orientation of enzymes on surfaces for ligand screening probed by force spectroscopy. Langmuir. 2006; 22(3): 887-92.

[14] Kassies R, van der Werf KO, Lenferink A, Hunter CN, Olsen JD, Subramaniam V, Otto C.Combined AFM and confocal fluorescence microscope for applications in bio-nanotechnology. J Microsc. 2005 217(Pt 1):109-16.

[15] Richter RP, Brisson A.QCM-D on mica for parallel QCM-D-AFM studies. Langmuir. 2004 May 25;20(11):4609-13.

[16] Felnerova D, Viret JF, Gluck R, Moser C. Liposomes and virosomes as delivery systems for antigens, nucleic acids and drugs. Curr Opin Biotechnol. 2004 Dec;15(6):518-29.

[17] Sapra P, Tyagi P, Allen TM. Ligand-targeted liposomes for cancer treatment. Curr Drug Deliv. 2005 Oct;2(4):369-81.

[18] Lee DC, Chang BJ, Yu L, Frey SL, Lee KY, Patchipulusu S, Hall C. Polymer cushions functionalized with lipid molecules. Langmuir. 2004 Dec 21;20(26):11297-300.

[19] Anrather D, Smetazko M, Saba M, Alguel Y, Schalkhammer T. Supported membrane nanodevices. J Nanosci Nanotechnol. 2004;4(1-2):1-22.

[20] Janshoff A, Steinem C. Transport across artificial membranes-an analytical perspective. Anal Bioanal Chem. 2006 385(3):433-51.

Samenvatting

Het doel van ons huidige werk is om wat van de geheimen bloot te leggen van een fascinerende biologische structuur, die een vitaal onderdeel vormt van elke levende cel. We zouden zelfs kunnen zeggen dat leven, althans in zijn huidige vorm, niet mogelijk zou zijn zonder deze alom aanwezige structuur. We hebben het hier over het biologisch membraan. Het begrenst niet alleen elke cel, zo voorkomend dat de celonderdelen zouden wegvloeien, maar het vormt ook compartimenten binnen eukaryotische cellen, waarbij het de organellen afbakent. Maar het biologisch membraan is veel meer dan een barrière. Het vormt een belangrijk middel bij het goed functioneren van de vele eiwitten – cellulaire machines, die de selectieve instroom en uitstroom van verschillende moleculen regelen, de communicatie tussen de cel en de naastgelegen cellen en de reactie van de cel op stimuli uit zijn omgeving.

Het skelet van het biologisch membraan bestaat uit verschillende lipide moleculen (zie figuur 1 in hoofdstuk 1 voor een schematische tekening van een biologisch membraan). Deze moleculen zijn amfifiel, wat wil zeggen dat ze zowel hydrofiele als hydrofobe groepen bevat. In een waterige omgeving vormen deze moleculen verschillende zelf-assemblerende structuren om hun hydrofobe groepen van het ongunstige contact met de waterige omgeving af te schermen. Een van deze structuren is de lipide bilaag, die gevormd wordt uit twee lagen van lipide moleculen die met hun hydrofobe groepen naar elkaar toe staan, zodat deze groepen op die manier worden afgeschermd tegen contact met de waterige omgeving. In deze vorm vormen lipide moleculen de ruggengraat van het biologische membraan, zo de grens vormend van de cel en cel organellen.

Membraaneiwitten, die een veelheid aan belangrijke functies vervullen voor het overleven van de cel, hebben op verschillende manieren met het membraan te maken. Veel van de membraaneiwitten steken met een of meer transmembrane gedeelten door het membraan. Het moge duidelijk zijn dat lipide/eiwit interacties belangrijk zijn voor het goed functioneren van de eiwitten. Deze interacties worden echter niet volledig begrepen. Het was daarom in dit onderzoek mijn doel om biologische membranen te onderzoeken, inzicht te krijgen in hun structuur en lipide/lipide en lipide/eiwit interacties, met behulp van Atomic Force Microscopy (AFM). Deze techniek maakt het mogelijk om biologische monsters zichtbaar te maken op een nanometer resolutie, en tegelijkertijd is het mogelijk om de Pico Newton krachten tussen moleculen te meten. Ook kan het monster fysiek bewerkt worden, en deze mogelijkheid is gebruikt om de grootte en oriëntatie van lipide moleculen in een membraan te bepalen. Bovendien is het met AFM mogelijk om in fysiologische omstandigheden te werken, en alle experimenten zijn uitgevoerd op kamertemperatuur en in een waterige omgeving, hetgeen bijdraagt aan de relevantie van de verkregen resultaten.

In het begin van mijn proefschrift heb ik een overzicht gegeven van de huidige kennis op het gebied van de membraanwetenschap. De AFM techniek werd beschreven en de mogelijkheden ervan besproken. In de volgende drie hoofdstukken zijn verschillende onderzoekshoofdlijnen gevolgd en afgerond. In hoofdstuk 2 zijn de krachten achter het intrigerende fenomeen van peptide aggregatie bepaald. Aangetoond werd dat de geordende streepjes (‘striated domains’, zie hoofdstuk 2, figuren 2 en 3), die gevormd worden vanuit geordende lineaire aggregaten van eiwitmoleculen, enkel voorkwamen in het geval van de gel-state bilaag, en niet waargenomen werden in vloeibaar-geordende of vloeibaar-ongeordende bilagen. Dit resultaat leverde bewijs voor het feit dat de aggregatie van de peptide veroorzaakt wordt door de hogere orde van de lipide moleculen in gel-state bilagen. Bovendien werd in dit hoofdstuk aangetoond dat, in de gescheiden fase vloeibaar-ongeordende – gel state bilagen, peptide moleculen zich voornamelijk bevinden in de minder geordende vloeibaar-ongeordende bilaag.

Met behulp van de kennis die in het tweede hoofdstuk van het proefschrift is opgedaan, is in hoofdstuk 3 de mogelijkheid om met behulp van AFM intermoleculaire krachten te meten gebruikt om de kracht waarmee een model peptide in de lipide bilaag wordt vastgehouden te meten. Hoewel het in de macroscopische wereld erg klein is, is de gemeten kracht van ~ 100 Piconewtons (dit is ongeveer 8 biljoen keer minder dan het gewicht van een gemiddeld mens) op moleculair niveau toch behoorlijk groot. De experimenten van dit hoofdstuk hebben verder aangetoond dat de gemeten kracht enigszins afhankelijk is van de exacte chemische samenstelling van het systeem. Dit gaf aan dat de stabiliteit van de incorporatie van een peptide in lipide bilagen wordt bepaald door een fundamentele eigenschap van het systeem. Om te bepalen wat deze fundamentele eigenschap precies is, zijn verdere experimenten uitgevoerd. Deze zijn geïnterpreteerd in de lijn van de bestaande theorie over de stabiliteit van intermoleculaire verbindingen. Uitgaand van het resultaat werd vastgesteld dat de interface tussen de bilaag en de waterige omgeving een zeer belangrijke factor in de stabiliteit van peptide incorporatie in een bilaag is (hoofdstuk 3, figuur 8).

In het laatste onderzoekshoofdstuk (hoofdstuk 4) heb ik de mogelijkheid van AFM gebruikt om niet alleen extreem kleine krachten te meten, maar om ook een van tevoren bepaalde kracht uit te oefenen op het onderzochte monster. Het doel van dit onderzoek was om inzicht te krijgen in een specifiek lipide molecuul, dat typerend is voor bacteriën. Dit belangrijke lipide molecuul, Lipide II genaamd (zie hoofdstuk 4, figuur 1), bouwt een bacteriële celwand (beschermende structuur dat de bacterie omgeeft) en is het doelwit van bepaalde antimicrobische geneesmiddelen. Met behulp van imaging en krachtsuitoefening is de grootte en oriëntatie van dit belangrijke molecuul in een bilaag vastgesteld (hoofdstuk 4, figuur 10). De experimenten in dit hoofdstuk hebben nuttige informatie opgeleverd, dat kan resulteren in een beter begrip van de werking van deze antimicrobische geneesmiddelen.

In het laatste hoofdstuk van dit proefschrift (hoofdstuk 5) worden de verkregen resultaten opgesomd en worden er enkele voorstellen gegeven voor mogelijk verder onderzoek op dit gebied.

Summary

The aim of the present work is to reveal some of the secrets of one fascinating biological structure, which is a vital part of every living cell. We even can speculate that the life itself would not be possible, at least in its contemporary form, without this all-pervasive structure. The object under question is the biological membrane. It defines not only the border of each cell, preventing the cell ingredients to dissipate in the surrounding, but also provides compartmentization within eukaryotic cells, defining cell organelles. But biological membrane is much more than just a simple barrier. It provides an appropriate medium, which ensures the proper work of the multitude of proteins - cellular machines, which provide selective influx and outflux of different molecules, communication between the cell and the neighbouring cells, and appropriate reaction of the cell to the stimuli from its surrounding.

Basically, the frame of the biological membrane consists of a variety of lipid molecules (see figure 1 in Chapter one for a schematic drawing of a biological membrane). These molecules are amphiphilic, which means that they feature both hydrophilic and hydrophobic parts. So in aqueous environment these molecules form a variety of self-assembling structures to protect their hydrophobic parts from the unfavourable contact with water environment. One of these structures is the lipid bilayer, formed from two planar layers of lipid molecules, which face each other with their hydrophobic parts, thus protecting them from contact with the aqueous environment. Arranged in this way lipid molecules form the backbone of the biological membrane, defining the boundaries of the cell and cell organelles.

Membrane proteins, which perform multitude of functions, on which depends the survival of the cell, are associated with the membrane in different ways. Many of the membrane proteins span the membrane with one or more transmembrane parts. It is obvious that lipid/protein interactions are important in determining the proper functioning of the proteins. However, these interactions are not completely understood. Therefore, in this study my goal was to investigate model biological membranes, getting insight into their structure and lipid/lipid and lipid/protein interactions, using Atomic Force Microscopy (AFM). This technique allows visualization of biological samples with nanometer resolution, and in the same time allows measuring Pico Newton forces between molecules. Mechanical manipulation of the sample also can be performed, and this possibility was also used to determine size and orientation of lipid molecules within a membrane. Moreover, the AFM allows operation in physiological conditions, and all experiments were performed at room temperature and aqueous environment, which contributes to the relevance of the obtained results.

In the beginning of this thesis I provided an overview on the contemporary knowledge in the field of membrane science. The AFM technique was also described and its possibilities discussed. In the following three experimental chapters of the study several main line of research were completed. In chapter 2 the driving forces for the intriguing phenomenon of peptide aggregation was determined. It was demonstrated that the striated domains (See Chapter 2, figure 2 and figure 3), which are formed from ordered linear aggregates of protein molecules, were present only in the case of gel-state bilayer, and could not be observed in liquid ordered or liquid disordered bilayers. This finding provided evidence that the aggregation of the peptide is cause by the high order of the lipid molecules in gel state bilayers. Moreover, in this chapter was demonstrated that in the phase separated liquid disordered – gel state bilayers peptide molecules are preferentially located in the les ordered liquid disordered bilayer.

Based on the knowledge, gained in the second chapter of the thesis, in chapter 3 the possibility of the AFM to measure intermolecular forces was used to determine the strength, by which a model peptide is held within the lipid bilayer. Although extremely small by the standards of the macroscopic world, the measured force of ~ 100 Piconewtons (this is approximately eight trillion times less than one average human being weighs) still is relatively large on molecular scale. The experiments of this chapter further demonstrated that the measured force weakly depends on the precise chemical composition of the system. This indicated that the stability of the peptide incorporation within model lipid bilayers is determined by some fundamental property of the system. To determine which precisely is this fundamental factor, additional experiments were performed. They were interpreted according to existing theory for the stability of the intermolecular bonds. Based on the result, the interface between bilayer and the aqueous environment was proposed as a main factor, governing the stability of peptide incorporation within a bilayer (Chapter 3, figure 8)

In the last experimental chapter (Chapter 4) I used the possibility of the AFM not only to measure extremely small forces, but also to exert a predetermined force on the investigated sample. The aim of this study was to gain insight into a specific lipid molecule, typical for bacteria. This important lipid molecule, named Lipid II (see Chapter 4, figure 1), builds a bacterial cell wall (protective structure, surrounding the bacteria) and is target for certain antimicrobial drugs. Combining imaging with force manipulation, the size and orientation this important molecule within a bilayer was determined (Chapter 4, figure 10). The experiments in this chapter provided valuable information, which can result in better understanding of the action of the antimicrobial drugs.

The last chapter of this thesis (Chapter 5) summarizes the achieved results and hypothesizes on some of the possible future development within this field.

Acknowledgments

And finally, here are the acknowledgments. Although not as difficult to write as the rest of this thesis, still there are so many people I would like to thank and I hope I would not forget somebody.

First of all, I would like to express my sincere gratitude to my promoter, Prof. Ben de Kruijff. More than six years ago he believed in a foreigner from a distant country and gave me the opportunity to work in a world-wide renowned scientific group, using state of the art equipment. Moreover, he showed me the fascinating world of the biological membranes. You were so precise, so quite often I felt under pressure to be as perfect as possible. But I realized this is the way the science should be done. I learned so much from you and in a fact sometimes I felt as Alice in Wonderland – all the time you showed me so many new things to see and new knowledge to gather. Ben, thank you for showing me how deep the rabbit hole of the science is...

I would also like to thank my co-promoter, Antoinette Killian, who was always helpful and willing to discuss my problems and ideas.

The whole group of Biochemistry of Membranes – there are too many people to mention them all – Hester, Peter, Jacob, Matthijs, Emma – thank you for being around, for the 10.30 coffee, for the Thursday cookies, for introducing me to different laboratory practices in my freshman year.

To Suat – my roommate in the University (in fact, we shared two offices) – thank you for your friendship. The IB evenings in this Turkish restaurant were really nice and entertaining. Keep going man, I wish you all the best in the science and in music...

To my "other" group – Jan, thank you for your supervision when I was around. Jeroen, Liesbeth, Anelia, Fiona - it was nice to be together. Thank you for the talks and the coffee which we had together. Laura, you helped me so much with the everyday administrative stuff – I really appreciate it!

Hilde – you are a great person, you introduced me to the art of working with the AFM and showed me so many tricks to overcome the bad moods of this sometimes terrible machine... I enjoyed talking to you and listening to your singing.

To my supervisor during my first years – Margot, thank you for always helping me and giving me the right advice. I hope you are getting well.

Last, but not least, from my "professional" list – many thanks to one of the most important persons in BvM – Irene van Duin - many, many thanks for being always helpful and cheering me up.

From my personal life – special thanks to my mother, Marinka.

Майко, благодарение на това, което си направила от мен, съм стигнал до тук. Благодаря и извинявай, че съм далеч толкова за дълго.

Of course, the whole “Bulgarian mafia” in Utrecht an Netherlands has my special thanks – Niki, Nina, Ivan, Peter, Dancho, Lubo, Beni, Reni, Marko, Amilia, Krasi – so often you brought light and cheer in my life.

And finally, my dearest girl, Toshka – thank you for finding me and for waiting for me all these long years. You give me something warm and nice to think about in all these rainy Dutch evenings. Each moment spent with you is a small miracle – let’s keep it this way. My thoughts are always with you through all the distances, which separate us now.

Autobiography

Dragomir Nikolov Ganchev was born on 2nd of May 1970 in the town of Veliko Tarnovo, Bulgaria. He completed his high education in the High School of mathematics "Vassil Drumev" in his native town and graduated in 1988. After two year service in the Bulgarian army (compulsory duty by that time) he started his higher education in Technical University – Sofia. He graduated in 1995 with a defense of a MSc thesis "High precision instrumental amplifier based on the principle of modulation/demodulation", becoming an engineer in electronics and automatics. In the autumn of the same year he joined the Laboratory of Thermodynamics and Physico-chemical Hydrodynamics and continued his education in Chemistry Faculty of Sofia University "St. Kliment Ohridski". He completed his second MSc. in the field of physical chemistry in 1997 with a defense of the thesis "Dynamic and static surface and interfacial tension of different surfactants". He continued to work as a researcher in the laboratory where he graduated until 2001, when he started his PhD research in Utrecht University, Department of Biochemistry of membranes. His PhD project was primarily focused on AFM investigation of model biological membranes.

In the moment he works in Case Western Reserve University, Department of Physiology and Biophysics as a post-doctoral scholar, studying the process of prion protein aggregation.

List of publications

Role of Betaine as Foam Booster in the Presence of Silicone Oil Drops. Langmuir, 2000; 16 (3), 1000-1013. Basheva, E. S.; Ganchev, D.; Denkov, N. D.; Kasuga, K.; Satoh, N.; Tsujii, K.

Capillary mechanisms in membrane emulsification: oil-in-water emulsions stabilized by Tween 20 and milk proteins. Colloids and Surfaces A: Physicochemical and Engineering Aspects, 2002; 209 (1), 83-104. N. C. Christov, D. N. Ganchev, N. D. Vassileva, N. D. Denkov, K. D. Danov and P. A. Kralchevsky

Sphingomyelin is much more effective than saturated phosphatidylcholine in excluding unsaturated phosphatidylcholine from domains formed with cholesterol. FEBS Letters, 2003; 547 (1-3), 101-106. Bianca Y. van Duyl, Dragomir Ganchev, Vladimir Chupin, Ben de Kruijff and J. Antoinette Killian

The Peptide Antibiotic Clavanin A Interacts Strongly and Specifically with Lipid Bilayers. Biochemistry, 2003; 42 (38), 11366-11372. van Kan, E. J. M.; Ganchev, D. N.; Snel, M. M. E.; Chupin, V.; van der Bent, A.; de Kruijff, B.;

Strength of integration of transmembrane alpha-helical peptides in lipid bilayers as determined by Atomic Force Spectroscopy, Biochemistry, 2004; 43 (47), 14987-14993. Dragomir N. Ganchev, Margot M. E. Snel, J. Antoinette Killian, Dirk T. S. Rijkers and Ben de Kruijff

Molecular organization in striated domains induced by transmembrane α-helical peptides in dipalmitoyl phosphatidylcholine bilayers, Biochemistry, 2005; 44 (1); 2-10. Emma Sparr, Dragomir N. Ganchev, Margot M.E. Snel, Anja N.J.A. Ridder, Loes M.J. Kroon-Batenburg, Vladimir Chupin, Dirk T.S. Rijkers, J.Antoinette Killian, Ben de Kruijff

Size and orientation of the Lipid II headgroup as revealed by AFM imaging; Biochemistry. 2006 May 16;45(19):6195-202, Dragomir N. Ganchev, Antoinette J. Killian, Eefjan Breukink, and Ben de Kruijff

Striated domains: self-organizing ordered assemblies of transmembrane alpha-helical peptides and lipids in bilayers, Biol Chem. 2006; 387 (3); 235-41 Ben de Kruijff , Antoinette J. Killian , Dragomir N. Ganchev, Hilde A. Rinia, Emma Sparr.